

Use of quantitative pathology to improve grading and predict prognosis in tumours of the gastrointestinal tract

Dordi Lea

Thesis for the degree of Philosophiae Doctor (PhD)
University of Bergen, Norway
2022

UNIVERSITY OF BERGEN



Use of quantitative pathology to improve grading and predict prognosis in tumours of the gastrointestinal tract

Dordi Lea



Thesis for the degree of Philosophiae Doctor (PhD)
at the University of Bergen

Date of defense: 14.01.2022

© Copyright Dordi Lea

The material in this publication is covered by the provisions of the Copyright Act.

Year: 2022

Title: Use of quantitative pathology to improve grading and predict prognosis in tumours of the gastrointestinal tract

Name: Dordi Lea

Print: Skipnes Kommunikasjon / University of Bergen

Scientific environment

This study was conducted at the Department of Pathology, Stavanger University Hospital, in collaboration with the Research Group of Gastrointestinal Surgery. Also, one of the subprojects was done in collaboration with the Gastrointestinal Translational Research Group. The doctoral dissertation is affiliated with the Department of Clinical Medicine (Klinisk Institutt 1, K1) at the University of Bergen, Norway.



Financial support was provided by grants from the Folke Hermansen Fond, Stavanger, Norway and CarciNor, Oslo, Norway.



FOLKE HERMANSENS FOND



CarciNor

Acknowledgements

I am extremely grateful for the ability to conduct this study in collaboration with many talented and knowledgeable people. Most importantly, my sincere appreciation goes to my main supervisor, Dr Einar Gudbjörn Gudlaugsson, for guiding me through this process. You have experience from different research projects both abroad and in-house, and your knowledge of pathology is almost unattainable. Your door is always open for a consult.

I am overwhelmingly thankful to my co-supervisor, Prof. Kjetil Søreide. Your visions and ability to put ideas into practice in research projects is an inspiration. Your effort in this study is more than one can expect from a co-supervisor, and I am very grateful that you introduced me to the ACROBATICC project and involved me in the ongoing projects in the Research Group for Gastrointestinal Surgery. Your skills in scientific writing are for which to strive.

To Prof. Jon Arne Søreide, your passion for neuroendocrine tumours is almost religious. You responded quickly and offered help in any possible way. Although you were not a co-supervisor, your effort and enthusiasm were at the level of one.

I would like to thank the head of the Department of Pathology, Susanne Buhr-Wildhagen. I am thankful that you gave me time in busy schedule to conduct research, even when we were behind in reporting the pathological samples. I am also grateful to all my co-workers in the Department of Pathology. I could not have performed this project without your support and willingness to undertake some of my duties. In addition, I value our friendship, either over 'Geirs coffee' during a quiz or at lunchtime. Especially thanks to Linda Hatleskog for her excellent linguistic skills, which have improved this thesis.

I would like to thank my collaborators, Dr Martin Watson and ass. Prof. Hanne R. Hagland, for their valuable contribution to the projects and to the ACROBATICC cohort. You gave me valuable input and friendship on this ride. To Ivar Skaland, I could not have learnt Visiopharm without your help and support. I would also like to

thank Ramesh Khajavi, who did fantastic work with the ACROBATICC cohort and all the surgeons at the Department of Gastrointestinal Surgery.

To Melinda Lillesand, Emma Rewcastle and Kirsten Breistein Pettersen, the projects could not have been conducted without your efforts and valuable company in the ‘room with no windows’.

My research experience began at the Norwegian University of Science and Technology (NTNU). I am thankful for the enthusiastic lecturers, especially Prof. Anna Bofin, who supervised my research thesis and Prof. Lars Slørdal and Prof. Olav Spigset, who showed me the rewarding side of research and supervised my master’s thesis.

I would like to thank all my family and friends. A special thanks to my sister for starting her teaching career when I was five and giving me a good academic start. I am also grateful to my parents for giving me a safe upbringing and regularly providing my family and me with dinner during the last few years, a very well appreciated gesture. I am also lucky to be surrounded by good friends, and I regard some of you as my extended family.

Finally, I would like to thank Stian for being a modern man, keeping the house tidy and serving dinner when I worked late or during the evenings. Thank you for supporting me through this process and for being my life partner. We got the best gift we could receive during this process when we got Daniel into our lives two years ago. This thesis is dedicated to you, Daniel.

‘If I have seen further, it is by standing on the shoulders of giants.’

Sir Isaac Newton

Abbreviations

American Joint Committee on Cancer (AJCC)

Artificial intelligence (AI)

Assessment of clinically related outcomes and biomarker analysis for translational integration in colorectal cancer (ACROBATICC)

Cluster of differentiation (CD)

Colorectal cancer (CRC)

Computer tomography (CT)

Chromogranin A (CgA)

Deoxyribonucleic acid (DNA)

European Neuroendocrine Tumor Society (ENETS)

Formalin-fixed paraffin embedded (FFPE)

Gastroenteropancreatic neuroendocrine neoplasms (GEP-NENs)

Haematoxylin and eosin (HE)

Immune checkpoint inhibitors (ICI)

Immunohistochemical (IHC)

Kirsten rat sarcoma (KRAS)

Proto-oncogene B-Raf (BRAF)

Major histocompatibility complex (MHC)

Mammalian target of rapamycin (mTOR)

Microsatellite instability (MSI)

Microsatellite stable (MSS)

Mismatch repair (MMR)

Neuroendocrine tumour (NET)

Neuroendocrine neoplasm (NEN)

Neuroendocrine carcinoma (NEC)

Phosphohistone 3 (PHH3)

Polymerase chain reaction (PCR)

Positron emission tomography (PET)

Ribonucleic acid (RNA)

Tumour-Node-Metastasis (TNM)

Abstract

Cancer represents a formidable health burden and was the second leading cause of death globally in 2018. In Norway, almost 35000 new cancer cases were reported in 2019. For colon cancer, the incidence and mortality rates in Norway are among the highest in the world. Furthermore, the tumour-node-metastasis (TNM) system used today is not optimal for selecting which patients should receive adjuvant therapy or not.

With the implementation of digital pathology in different pathology departments, there will be better opportunities for digital image analysis, a tool aimed at giving a more reproducible and objective diagnosis than subjective evaluation in a microscope. In digital image analysis, a computer programme is used for the quantification of different biomarkers. This can improve cancer diagnostics because several biases in manual evaluation can be reduced or avoided. One of the challenges in pathology is intra-and inter-observer variability of prognostic and predictive biomarkers. This especially applies for gastroenteropancreatic neuroendocrine neoplasms (GEP-NENs), in which the proliferation marker Ki67 is important for grading (1–3), prognosis and treatment of patients. Several studies have shown inter- and intra-observer variations in the manual evaluation of Ki67 positivity, which can be improved with digital image analysis. This is important because the interpretation of the immunohistochemical staining of different biomarkers, such as Ki67, often influences patient prognosis and treatment.

The immune system, especially the number of T-cells in and around the tumour, has been investigated as a promising biomarker for predicting prognosis and survival in colorectal cancer (CRC). The immune system is closely linked to microsatellite instability (MSI) in CRC, and MSI-high CRC has been shown to respond well to immune therapy. A TNM-immune is suggested based on scoring of the number of T-cells in the tumour centre and the invasive margin using digital image analysis.

In this study, we explored the correlation between T-cells in presurgical blood samples and T-cells in the invasive margins and the tumour centres in CRC with

digital image analysis in a feasibility study and found a correlation. Furthermore, we used digital image analysis to calculate the immune score in colon cancer patients based on immunohistochemical (IHC) staining of cluster of differentiation (CD)3+ and CD8+ T-cells in invasive margins and tumour centres in a prospective cohort. This immune score corresponded strongly with known clinicopathological features, such as stage and MSI status.

Also, we evaluated digital image analysis as an objective assessment tool for two different proliferation markers in GEP-NENs: Ki67 and Phosphohistone 3 (PHH3). We compared manual (visual) evaluation of Ki67 from pathology reports with digital image analysis of Ki67 and found excellent agreement, but there is a tendency to upgrade cases from grade 1 to grade 2 with digital image analysis. For the digital image analysis of PHH3, the measurements were more diverging.

The data presented show the use of digital image analysis in two settings: developing an immune score as a prognostic marker in colon cancer and providing an objective and reproducible evaluation of proliferation in neuroendocrine neoplasms. With the transition to digital pathology, digital image analysis can be implemented in daily diagnostics. This implementation requires more research for the validation of the different methods. With time, digital image analysis is expected to be utilized for tasks performed by pathologists today.

List of Publications

- I. Hagland HR*, **Lea D***, Watson MM, Søreide K; *Correlation of Blood T-Cells to Intratumoral Density and Location of CD3+ and CD8+ T-Cells in Colorectal Cancer*; *Anticancer Research* 2017; 37 (2):675–684.
- II. **Lea D**, Watson MM, Skaland I, Hagland HR, Lillesand M, Gudlaugsson E, Søreide K; *A template to quantify the location and density of CD3+ and CD8+ tumor-infiltrating lymphocytes in colon cancer by digital pathology on whole slides for an objective, standardized immune-score assessment*; *Cancer Immunology Immunotherapy* 2021; 70(7):2049–2057.
- III. **Lea D**, Gudlaugsson EG, Skaland I, Lillesand M, Søreide K, Søreide JA; *Digital image analysis of the proliferation markers Ki67 and phosphohistone H3 in gastroenteropancreatic neuroendocrine neoplasms: accuracy of grading compared to routine manual hot spot evaluation of the Ki67 index*; *Appl Immunohistochem Mol Morphol* 2021; 29(7):499–505.

*These authors contributed equally to this study.

The published papers are reprinted with permission from their respective publishers or under the terms of the Creative Commons attributions. All rights reserved.

Contents

Scientific environment	3
Acknowledgements.....	4
Abbreviations	6
Abstract	8
List of Publications	10
Contents	11
1. Introduction	14
1.1 <i>Digital pathology</i>	15
1.1.1 Background	15
1.1.2 Whole slide imaging.....	16
1.1.3 Digital image analysis.....	17
1.1.4 Advantages and disadvantages of digital pathology.....	19
1.2 <i>Cancer</i>	24
1.2.1 Hallmarks of cancer.....	25
1.3 <i>Colorectal Cancer</i>	27
1.3.1 Epidemiology and aetiology.....	27
1.3.2 Pathogenesis	30
1.3.3 Microsatellite instability in colorectal cancer	32
1.3.4 Diagnosis and treatment.....	34
1.3.5 Histopathology and staging	35
1.3.6 Prognosis and prediction	40
1.4 <i>Neuroendocrine Neoplasms</i>	41
1.4.1 Epidemiology and aetiology.....	41
1.4.2 Pathogenesis	42
1.4.3 Diagnosis and treatment.....	44
1.4.4 Histopathology and staging	46
1.4.5 Prognosis and predication	50
1.5 <i>Cancer and the immune system</i>	52
1.5.1 The immune system in colorectal cancer	57
1.5.2 Immunoscore	60

1.6	<i>Proliferation in cancer cells</i>	62
1.6.1	Mitotic activity	63
1.6.2	Ki67.....	64
1.6.3	Phosphohistone H3	65
2.	Aims of the study	67
3.	Methods	68
3.1	<i>Study population</i>	68
3.2	<i>Material and data collected</i>	69
3.2.1	ACROBATIC.....	69
3.2.2	GEP-NENS cohort.....	69
3.2.3	Enhancing the quality and transparency of health research	70
3.3	<i>Statistical analysis</i>	71
3.4	<i>Techniques</i>	72
3.4.1	Flow cytometry	72
3.4.2	Multiplex polymerase chain reaction and fragment analysis	74
3.4.3	Immunohistochemistry	76
3.4.4	Digital image analysis	77
4.	Results	82
5.	Discussion	84
5.1	<i>Determine immune status in colorectal patients</i>	84
5.2	<i>Immune score for colon cancer</i>	85
5.3	<i>Digital image analysis of proliferation markers in neuroendocrine neoplasms</i>	86
5.4	<i>Methodological considerations and limitations</i>	87
5.4.1	Study population	87
5.4.2	Reference standard	88
5.4.3	Digital image analysis	89
6.	Conclusion and future perspectives	92
7.	References	94
8.	Figure credits	114
9.	Errata	117

10. Papers I – III	118
---------------------------------	------------

1. Introduction

This PhD thesis comprises two subprojects. First, a subproject with quantification of T-cells in colorectal cancer (CRC). **Papers I and II** are based on this subproject. The second subproject is on quantifying proliferative markers in neuroendocrine neoplasms (NENs) of the gastrointestinal tract using digital pathology. **Paper III** is based on this subproject.

The common denominator for this thesis is using digital image analysis to quantify different cell types in cancers of the gastrointestinal tract. For the first subproject, we quantified T-cells, and in the second subproject, we quantified proliferative tumour cells.

In Norway, a national project for implementing digital pathology is currently running, and all pathology departments in the region of Helse Vest, Norway, are scheduled to be fully digitalised in 2021/22. With this transformation, the adaption of existing grading systems must be integrated and implemented in digital pathology. With this adaptation, software offering digital image analysis can be integrated with diagnostics, either as supplementary software or the software used for viewing slides for the diagnostics. The benefit of integrating digital image analysis into diagnostics is that measurements can be made objectively and reproducibly. However, for this integration to occur, research is needed to develop methods, ensure that the methods are validated and give prognostic information similar to the manual evaluation performed today.

This thesis developed and explored two different digital image analysis methods. We aim to use these methods to give prognostic information to patients after the methods' validation. There is a need for more objective measurements of prognostic markers in pathology, and this thesis can contribute to such knowledge. After validation, we aim to integrate the methods into the daily diagnostics at pathology departments, as digital pathology is introduced in different departments.

1.1 Digital pathology

1.1.1 Background

Since the start of modern pathology, when Rudolf Virchow started describing the disease in the microscope, it has been the workhorse for pathologists to investigate tissues, understand the disease and give details about biology and formally stage disease severity for prognosis. While this is a refined art and a learned process with criteria and consensus developed over decades of practice, the current use of the human eye and mind is limited by subjective interpretation, leading to inter- and intra-observer variabilities. Several attempts have been made to overcome these shortcomings in pathology over the decades, such as using standardised criteria to grade disease and equipment like grid filters in the microscope when counting cells. Due to digital technology advancements in pathology, digital image analyses have become a tool to overcome the obstacles of subjective interpretation. Furthermore, digital image analysis, if performed correctly, can produce precise and highly reproducible results¹.

A virtual slide is a scanned slide image that is an exact copy of a physical slide image. However, the scanned slide image is evaluated on a computer screen instead of using a light microscope. During the last two decades, virtual microscopy/whole slide imaging technology has developed substantially, with several companies offering solutions for telepathology/digital pathology imaging systems².

Digital pathology requires digital platforms to capture, store, share, analyse and report on pathological examination. This includes digitalising the whole laboratory process, from registering a specimen to reporting the final diagnosis³. Today, several pathology departments worldwide have been digitalised and have used whole slide imaging in routine practice^{4, 5}.

Digital pathology can be divided into *whole slide imaging* and *digital image analysis*. Compared to manual observation utilising the human eye alone, digital pathology provides opportunities for a more consistent and quantitative evaluation^{6,7}. Using digital image analysis also provides opportunities for different morphometric measurements that are not possible with a light microscope⁸.

1.1.2 Whole slide imaging

Whole slide imaging requires dedicated equipment and an IT infrastructure. The technical requirements for whole slide imaging are image acquisition, storage, processing and visualisation⁹. In addition, both trained personnel and specific quality control steps are required to ensure that the scans are satisfactory³. Image acquisition is both image capture by a digital scanner and image display. For optimal scanning, it is important that the tissue section has optimal thickness, and that the tissue is placed in the slide's centre. Artefacts of the microtomy and mounting must be avoided. The resolution of a virtual slide should be at least x20 magnification, but, for some types of slides, there is a higher diagnostic accuracy with x40 magnification¹⁰, which unfortunately also increases the scanning time and requires more storage space. The pathologist can view the virtual slide on an image-viewing software locally or remotely (**Figure 1**). Most imaging viewing software programmes offer the opportunity to annotate on the virtual slide. Some imaging software programmes are more advanced and offer various options for digital image analysis.

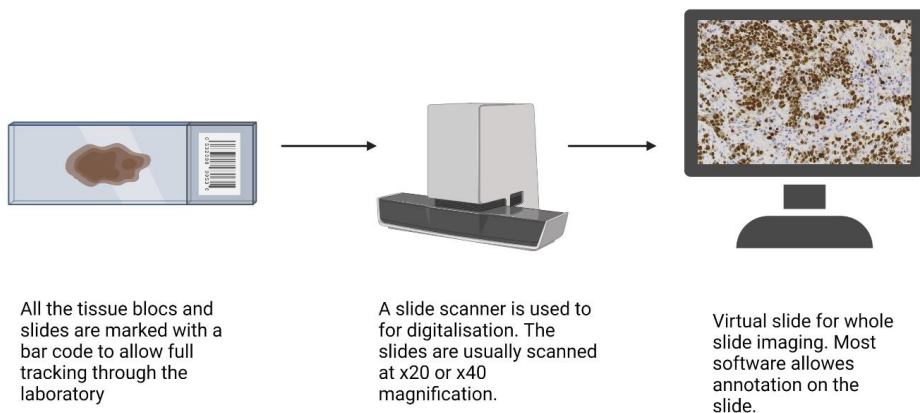


Figure 1: Whole slide imaging in a digital workflow in a pathology department. Created with BioRender.com.

1.1.3 Digital image analysis

Image analysis is a specific discipline that aims to obtain meaningful information from images in an objective and reproducible manner¹. Analysing images with objective tools began as early as the 17th century when Leeuwenhoek developed a system to measure microscopic objects¹¹. There has been a development in pathology, with a transition from qualitative information to semi-quantitative and quantitative evaluation of pathological features and biomarker expression, such as IHC expression (**Figure 2**)¹². An example is the percent positivity of the proliferation marker Ki67 of tumour cells in neuroendocrine neoplasm (NEN). This development occurs independent of digital pathology, but digital image analysis may be a helpful tool and may improve quantitative measurements. One of the challenges in pathology is intra- and inter-observer variability of prognostic and predictive biomarkers¹³⁻¹⁵, hence the need for objective and reproducible quantitative measurements using digital image analysis.

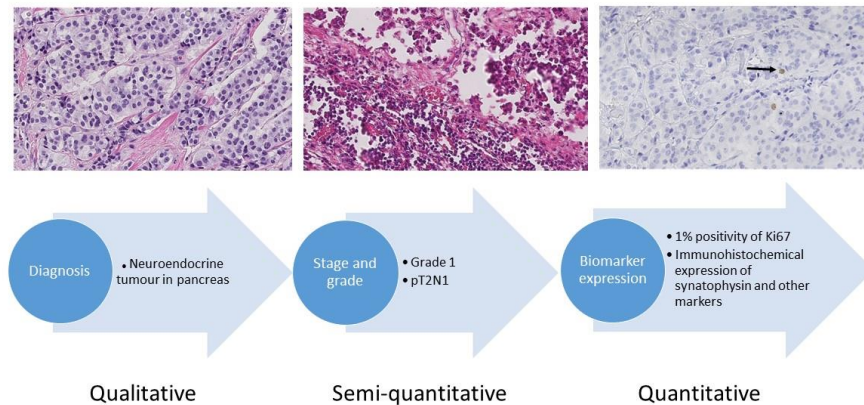


Figure 2: Evolution in pathology. Pathology has developed from describing the tissue and giving a diagnosis to giving more quantifiable data with grading and then using biomarkers such as immunohistochemistry for grading and quantification. This example shows the development in diagnosing neuroendocrine neoplasms.

Digital image analysis can be area based, cell based, and measurements pertaining to objects in the tissue aside from cells⁸. Digital image analysis can be used for several tasks in pathology, including the measurement of the staining of a protein with IHC or the measurement of size or area on a virtual slide. For some IHC markers, there are semiquantitative evaluations of staining intensity available, for example, human epidermal growth factor 2 in breast cancer, where a tier scoring system from zero to 3+ in $>/< 10\%$ of the tumour cells is used diagnostically. However, difficulties are encountered in determining whether the tumour is 1+ or 2+ with manual evaluation¹⁶. The College of American Pathologists has developed guidelines for quantitative image analysis with digital image analysis for human epidermal growth factor 2 IHC in breast cancer, which may aid in scoring human epidermal growth factor 2¹⁷. Unfortunately, there is a lack of similar guidelines for other IHC markers analysed by quantitative image analysis. By introducing personalised medicine and individualised therapies related to IHC assessments, many IHC analyses will likely require digital

image analysis for reliable quantitative and more objective measurements in the future¹.

An emerging field in digital image analysis is the development of artificial intelligence (AI). AI refers to the simulation of the human mind in computer systems programmed to think like humans and mimic their actions, such as learning and problem-solving¹⁸. This is a more complex form of digital image analysis than quantitative image analysis, in which the computer programme learns and interprets the data based on training. The learning process can be supervised or unsupervised. Supervised learning has a defined set of outputs compared to unsupervised learning, whose output is not predefined^{19, 20}. AI can be divided into machine learning and deep learning. Machine learning is the ability to learn without being directly programmed, while deep learning is a subset of machine learning using artificial neural networks, in which statistical models are established through input data^{18, 21}. Using deep neural networks, these computer algorithms can be used to detect malignant tissue in a histological specimen²² or give prognostic information to guide treatment (e.g. adjuvant therapy in CRC²³). An example from gastrointestinal pathology is the development of multiple deep learning algorithms, where the computer could classify several types of colorectal polyps, including hyperplastic, sessile serrated, traditional serrated, tubular and tubulovillous/villous polyps with an overall accuracy of 93%²⁴. Deep learning algorithms like this can help in colorectal screening programmes to identify high-risk polyps for further evaluation by a pathologist.

1.1.4 Advantages and disadvantages of digital pathology

A transition to a digital workflow likely provides several advantages, including easier sharing of slides for consultation with other pathologists, collaboration with interdisciplinary and remote research teams or during routine practice by the contribution of pathology in multidisciplinary clinical teams. It can also help to standardise teaching¹. One of the major benefits of digital pathology is the

opportunity of remote consulting. This technology is important, especially in countries with a shortage of pathologists^{25, 26}, and in other countries like Norway, with long distances and a lack of or limited pathology services at many small hospitals²⁷. Furthermore, with the evolving subspecialisation in pathology, there is an increasing need for consultation among pathologists. Digital pathology may facilitate this²⁸.

Several technical aspects of digital pathology need to be addressed. First, the hardware and storage capacity are important. Each scanned slide is currently about 0.5–4.0 GB, and huge storage capacity, both locally and in a cloud is necessary²¹. The computer must be powerful enough to process the images rapidly and upload/download the data to storage. So, both the intranet and the internet capacity are critical^{21, 29}. Compared to a traditional glass slide, the scanned slide does not break, fade or get lost³⁰. Thus, the organisation of archived digitized slides is easier than physical filing¹. Also, there is evidence that digital pathology will increase safety with barcode identification and thus improve quality and efficiency³. A study by Nakhleh and co-workers in 136 institutions found that the overall mislabelling of cases occurred in about 1.1 pr. 1000³¹. The rates for specimens, blocks and slides were 1.0, 1.7 and 1.1, respectively. Only 27% of the laboratories in this study had barcoding, which dramatically reduced the error rate³¹. One large study found that misidentification errors were reduced by 55% when barcoding was implemented for the throughput of an entire laboratory³². Barcoding allows full laboratory tracking, which reduces misidentification errors and increases efficiency³³.

A meta-analysis showed that whole slide imaging was discordant in about 4% of the cases compared with light microscopy. Most of this discordance was related to diagnosing and grading dysplasia (32%) or to the inability to find small objects (10%)³⁴. A study that assessed mitosis in breast cancer found a reduction of 20% when counting mitosis using whole slide imaging compared with light microscopy³⁵. This illustrates the need for automated measurements using digital image analysis. Automated measurements of IHC staining can give more precise and reliable results,

reducing the under- and overtreatment of patients³⁶. Digital quantification of histopathological parameters, such as steatosis or fibrosis, has also been more precise and reproducible than manual quantification of the same features³⁷. With digital image analysis, data can be extracted in a highly reproducible fashion via specialized software, which is a great benefit of this technology⁸.

With whole slide imaging, AI and machine learning are facilitated²², and promising results using AI in histopathology have been shown in several studies^{18, 23, 24}.

Algorithms, as delineated in **Figure 3**, may be helpful in routine diagnostics in the future.

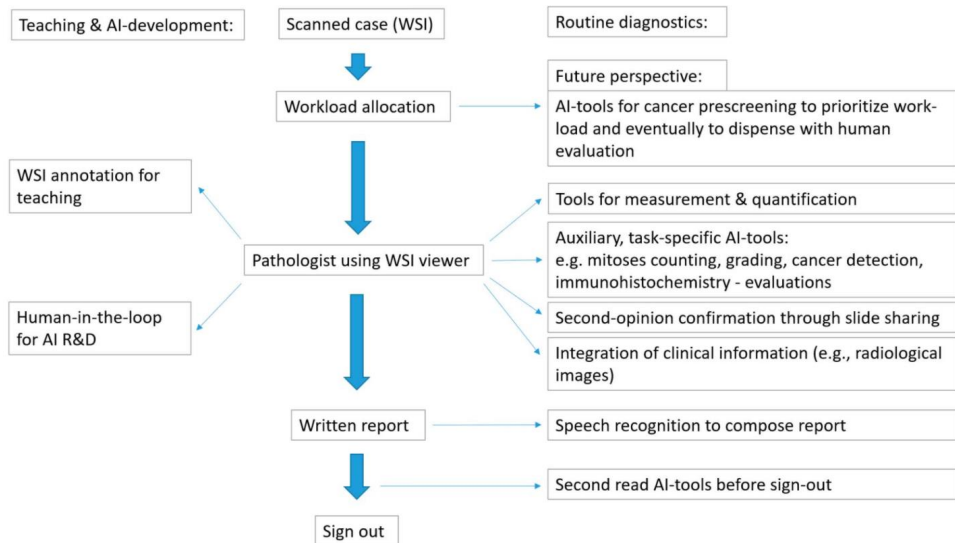


Figure 3: Processing of whole slide imaging (WSI). Potential workflow at a given department of pathology in the future. Reprinted under CC BY 4.0 with permission from³⁸. Copyright © MDPI 2020.

Digital image analysis likely yields more precise and reproducible results, which may partly be explained by reducing many biases that influence manual scoring, including visual and cognitive traps (**Table 1**)³⁹. Biases are systematic errors that can affect scientific investigations and destroy the validity of a study^{40, 41}. There are several visual traps in manual scoring, such as the illusion of size, where the perception of

size is influenced by the context in which it is displayed, which is the Ebbinghaus illusion (**Figure 4**)⁴². Other visual traps are also present in manual scoring, such as ‘inattentional blindness’, in which one fails to observe salient features when engaged in a different task^{43, 44}. For example, in a study of chest X-rays, 60% of radiologists failed to observe a missing left medial clavicle⁴⁵. The perception of colour and hues also depends on their context and the individual who does the evaluation^{42, 46}. In addition, there are several cognitive traps. Pathologists tend to avoid extreme ranges when assigning pathology scores⁴⁷. Furthermore, measurements tend to be given and end at a value of 0 or 5, for example, in blood pressure measurements^{48, 49}. The same would probably apply to the manual scoring of percentages in pathology. A pathologist may also be influenced by context bias when evaluating a sample⁵⁰. For example, if a disease is prevalent, it is more likely to consider a sample as abnormal when viewed together with other samples showing high disease prevalence. One of the most important cognitive biases is the predisposition to seek informative support for a favourable hypothesis⁵¹. The introduction of digital pathology and digital image analysis will probably reduce bias, such as the ones mentioned above and enhance the accuracy and reproducibility of different biomarkers, such as the interpretation of IHC stains¹.

Visual and cognitive traps where the effect can be diminished by digital image analysis	
Visual traps	Brief description
Illusion of size	Perception of an object's size is influenced by the context in which it is displayed
Inattentional blindness	The phenomenon of failing to observe salient features or events when engaged in a different task
Perception of colour and hues	Perception of colours and hues depends on their context
Checker shadow illusion	Perception of a surface's brightness is influenced by our knowledge of how it should appear, even if it is covered by a shadow
Lateral inhibition	A tendency for activated neurons to influence neighbouring neurons in the visual pathway, yielding an increased ability to respond to edges of surfaces
Cognitive traps	
Confirmation bias	The predisposition of people to seek information supportive of a favoured hypothesis
Avoidance of extreme ranges	Tendency to avoid extremes of ranges when assigning pathology scores
Diagnostic drift	The situation in which scoring values vary slightly and in a consistent fashion during a study
Number preference	Predisposition to assign numerical scores ending in 0 or 5
Context bias	Predisposition to consider a sample as abnormal when viewed in series with other samples showing a high disease prevalence but not when the sample is interpreted as part of a group with lower disease prevalence
Gambler's fallacy	Inability to consider individual samples and endpoints (e.g. cytoplasmic versus membrane staining in IHC) as events independent from previous and following slides or scoring events

Table 1: Visual and cognitive traps that can be reduced with digital image analysis. Adapted with permission from³⁹. Copyright© College of American Pathologists 2017.

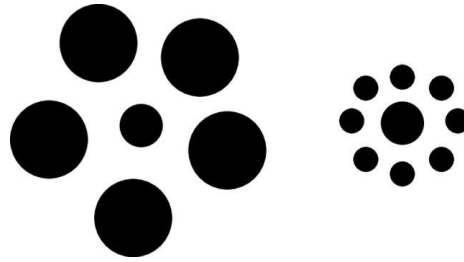


Figure 4: Ebbinghaus illusion. Although the inner circles are the same size, the surrounding circles affect how we interpret the size. Reprinted with permission from⁵². Copyright© Sage 2015.

1.2 Cancer

Cancer represents a formidable health burden and was the second leading cause of death globally in 2018. About 1/6 of deaths are due to cancer⁵³. According to a recent report from the Cancer Registry of Norway, over 35 000 new cancer cases (54.1% men) were reported annually, and 10981 deaths from cancer were encountered⁵⁴.

The cancer formation process is called carcinogenesis. In this process, various biological events and molecular changes are involved. Several genetic changes lead to abnormal cell division and cause normal cells to transform into cancer cells⁵⁵. For cancer to develop, genes that regulate cell growth and differentiation must be altered by genetic or epigenetic changes⁵⁶. An epigenetic change is a phenotype change without altering the DNA sequence (e.g. DNA methylation or histone modification)⁵⁷.

Genetic alterations are usually somatic events and take a long time to accrue (hence, the debut of cancer is usually in the age groups 60–70s), but a germline mutation predisposes a person to cancer at a much earlier age (usually in their early 30s or 40s)⁵⁶. Driver mutations are causal in the neoplastic process and are positively selected during carcinogenesis. They often occur in genes that regulate cell division, apoptosis and deoxyribonucleic acid (DNA) repair. Passenger mutations are biologically neutral

and provide no advantage to the tumour but are retained by chance during repeated cell division and clonal expansion⁵⁸.

In carcinogenesis, these genetic changes affect two broad categories of genes: proto-oncogenes and tumour suppressor genes. Proto-oncogenes encode proteins that control cell proliferation and or/apoptosis⁵⁶. These may be normal genes expressed at inappropriately high levels or altered genes with novel properties. Tumour suppressor genes inhibit cell division, survival or other properties of cancer cells and are often disabled by cancer-promoting genetic changes⁵⁹. An important difference between oncogenes and tumour suppressor genes is that oncogenes result from the *activation* (switching on) of proto-oncogenes, whereas tumour suppressor genes cause cancer when they are *inactivated* (switched off)⁶⁰.

1.2.1 Hallmarks of cancer

Our understanding of carcinogenesis involves several other aspects besides genetic changes. Several alterations are found in cancer, and these have been called *Hallmarks of cancer*⁶¹ in a publication by Hanahan and Weinberg in 2000. The list included six functional acquired capabilities: sustaining proliferative signalling, evading growth suppressors, resisting cell death, enabling replicative immortality, inducing angiogenesis, activating invasion and metastasis⁶². A decade later, two more hallmarks and two enabling characteristics were added, see **figure 5**⁶².

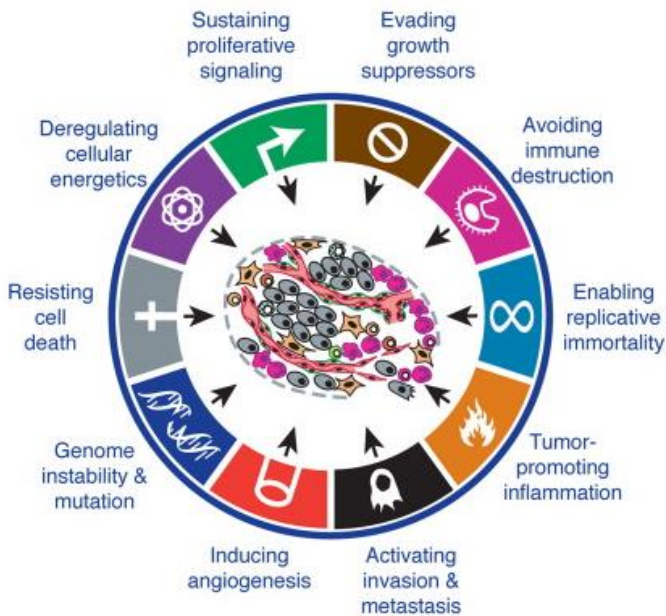


Figure 5: Hallmarks of cancer. Adapted with permission from⁶². Copyright © Elsevier Inc. 2011.

The most fundamental trait of a cancer cell is its ability to sustain continuous proliferation. Normally, proliferation is controlled by the release of growth-promoting signal molecules that regulate the cell cycle to ensure the homeostatic maintenance of normal tissue. Cancer cells deregulate these signals. In addition, there is resistance to cell death, which adds to the uncontrolled proliferation of cancer cells⁶². Furthermore, cancer cells develop the ability to avoid destruction by the immune system, which aids in their resistance to cell death⁶³. For cancer cells to survive and metastasis to other organs, angiogenesis and modification of the tumour microenvironment are critical to access nutrients. In addition, there is a gain of telomerase in cancer cells, which has a life-prolonging effect⁶⁴.

1.3 Colorectal Cancer

1.3.1 Epidemiology and aetiology

Worldwide, CRC represents a formidable health burden, with an estimated 72% increase in cases towards 2040⁶⁵. It is the third most common cancer type and the second most common cause of death from cancer worldwide (**Figure 6**)^{66, 67}. Despite the improvements in surgical and oncological treatments over the last decade⁶⁸, about half of all patients will develop metastasis and eventually die from disseminated disease^{69, 70}. The incidence of CRC varies greatly, and about 60% of all deaths occur in countries with a high or very high human development index⁷⁰.

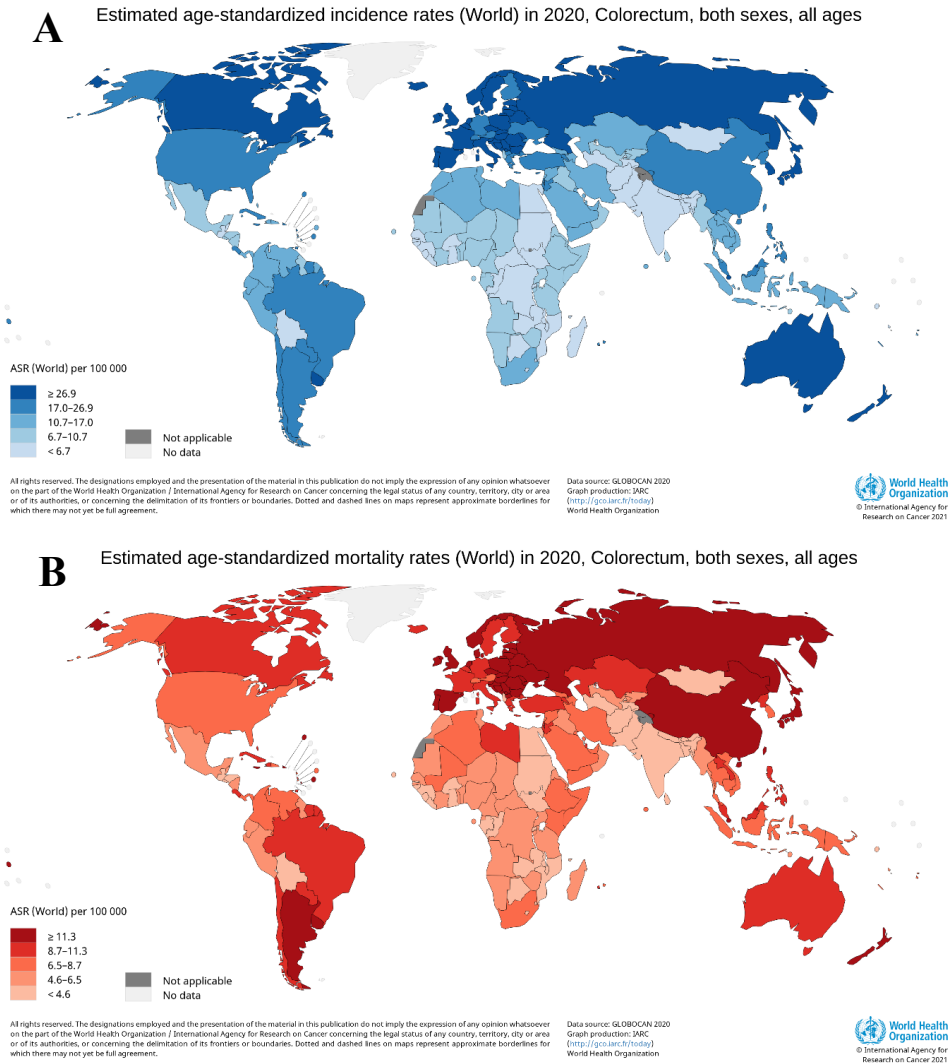


Figure 6: Incidence (A) and mortality rates (B) of colorectal cancer in the world. Reprinted with permission from⁷¹. Copyright© International Agency for Research on Cancer IARC 2020.

In Norway, almost 4500 patients were diagnosed with CRC in 2020. It is the second leading cause of cancer death in Norway, following lung cancer. Of CRC, about 2/3 is colon cancer⁵⁴. For decades, incidence rates for both colon and rectal cancer have been on the rise in Norway. However, the incidence rate of rectal cancer has levelled

since the 1990s, and the mortality rate is about half of what it used to be⁵⁴. For colon cancer, the incidence and mortality rates in Norway are among the highest in the world^{54, 66}.

Incidence rates are influenced by lifestyle factors, such as diet and obesity, while mortality rates depend on the stage of the disease at the time of diagnosis and the available treatment options⁷². In many low-income countries, adjuvant therapy is not available⁷³. Screening programmes may have contributed to the decrease in mortality rates seen in many countries, such as Israel, Japan, the United States⁷⁴ and several European countries⁷⁵. In Norway, a national screening programme for CRC is scheduled to start in 2022⁷⁶.

Both hereditary and environmental risk factors play a role in development of CRC (**Figure 7**)⁷⁷. Positive family history is a risk factor for CRC⁷⁸, but only a subgroup of approximately 5–7% is affected by a well-defined hereditary CRC syndrome, such as Lynch syndrome or familial adenomatous polyposis^{79, 80}. People with a positive family history of CRC, but where the genetic pathway is unknown, will have a moderately increased risk of developing CRC compared with the general population⁸¹.

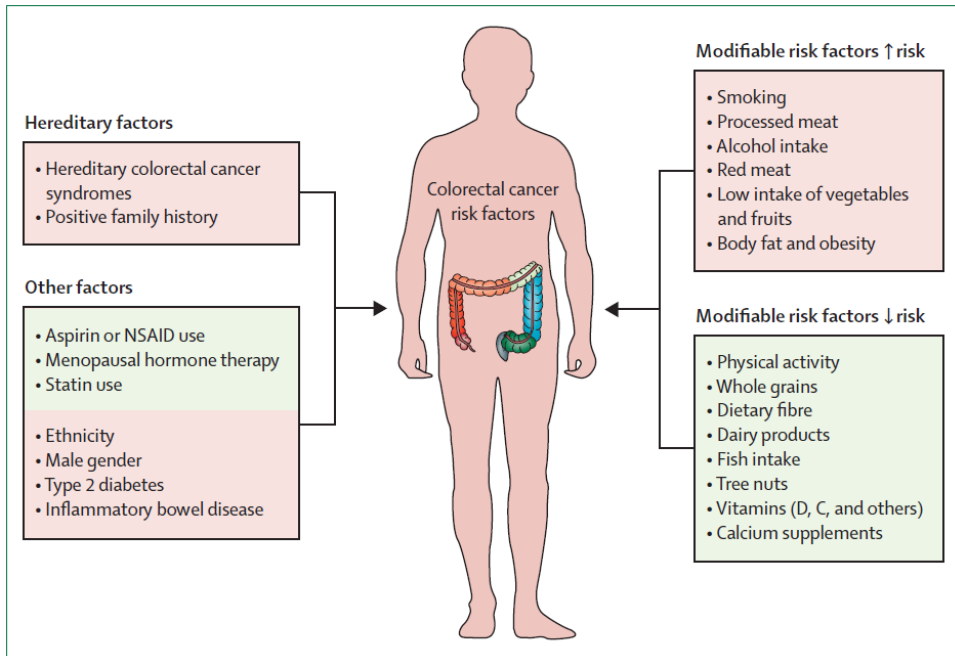


Figure 7: Risk factors for the development of colorectal cancer. Reprinted with permission from⁷⁷ Copyright © Elsevier Ltd 2019.

1.3.2 Pathogenesis

Carcinogenesis was first described for CRC in the 1990s and referred to as the adenoma–carcinoma sequence (**Figure 8**)^{82, 83}. Although our understanding of carcinogenesis in CRC is more complex today⁷⁷, this model illustrates the molecular events in the most common pathway of CRC leading to precancerous disease (adenoma) before developing into invasive carcinoma. The commonest genetic changes in this pathway include alterations seen in adenomatous polyposis coli, tumour protein 53 and the KRAS (Kirsten rat sarcoma) gene, which are present in 81%, 60% and 43% of sporadic CRCs, respectively⁸⁴. About 70-90% of CRC develop via this pathway⁸². The other development pathways are the serrated neoplasia pathway (10–20%) and the microsatellite instability pathway (2–7%) (**Figure 9**).

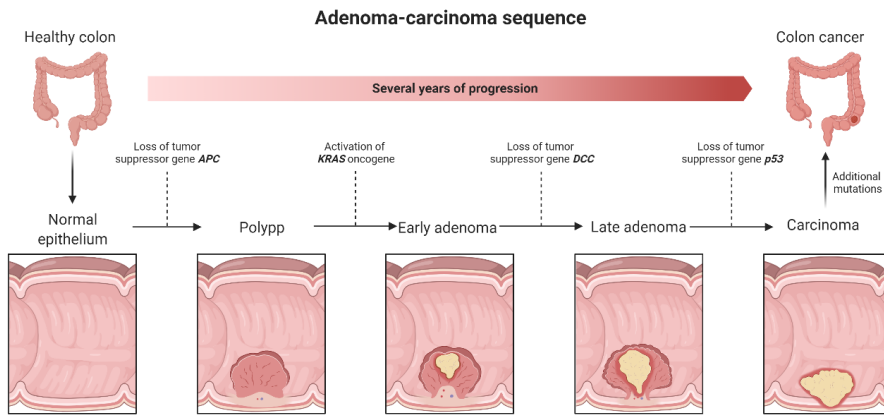


Figure 8: Adenoma-carcinoma sequence. Development of cancer through different genetic changes, which promote tumour development. Adapted with permission from⁶³ using BioRender.com. Copyright© Cell Press 1990.

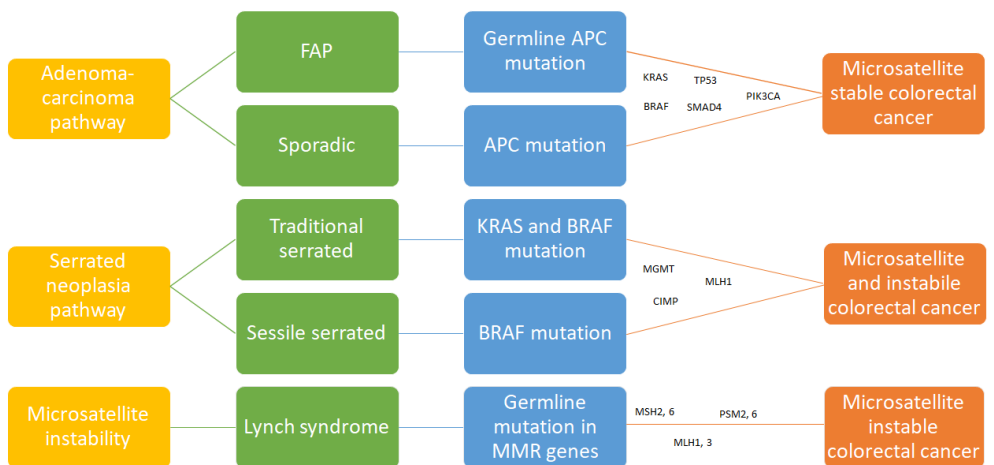


Figure 9: The three different developmental pathways of colorectal cancer and their associated hereditary syndromes and molecular genetic changes. Abbreviations: FAP: Familial adenomatous polyposis, APC: adenomatous polyposis coli, TP53: tumour protein 53, KRAS: Kirsten rat sarcoma, BRAF: Proto-oncogene B-raf, MMR: Mismatch repair, PIK3CA: phosphatidylinositol-4,5-bisphosphate 3-kinase catalytic

subunit alpha, MGMT: O(6)-methylguanine-DNA methyltransferase MLH: MutL homolog 1, CIMP: CpG island methylator phenotype, MSH: MutS homolog, PSM: protein signalling modulator. Adapted with permission from⁷⁷. Copyright © Elsevier Inc. 2019.

1.3.3 Microsatellite instability in colorectal cancer

A microsatellite is a stretch of repetitive DNA, where certain DNA motifs (typically 1–6 base pairs) are repeated in the genome⁸⁵. Microsatellites comprise mononucleotides, dinucleotides or higher-order nucleotides such as (A)_n or (CA)_n⁸⁶, and are present in about 3% of the human genome⁸⁷. Microsatellites are often referred to as short tandem repeats or simple sequence repeats. Due to their repetitive structure, microsatellites are particularly prone to replication errors and have a higher mutation rate than other segments of DNA⁸⁸. These errors are normally repaired by the mismatch repair (MMR) system⁸⁶. MSI is a state of genetic hypermutability that results from an impaired MMR system. Thus, MSI is phenotypic evidence that the MMR system is not functioning normally. Deficient in the MMR system are either caused by germline mutation (Lynch syndrome), somatic mutation or epigenetic silencing⁸⁶.

In 1993, several papers reported the presence of MSI as a frequent molecular phenomenon in CRC⁸⁹⁻⁹¹. MSI was found in Lynch syndrome patients, linked to a specific genetic locus (D2S123)⁸⁹ subsequently identified as one of the MMR genes. 15–20% of CRCs have MSI. About 2–3% of these have Lynch syndrome, an autosomal dominant genetic disorder with defect MMR genes⁹²⁻⁹⁵. There is a correlation between MSI and tumours in the proximal colon and increased patient survival⁹⁰. MSI is reported in several other tumour types, such as endometrial, ovarian and gastric carcinoma⁹⁶.

MSI can be detected by polymerase chain reaction (PCR) of specific microsatellite repeats or IHC staining of different MMR proteins. In Bethesda in the late 1990s, a consensus conference established a panel of microsatellite markers to diagnose MSI

in CRC. Microsatellite instability is defined as ‘a change in length due to either insertion or deletion of repeating units, in a microsatellite within a tumour when compared to normal tissue’⁹⁶. The guidelines suggest a panel of five microsatellite loci to assess instability, known as the *Bethesda panel*. Originally, it included five microsatellite loci, two mononucleotides (BAT25 and BAT26) and three dinucleotides (D5S346, D2S123 and D17S250)^{86,96}. The panel has later been debated and revised and now includes five monomorphic repeats, where the dinucleotides have been replaced by the mononucleotides NR-21, NR24 and NR27. The Bethesda guidelines also describe three different classes of CRC based on MSI status. These classes were MSI-high, showing MSI at $\geq 2/5$ loci, MSI-low, with instability at 1/5 loci, and MSS CRCs, where no instable marker was detected out of the suggested five⁹⁶.

IHC staining for MMR proteins was first successfully performed in 1996⁹⁷. Today, the recommended panel includes MLH1, MSH2, MSH6 and PMS2⁹⁸. Normally, cancer cells will show nuclear staining for MMR-proteins. Loss of one or more of these proteins/negative staining is pathologic and suggests mismatch repair defects, either sporadic or inherited (Lynch syndrome)⁹⁸. In cases of difficult interpretation of the IHC stain, a more sensitive method of PCR is recommended⁹⁹. In general, IHC and PCR-based analysis for MSI/MMR show good concordance¹⁰⁰, but weak or heterogeneous staining of MMR proteins might be difficult to interpret¹⁰¹.

Testing for MSI and/or examining MMR proteins with IHC is recommended in patients with CRC, who at the time of diagnosis are less than 60 years of age, have high-risk stadium II or following the Norwegian national guidelines, are eligible for adjuvant therapy¹⁰². If a patient is MSI-high and/or has lost MMR proteins, further PCR analysis to check for proto-oncogene B-raf (BRAF) mutation and/or MLH1 promoter hyper-methylation is recommended. If these are absent, genetic counselling and testing for Lynch syndrome are warranted¹⁰³.

EMAST

An alternative form of MSI is found in tetranucleotide-based microsatellites and is labelled Elevated Microsatellite Alterations at Selected Tetranucleotides or EMAST^{104, 105}. While MSI with repetitive mono- and dinucleotides has been extensively investigated, less is known about EMAST. Currently, the prognostic value, molecular mechanisms and clinical implications of EMAST are unclear. Thus, there are no consensus guidelines regarding EMAST. In CRC, EMAST is more often found in elderly and female patients and tumours of the proximal colon. It is associated with longer recurrence-free survival¹⁰⁶.

1.3.4 Diagnosis and treatment

CRC patients present with a wide range of symptoms. The most common symptoms are changes in bowel habits, occult or overt rectal bleeding, anaemia and abdominal pain. However, many patients are asymptomatic⁷⁷. In diagnosing CRC, colonoscopy is the reference standard¹⁰⁷. This examination allows for biopsy or even the removal of small lesions. In addition, computer tomography (CT) colonography is done, and in cases of rectum cancer, magnetic resonance imaging. CT scans of the liver and thorax are also performed following Norwegian national guidelines¹⁰². For advanced diseases, positron emission tomography (PET) may be performed. Measuring the tumour marker carcinoembryonic antigen in blood at the time of diagnosis is recommended¹⁰⁸. A high level of carcinoembryonic antigen is associated with a worse prognosis, and can be useful in monitoring the disease after surgery¹⁰⁹.

Surgical resection is the recommended treatment for patients with non-metastatic CRC. Tumour location, depth of invasion and vascular structure in the area determine the extent of the resection. For rectal cancer, total mesorectal excision is performed, either with or without preoperative radiotherapy. In patients with metastatic disease in the liver or lung, curative resection of metastases might be possible. Other options include microwave ablation or stereotactic radiotherapy of the metastases. More

options are becoming available, notably personalised treatment like immunotherapy in patients with MSI-high tumours or epidermal growth factor receptor inhibitors¹⁰². For patients with non-curative disease, palliative surgery might be an option. Depending on the disease stage, patients might be offered radiotherapy or systemic chemotherapy following primary surgery or as a primary treatment in a palliative setting^{77, 102}.

1.3.5 Histopathology and staging

Pathology staging is done using the tumour-node-metastasis (TNM) system (**Figure 10**)¹¹⁰, American Joint Committee on Cancer (AJCC) 8th edition. The TNM system compiles information of importance to the patient's prognosis. A standardised gross pathology and microscopic histopathology template is used for reporting relevant findings and stages. The pathologist's evaluation of the resected specimen provides information necessary in deciding which patients are eligible for adjuvant treatment, as this depends on whether there is metastasis to the lymph nodes or distant metastasis¹¹⁰. We used the AJCC 7th edition for **Paper I**, and for **Paper II**, we used the AJCC 8th edition (**Figure 11**). Minor changes were made in the TNM classification from the 7th to the 8th edition, with an expansion of the M category, as M1c was added for peritoneal metastasis¹¹¹. Peritoneal metastasis was previously encompassed in M1b. The AJCC 8th edition offers a personalised approach to diagnosing and treating CRC, including the use of molecular markers for somatic and germline mutations leading to mismatch repair deficiency or microsatellite instability and RAS/RAF pathway mutations, such as KRAS, NRAS and BRAF^{110, 111}.

Tumour-Node-Metastasis (TNM)

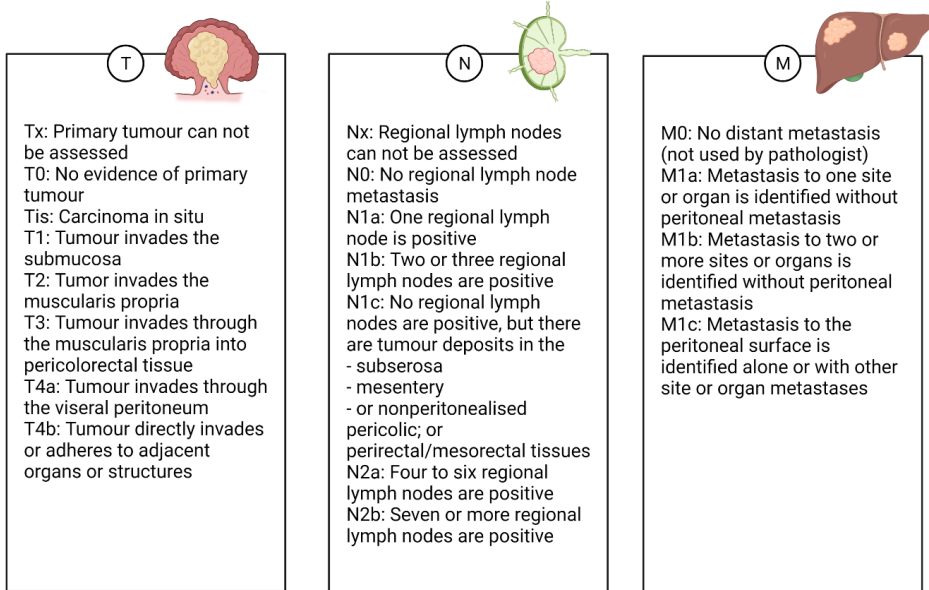


Figure 10: Tumour-node-metastasis (TNM) classification of colorectal cancer. Used with permission of the American College of Surgeons, Chicago, Illinois. The source of this information is the American Joint Committee on Cancer (AJCC) Cancer Staging System (2020)¹¹⁰. Created with BioRender.com.

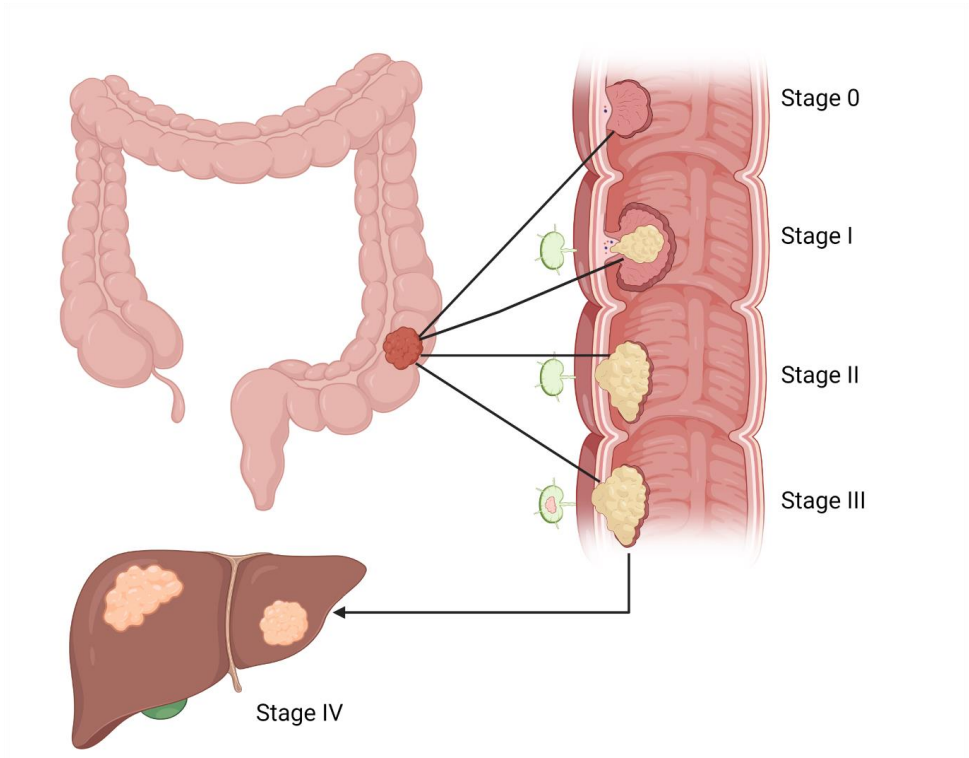


Figure 11: American Joint Committee on Cancer (AJCC) Colorectal Cancer Staging, 8th edition¹¹⁰. Used with permission of the American College of Surgeons, Chicago and Illinois. The source of this information is the AJCC Cancer Staging System (2020). Created with BioRender.com.

According to the latest WHO classification¹¹², several histopathological parameters are recommended in the pathology report. These are tumour size and location, histological subtype, tumour grade, depth of invasion, presence of lymphatic and/or vascular infiltration, perineural growth, lymph node status, tumour budding^{113, 114}, resection margins, presence of treatment response if neoadjuvant therapy, MSI-status, immune response and presence or absence of relevant mutations¹¹². **Figure 12** shows a photo of a surgical specimen with the corresponding histological image.

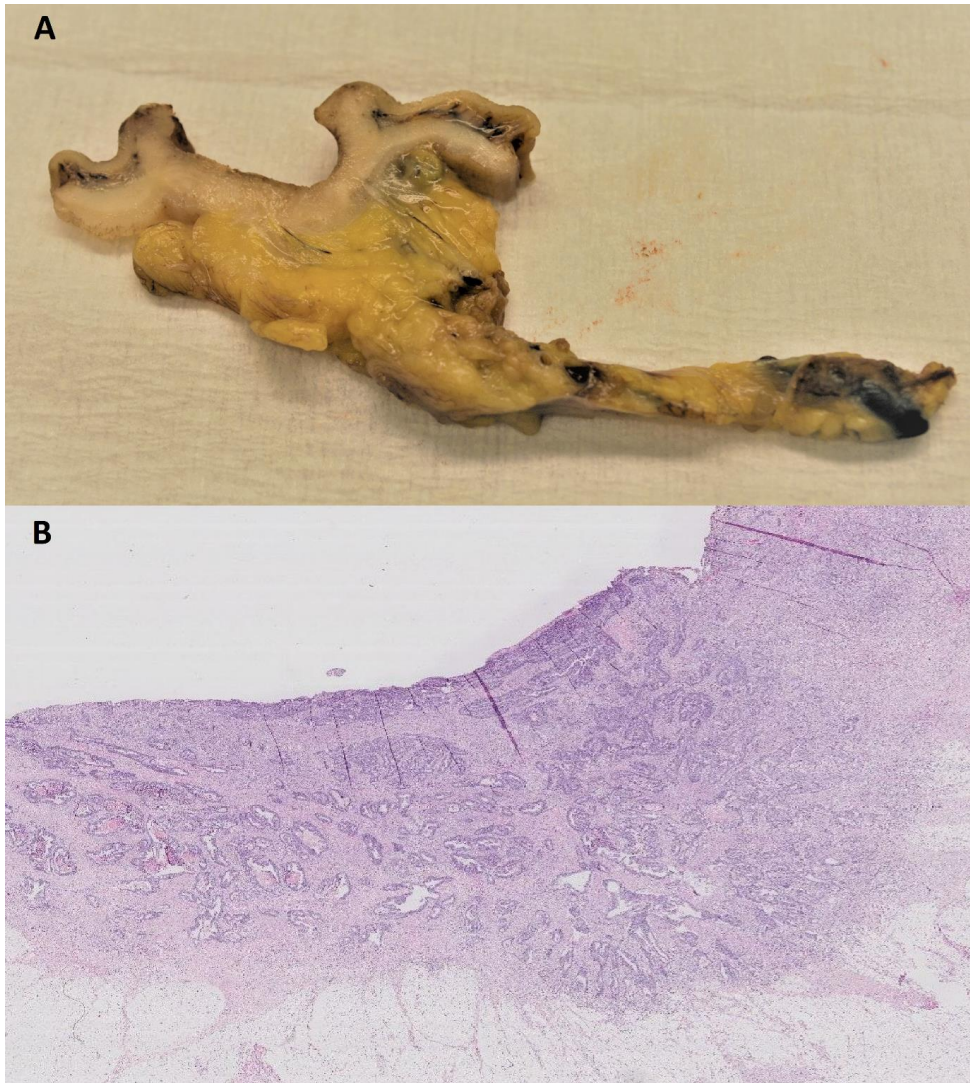


Figure 12: A: Cross sections through a colon cancer specimen. B: Haematoxylin and eosin staining x11.5 of the same tumour as A, showing an invasive adenocarcinoma. In both images, you can see tumour infiltration through the muscularis propria and into pericolic tissue. This is classified as a T3 tumour, according to the Tumour-Node-Metastasis system.

Challenges of the TNM system

The TNM system¹¹⁰ is the most widely used staging system for CRC. It is easy to use and allows for a fairly accurate estimation of prognosis^{115, 116}. However, the TNM system is imperfect in defining appropriate subgroups of patients and guiding treatment beyond surgical resection¹¹⁷. The TNM-system does not permit discrimination between ‘good’ and ‘bad’ cancers within the same stage. In fact, up to 20% of stage II patients may still die of recurrent disease¹¹⁸. For stage III patients, about half of the patients are cured by surgery alone, and about 20% benefit from adjuvant therapy¹¹⁹. The TNM system largely leaves the decision of adjuvant treatment up to lymph node status. Consequently, due to the current guidelines for adjuvant chemotherapy, there is a risk of under- and overtreatment of patients^{120, 121}.

Concerns have been raised regarding updates in the newest editions of the TNM-system. Critiques claim that existing system elements are not evidence-based and question making changes without a basis in systematic empirical investigation^{122, 123}. Specifically, they question keeping the subdivision of T4 into T4a (invasion of visceral peritoneum) and T4b (invasion of adherent structures and/or organs), as studies have not confirmed a difference in outcome between these two¹²⁴.

The definition of tumour deposits has been altered several times, as new editions of the TNM classification have been published. The reason for this is criticism regarding the use of unpublished data and difficulties in understanding the definition¹²⁵. Thus, pathologists use different versions of the TNM-classification¹²⁶. This reduces validity and hampers comparison of results across regions, as patients may be down-/up-staged according to the variation in definitions. The challenges of the TNM system illustrate the need for other prognostic markers to better determine optimal treatment of CRC in the future.

1.3.6 Prognosis and prediction

Based on figures from the Cancer Registry of Norway, the five-year relative survival rate for colon cancer is 69.4% for men and 71.3% for women, and the corresponding figures for rectum cancer are 71.4% and 72.4%, respectively⁵⁴. Thus, during the last five years, CRC survival rates have increased slightly for both men and women⁵⁴. In Europe, decreasing mortality rates for CRC has been ascribed to reduced prevalence of risk factors and/or improved treatment¹²⁷. In addition, CRC screening has had an effect in some countries^{74, 128} but has not yet been generally established in Norway.

In addition to the TNM system and histopathological parameters, there are several other predictive biomarkers in CRC, including the ras-genes and BRAF. Mutations in the ras-genes (HRAS, NRAS and KRAS) are found in about 30% of human cancers¹²⁹. For primary colon cancer, KRAS is found in about 32%, NRAS in about 3% and BRAF in about 14% of the cases¹²⁹. About half of the patients with metastatic CRC have mutations in KRAS and NRAS. This excludes them from receiving epidermal growth factor receptor directed therapy¹³⁰. BRAF mutation is found in about 7–8% of patients with metastatic CRC^{130, 131}. Mutations in either KRAS or BRAF are associated with reduced progression-free survival and overall survival¹³². For NRAS, the data is sparser, but a meta-analysis indicates that NRAS is associated with poor overall survival, especially in western countries¹³³. There have been clinical trials with BRAF inhibitors, either alone or in combination with other therapies, but the results have been quite disappointing¹³⁴.

MSI status is another predictive biomarker. About 3–5% of patients with metastatic CRC have MSI-high tumour or deficient MMR proteins¹³⁵. Although MSI-high is a marker of less aggressive disease in a primary CRC^{136, 137}, the opposite is the case in metastatic CRC, where MSI-high is associated with a worse overall survival¹³⁸. MSI reduces the effect of fluorouracil-based chemotherapy^{139, 140}. In sporadic cases of MSI, approximately 40–60% have a BRAF mutation. Lynch syndrome is associated with wild type BRAF¹⁴¹. Both MSI and BRAF mutations in metastatic CRC are

independent markers of poor prognosis regarding progression-free survival and overall survival¹⁴².

The effect of immune check point inhibitors (ICI) in CRC is being investigated in several clinical trials, as studies have shown an effect on Programmed cell death 1/Programmed cell death ligand-1 and cytotoxic T-lymphocyte-associated protein-4 inhibition in MSI-high CRC^{135, 143, 144}. In Norway, MSI-high CRC can receive ICI as part of ongoing clinical trials¹⁰².

1.4 Neuroendocrine Neoplasms

1.4.1 Epidemiology and aetiology

Gastroenteropancreatic neuroendocrine neoplasms (GEP-NENs) belong to a heterogeneous family of rare epithelial neoplasms originating from the pancreas or the gastrointestinal tract. GEP-NENs include both neuroendocrine tumours (NET) and neuroendocrine carcinoma (NEC), with detrimental prognoses for most NEC patients¹⁴⁵. GEP-NENs are characterized by heterogeneous clinical patterns, a relatively indolent growth rate and the ability to secrete peptide hormones and biogenic amines¹⁴⁶⁻¹⁴⁸. GEP-NENs are divided into *functional* tumours (which secrete hormones or peptides, causing clinical symptoms or syndromes) and *nonfunctional* tumours.

Many patients with well-differentiated NENs, even those with advanced disease at the time of diagnosis, can survive for several years¹⁴⁹⁻¹⁵¹. Although rather rare, due to the low mortality rates, GEP-NENs are the most prevalent gastrointestinal malignancy, second to CRC¹⁴⁶. According to the international literature, the incidence of GEP-NENs is 2.39 per 100,000 inhabitants/year worldwide, and the prevalence is 35 per 100,000/year worldwide¹⁵². In Norway, the incidence is 5.83 per 100,000

inhabitants/year¹⁵³, which complies with recent reports from different regions, suggesting that the incidence is higher and increasing^{149, 154}. Increased awareness by clinicians and improved diagnostics, such as IHC and radiological imaging, may in part explain this increase¹⁵⁵. Five-year survival rates vary between 40–100% according to the tumour site and stage of disease^{156, 157}. Gastrointestinal NENs are more common in women with a median age of 57 years¹⁵⁸. About 13% of gastrointestinal NENs have metastasis at the time of diagnosis¹⁵⁹. The most common site for metastasis is the liver, followed by lung, bone and brain¹⁵⁸.

Most NEN is sporadic¹⁶⁰. However, some reports of NEN in the lower gastrointestinal tract are associated with hereditary colorectal syndromes, such as familial adenomatous polyposis and Lynch syndrome¹⁶¹. Furthermore, NET can be seen in the pancreas or gastrointestinal tract as a part of hereditary syndromes, such as multiple endocrine neoplasia type 1, von Hippel-Lindau syndrome, neurofibromatosis type 1 and tuberous sclerosis complex¹⁶². These hereditary syndromes usually involve the pancreas, but also the occurrence of NETs outside the gastrointestinal tract.

1.4.2 Pathogenesis

Neuroendocrine tumours as an entity were described in 1907 by Siegfried Oberndorfer (1876–1944). He described them as small tumours of the intestine and called them *Karzinoid Tumoren*, which means ‘cancer-like’. This term was used because of its indolent clinical behaviour¹⁶³. For many years, ‘carcinoid tumours’ has been the terminology for these tumours, but this is now outdated and not recommended¹¹².

NENs in the gastrointestinal tract originate from enterochromaffin cells and enterochromaffin-like cells¹⁶⁴. Pancreatic NENs are thought to develop in the islets of Langerhans¹⁴⁸, but alternative origins have also been suggested¹⁶⁵. NETs are

characterised by the high-density expression of somatostatin receptors, which modulate proliferation and protein synthesis in addition to hormone secretion. NEC, in contrast, have fewer somatostatin receptors¹⁴⁸.

The pathogenesis of NENs is not fully understood. The heterogeneity of these tumours, from indolent to highly aggressive, suggests that it is multifactorial. In the molecular pathogenesis of NET, aberrant activation of signalling by the mammalian target of rapamycin (mTOR) is a hallmark, regardless of the primary site¹⁴⁸ (**Figure 13**). mTOR modulates cell survival, proliferation, angiogenesis and metabolism. Mutations in the mTOR pathway are observed in approximately 15% of pancreatic NET^{166, 167}. In hereditary syndromes, such as tuberous sclerosis, which is associated with pancreatic NET, there are losses of function mutations in two tumour suppressor genes (TSC1 and TSC2) that inhibit mTOR¹⁶⁸. Phosphatase and tensin homolog (PTEN), which regulate mTOR activity through the Akt pathway, and TSC2 are downregulated in approximately 75% of pancreatic NETs, and their low expression is associated with shorter disease-free and overall survival¹⁶⁹. Studies of molecular pathways in NENs have shown high expression of proangiogenic molecules, such as angiogenic cytokine vascular endothelial growth factor¹⁷⁰. Several vascular endothelial growth factor inhibitors have shown clinical effects on some NENs, particularly in pancreas^{171, 172}.

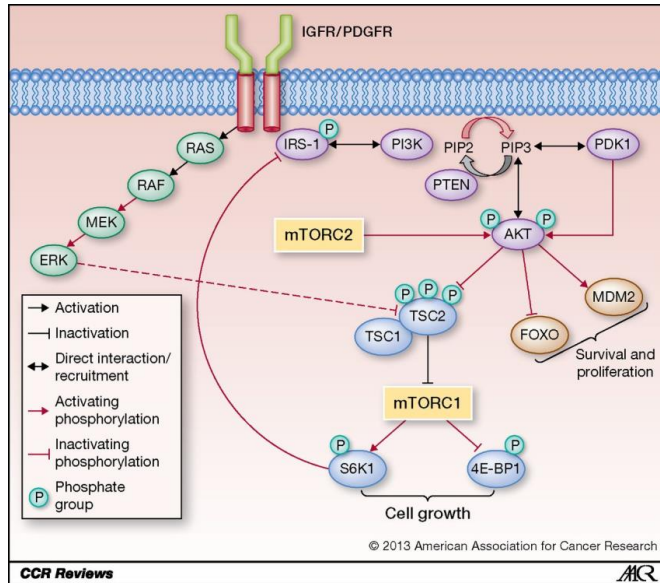


Figure 13: Schematic representation of the mammalian target of rapamycin (mTOR) pathway and associated regulatory circuitries. mTOR exists as two different complexes (mTORC1 and mTORC2) that are activated through different signalling cascades. Here is depicted the activation of mTORC1 by receptor tyrosine kinases–triggered signalling. Positive and feedback regulatory loops are also described. Abbreviations – PIP2: phosphatidylinositol (4,5)-bisphosphate, ERK: extracellular signal-regulated kinase, IGFR: insulin-like growth factor receptor, MEK: MAP–ERK kinase, PDGFR: platelet-derived growth factor receptor, PI3K: phosphoinositide 3-kinase, PIP2: phosphatidylinositol (4,5)-bisphosphate, PIP3: phosphatidylinositol (3,4,5)-triphosphate. Republished with permission from¹⁶⁸. Copyright© American Association for Cancer Research 2013.

1.4.3 Diagnosis and treatment

The clinical symptoms depend on the tumour localisation and stage of the disease. In some locations (i.e. appendix, rectum and stomach), a NEN is often an incidental finding. Patients with GEP-NENs may have general cancer-associated symptoms, including loss of appetite, unexpected or unintended weight loss and fatigue. In addition, there might be localised symptoms, such as pain or obstruction, depending on where in the body the tumour is located. Functional tumours usually lead to diarrhoea and facial flushing. The patient might also experience hyper-or

hypoglycaemia, gastric ulcers, skin rashes, wheezing, tachycardia or high blood pressure, determined by which hormone is produced. The combination of symptoms related to the release of serotonin is called carcinoid syndrome¹⁷³. About ¼ of patients with GEP-NENs have hormone hypersecretion symptoms¹⁷⁴. NEN in the distal colon and rectum or NEC is rarely associated with hormonal syndrome/carcinoid syndrome¹⁷⁵.

For diagnosing GEP-NENs, a biopsy of the tumour is recommended. In addition, biochemical markers such as serum-chromogranin A (CgA), are measured in blood. Serum-CgA is a predictor of outcome¹⁷⁶ and correlates with tumour progression or regression¹⁷⁷. Measuring other markers in blood such as gastrin, insulin, somatostatin and other endocrine markers is recommended, depending on tumour location¹⁷⁵. Several imaging techniques are also used. Multidetector CT and/or magnetic resonance imaging with intravenous contrast are usually performed¹⁷⁵. PET is increasingly used to gain information about functionality in tumours. Several tracers can be used for PET evaluations of NEN patients, including F-deoxyglucose (i.e. measures glucose metabolism in the tumours) of poorly differentiated NENs and Gallium-DOTATOC (i.e. detects one of the somatostatin receptors) in well-differentiated NENs. Somatostatin receptor imaging is used for tumour staging, monitoring tumour recurrence and evaluating eligibility for peptide receptor radionuclide therapy¹⁷⁸.

Surgery is the recommended treatment for NEN and should always be considered¹⁷⁵. While curative surgery is not always possible, even in advanced disease, debulking surgery is considered beneficial to ease symptoms from local large tumour masses and reduce tumour volumes to alleviate therapy-resistant and debilitating endocrine effects¹⁷⁹. However, even when surgery with curative intent is employed, several patients will eventually present with recurrent disease.

A better understanding of the biology of this disease and the development of novel diagnostic approaches and treatment options have increased the complexity of the clinical management of NENs^{148, 180}. Other therapies include chemotherapy in

advanced pancreatic NET, GEP-NET grade 3 and NEC¹⁷⁵. Somatostatin analogues are used as symptomatic and anti-proliferative treatment¹⁸¹. Patients with functional tumours might benefit from tryptophan hydroxylase inhibitors. Peptide receptor radionuclide therapy is used in inoperable or metastatic NEN with high tumour uptake on somatostatin receptor imaging. Several other molecular-targeted therapies are being introduced. Examples include an inhibitor of the mTOR pathway (Everolimus) and a tyrosine kinase inhibitor (Sunitinib) in pancreatic NEN¹⁷⁵.

1.4.4 Histopathology and staging

On histopathological examination, NET is a well-defined cellular tumour with uniform round to ovoid cells. The cytoplasm is amphophilic or eosinophilic. Nuclei are enlarged, often with a stippled salt-and-pepper-type pattern of the chromatin (**Figure 14A**). Tumour cells may have a nested, solid, trabecular or pseudoglandular growth pattern¹⁸². NECs, however, are poorly differentiated tumours and often show bleeding or necrosis and destruction of surrounding normal tissue (**Figure 15**)¹⁸².

The diagnosis is based on morphological features and a positive IHC staining for synaptophysin and/or CgA (**Figure 14BC**). Synaptophysin is a glycoprotein that occurs in the presynaptic vesicles of neurons and the small vesicles of normal and neoplastic neuroendocrine cells. CgA is one of several soluble proteins located in the matrix of the secretory granules of many neuroendocrine cells¹⁸³. The proliferation marker Ki67 is performed for grading¹¹². Different IHC markers might be used to indicate primary tumour sites, such as CDX2, for the gastrointestinal tract. IHC can also be used to detect endocrine production, such as gastrin or insulin, in functional tumours (**Figure 14D**).

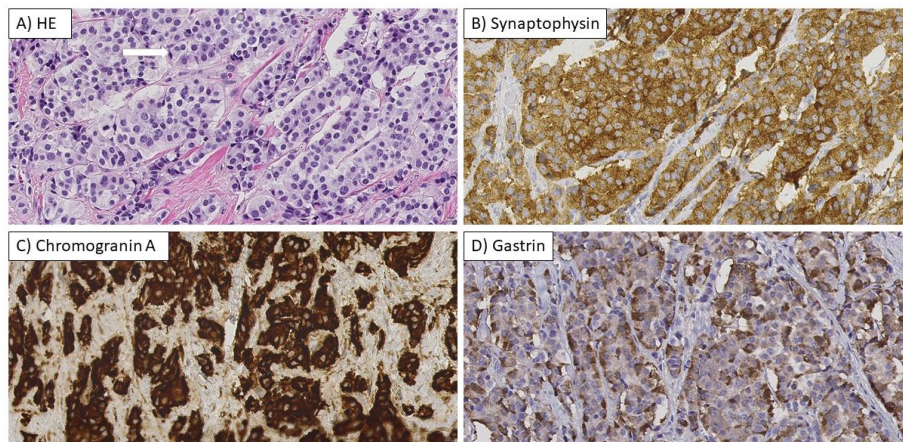


Figure 14: A) Haematoxylin and eosin (HE) staining of primary neuroendocrine tumour in pancreas x400. Arrow marks the nest of tumour cells. B) Positive immunohistochemical (IHC) staining of synaptophysin in tumour x400. C) Positive IHC staining of chromogranin A in tumour x400. D) Positive IHC staining of gastrin in tumour x400.

The nomenclature and classification of NENs have changed over the last decades. There is no uniform classification of morphology or grading that covers all anatomical sites. For example, the nomenclature of GEP-NENs and NEN in the lung are different¹⁸⁴. NEN was grouped into three categories in the 2000 WHO classification: well-differentiated endocrine tumours, well-differentiated endocrine carcinomas and poorly-differentiated carcinomas¹⁸⁵. In 2006, the European Neuroendocrine Tumour Society (ENETS) proposed a new classification of GEP-NENs based on mitotic count and Ki67 index¹⁸⁶. This was adapted and modified in the WHO grading system (2019) for GEP-NET, which is in use today¹¹².

Grading is based on mitotic activity, estimated either by counting mitosis on HE-stained slides or by calculating the percentage of Ki67-positive cells in a hot spot (**Table 2**)^{112, 187}. In the case of discordance between the two, the highest grade should be applied¹¹². It has, however, been shown that the Ki67 index more accurately predicts prognosis than mitotic count¹⁸⁸.

	Grade	Mitotic count, per 2 mm ² *	Ki-67%*
NET Grade 1	Low	1	< 3
NET Grade 2	Intermediate	2–20	3–20
NET Grade 3	High	> 20	> 20
LCNEC	High [†]	> 20	> 20
SCNEC	High [†]	> 20	> 20
MiNEN	Variable	Variable	Variable

LCNEC: Large-cell neuroendocrine carcinoma, MiNEN: Mixed neuroendocrine–non-neuroendocrine neoplasm, NEC: Neuroendocrine carcinoma, NET: Neuroendocrine tumour, and SCNEC: Small-cell neuroendocrine carcinoma

* Mitotic rates are expressed as the number of mitoses/2 mm² as determined by counting in 50 fields of 0.2 mm² (i.e. in a total area of 10 mm²); the Ki67 proliferation index value is determined by counting at least 500 cells in the regions of highest labelling (hot spots), which are identified at scanning magnification.

[†] Poorly differentiated NECs are not formally graded but are considered high-grade by definition.

Table 2: Grading of gastroenteropancreatic neuroendocrine neoplasms according to World Health Organization (2019)¹¹².

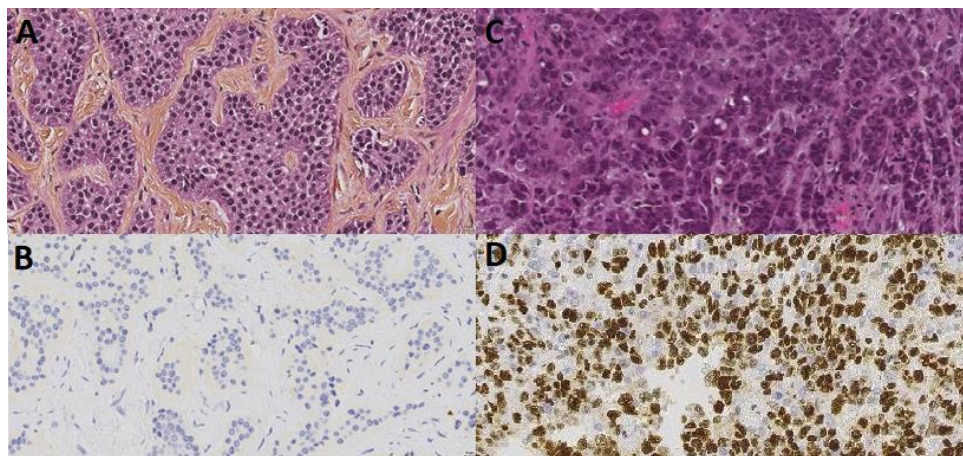


Figure 15: Neuroendocrine tumour grade 1 (A) and large cell neuroendocrine carcinoma grade 3 (B) and immunohistochemical staining of the proliferation marker Ki67 in the same tumours (C and D).

NET grade 3 and NEC can be difficult to discriminate from one another, and additional analyses may be helpful¹⁸⁹. Genetic alterations in tumour protein 53 and/or Retinoblastoma protein 1 are frequently seen in poorly differentiated NENs and can

be demonstrated by IHC¹⁹⁰. Analysis of mutations in BRAF might be an option in selected cases when BRAF/MEK inhibitor treatment is considered¹⁷⁵.

Staging is done according to the AJCC 8th edition¹¹⁰. The staging of NET (grades 1 to 3) depends on the primary organ. NEC and MiNEN are staged as primary carcinomas in their respective primary organs^{110, 112}.

Challenges with grading

Grading poses several challenges for the pathologist. Mitotic count is time consuming, and it is often difficult to identify mitosis in tumour cells^{191, 192}. In addition, it requires 10 mm² of tumour tissue, which makes it less convenient for biopsies^{74, 112}. For Ki67, controversies exist regarding what to count and how to do the count¹⁹³. Several methods have been proposed. A study by Tang and co-workers recommended either doing a manual count of 2000 cells or using digital image analysis¹⁵. Another study recommended counting at a camera captured or printed picture¹⁴. For Ki67, counting > 500 – 2000 cells is time-consuming, which may lead to an eyeball estimate as a shortcut in a busy routine practice¹⁵. In addition, the identification of a ‘hot spot’ in a section is sometimes difficult¹³. These difficulties may partly explain the reported poor intra-and inter-observer reliability of grading¹⁵. Furthermore, since the WHO defined NET grade 3 as a distinct entity, the challenge of differentiating between NET grade 3 and NEC has presented itself. There is no cut-off proliferation value to separate these two entities, as Ki-67 values are overlapping. Also, follow-up data on both are sparse¹⁹⁴ (**Figure 16**).

Tumour heterogeneity and the fact that different locations have different prognoses is another challenging issue¹¹⁰, as this makes it difficult to compare grading between different organs and to ensure correct treatment for these patients.

Differences in procedures for fixation and processing of the tissue and IHC of Ki67 may lead to differences in grading between laboratories¹⁹⁵. While automated IHC

staining is recommended, this option is not available at all laboratories.

Standardisation of protocols, such as external quality control, may help improve staining quality and reproducibility^{192, 196}.

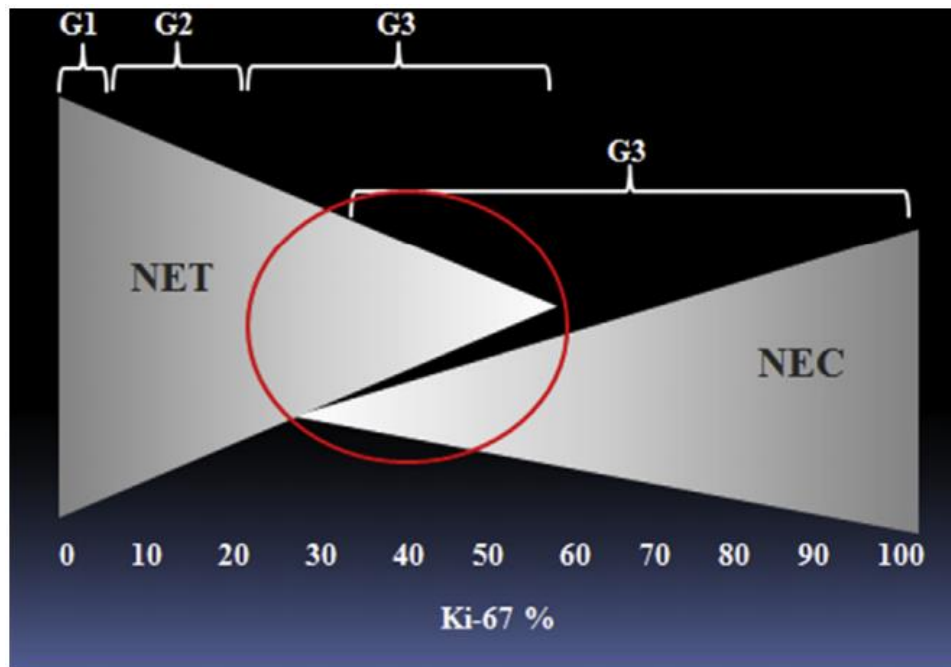


Figure 16: Neuroendocrine neoplasms' separation according to grade, Ki-67 and morphology. The red circle shows the overlap in the Ki-67 index between neuroendocrine tumour (NET) grade 3 and neuroendocrine carcinoma (NEC). Republished with permission from¹⁹⁴. Copyright© Elsevier Science & Technology Journals 2018.

1.4.5 Prognosis and predication

There is no national cancer statistics registry specifically for GEP-NENs in Norway. Existing statistics are often deficient because only malignant tumours are registered, and NEN outside the gastrointestinal tract are registered together with GEP-NENs. A Norwegian study, based on data from the period 1993 to 2015 in the Cancer Registry of Norway, found that the 5-year relative survival rate in patients with low/intermediate aggressive NENs was 64.8% (95% CI, 63.3–66.2). In patients with

highly aggressive NENs, the rate was 8.4% (95% CI, 7.8–9.1). In the same study, multivariable analysis showed that gender, age and stage at the time of diagnosis and primary site were all predictors of outcome, independent of grade. In addition, survival improved significantly during the period¹⁴⁵. However, the study included all organs in the body. The primary location in the lung was the most common tumour site. This might hamper the interpretation of the results.

A recent study based on data from the Southwestern region of Norway showed a median overall survival of 183 months for GEP-NENs, with 5- and 10-year survival rates of 66% and 57%, respectively. The significant determinants of overall survival were age, WHO tumour grade and surgery as primary treatment¹⁹⁷. The same study found that the occurrence of different WHO grades varied between different organs. For example, grade 3 tumours were more commonly found in the stomach, pancreas, colon and rectum. Other population-based studies have demonstrated that sex, tumour differentiation, stage and primary site were independent predictors of overall survival^{149, 150}, but these studies also included tumour locations outside of the gastrointestinal-pancreatic area.

Since prognosis depends on grade and location, survival data vary significantly between organs. The five-year survival of GEP-NET is directly related to the restriction of the disease (i.e. primary tumour) and the occurrence of (distant) metastases: 96% (localised), 77% (nodal), 73% (liver) and 50% (extrahepatic metastases)¹⁹⁸. For the appendix, most tumours are grade 1 and < 1 cm in size. In this group, the 5-year survival rate is close to 100%, while for patients with metastatic NEC, it is less than 10%¹⁷⁵.

The prognostic relevance of tumour grading was first proposed in Europe¹⁹⁹ and eventually embraced by clinicians worldwide²⁰⁰⁻²⁰². Tumour grade may also serve as a predictive factor in selecting GEP-NEN patients for chemotherapy²⁰², particularly in cases with a well-differentiated morphology despite a high Ki67 index (>55%)²⁰³. NET does not progress to NEC¹⁸², but NET can have a NEC component¹⁹⁰.

As mentioned, serum CgA is an important prognostic marker and marker of tumour progression. It may also be a predictive indicator of progression-free survival and overall survival²⁰⁴. However, serum CgA is only elevated in about 50–70% of NEN patients, and there are few prospective studies on serum CgA in NEN patients²⁰⁵.

The role of other emerging biomarkers is not determined, including the tumour mutational burden or programmed cell death ligand 1 expression in exploring the possibilities for immunotherapy^{206, 207} or treatment options targeting different somatic and germline mutations, especially in the mTOR pathway¹⁶⁶. Biomarker panels in liquid biopsies, such as NETest™, are another interesting emerging possibility²⁰⁸.

1.5 Cancer and the immune system

In 1863, Rudolf Virchow deduced leucocytes in neoplastic tissues and connected inflammation and cancer. Virchow suggested that the ‘lymphoreticular infiltrate’ reflected the origin of cancer at sites of chronic inflammation²⁰⁹. We now know that cancer-related inflammation plays a key role as a contributor to cancer progression, both in the tumour microenvironment and the induction of genetic instability and has been described as the seventh hallmark of cancer²¹⁰. Inflammation is now included in the ‘Next generation of Hallmarks of cancer’⁶².

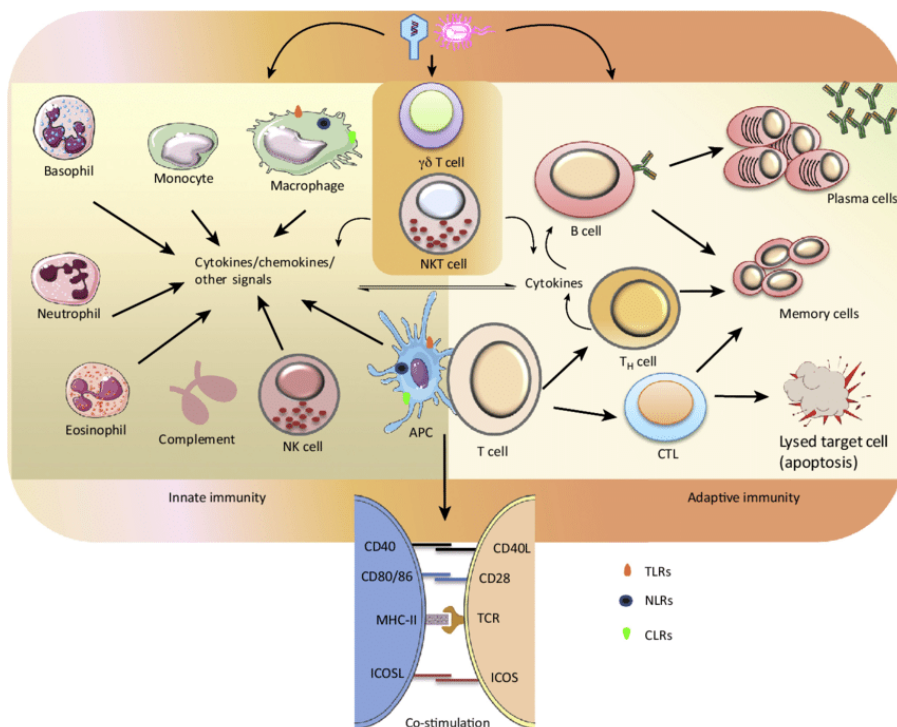
Globally, about 1/4 of cancers are related to infection and chronic inflammation²¹¹. Out of these, it is estimated that 1/8 are directly caused by infection and the resulting inflammation²¹². Examples are *Helicobacter pylori* as a cause of gastric cancer and the human papillomavirus in developing cervical cancer²⁰⁹. The rest are due to other causes of chronic inflammation, such as chemical, physical or autoimmune disease^{213, 214}.

The immune system comprises two parts: the *innate* and the *adaptive* or *acquired* immune system. The innate immune system is ‘what we are born with’ and is at the

front line of defence. Evolutionary, this is an older defence mechanism than the adaptive immune system, which is more specialised. However, both systems contribute to the destruction of pathogens using both humoral immunity components and cell-mediated immunity (**Figure 17**).

The innate immune system uses toll-like receptors to recognise pathogens. Most of the cells in the innate immune system are derived from multipotent stem cells in the bone marrow and perform phagocytosis. These cells express 'self-proteins' on their surface, along with major histocompatibility complex (MHC) class I, thus helping other components of the immune system discriminate 'self' from 'not-self'. The innate immune system also has antigen-presenting cells with MHC class I or II, presenting protein antigens to adaptive immune cells. In addition, some antigen-presenting cells, such as dendritic and B-cells, contain MHC classes I and II on their cell surface⁶³.

The adaptive immune system relies on the recognition of antigens and the activation of T-cells or B-cell production of antibodies²¹⁵. T-cells enable the immune system to recognize foreign antigens through an interaction between their T-cell receptors and peptide epitopes presented by MHC class I molecules on cancer cells. This activation requires the co-stimulation of a CD28²¹⁶. B-cells modulate immune response and inflammation through antibody production and promote T-cell activation and proliferation through antigen presentation²¹⁷. B-cells also produce different pro-inflammatory cytokines and promote co-stimulation and the activation of other types of immune cells²¹⁸.



Trends in Pharmacological Sciences

Figure 17. Innate and Adaptive Immune Systems. The innate immune system provides a nonspecific response against invading pathogens. This response is mediated by various immune cells (granulocytes, monocytes, macrophages, dendritic cells, neutrophils, basophils and natural killer cells), and active molecules as proteins of the complement cascade) through the recognition of pathogens. The innate immune response shapes adaptive immunity, resulting in the production of antigen-specific T and B lymphocytes. Abbreviations – APCs: antigen-presenting cells, CD: cluster of differentiation, CLRs: C-type lectin receptors, CTL: cytotoxic lymphocytes, ICOS: inducible T-cell costimulatory, MHC: major histocompatibility complex, NKT: natural killer T-cells, NLRs: nucleotide-binding, oligomerization domain (NOD)-like receptors, TCR: T-cell receptor, TLRs: Toll-like receptors. Adapted with permission from²¹⁹. Copyright© Cell Press 2017.

The immune system protects the organism from harmful endogenous and exogenous events. For instance, inflammation is a normal response to infection and is also part of the wound-healing process after an injury. The inflammatory process releases different chemical mediators, such as cytokines, to recruit immune cells and growth factors, stimulating tissue growth and neovascularisation. This is something cancer cells take advantage of²²⁰. The inflammatory cells are part of the tumour microenvironment, which surrounds the tumour cells. The tumour microenvironment

harbours different components, such as extracellular matrix, blood and lymphatic vessels and several cell types, including fibroblasts and immune cells, such as neutrophils, lymphocytes, natural killer cells, tumour-associated macrophages and dendritic (antigen-presenting) cells²²¹. Thus, there is a complex interaction between immune cells and cancer cells in the tumour microenvironment, and tumour microenvironment-associated cells play an important part in tumour development and growth (**Figure 18**)⁶².

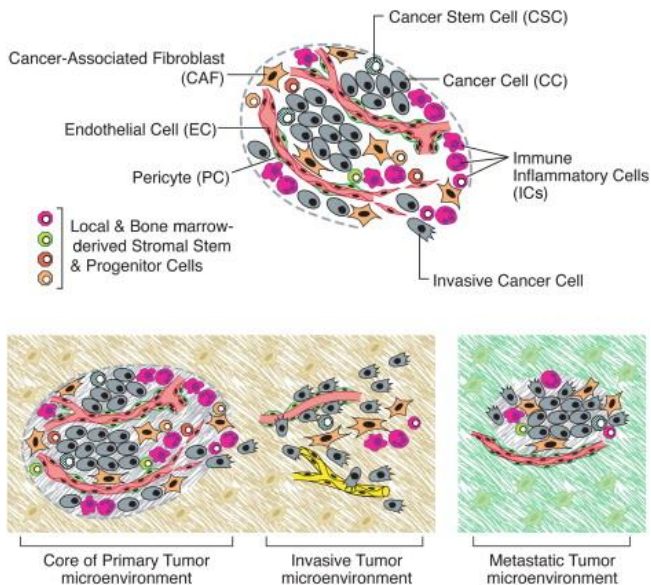


Figure 18: Cells in the tumour microenvironment. Reprinted with permission from ⁶² Copyright © 2011 Elsevier Inc.

The immune system can work as both an agonist and an antagonist in cancer development and progression (**Figure 19**). First, the immune system recognises tumour antigens on the surface of cancer cells or from antigen-presenting cells. This initiates an immune response. Tumour-promoting inflammatory cells include macrophages (several subtypes), mast cells, neutrophils and T- and B-cells. These cell types produce several signal molecules that mediate their tumour-promoting effects, such as tumour growth factor, angiogenic growth factor, chemokines and

cytokines. Tumour-promoting inflammatory cells also produce proangiogenic and/or proinvasive matrix-degrading enzymes, which may help the cancer cells to proliferate, invade normal tissue and metastasise⁶². On the antagonist side, the innate immune system induces antibody-induced complement-mediated lysis²²². The adaptive immune system induces an anti-tumour response, activating both cytotoxic T-cells that can kill the cancer cells and B-cells, producing antibodies directed against the cancer cells. Tumour-associated macrophages can have antagonistic and agonistic effects. They can kill tumour cells but may also produce growth factors and protease enzymes, which can stimulate tumour cell proliferation²⁰⁹.

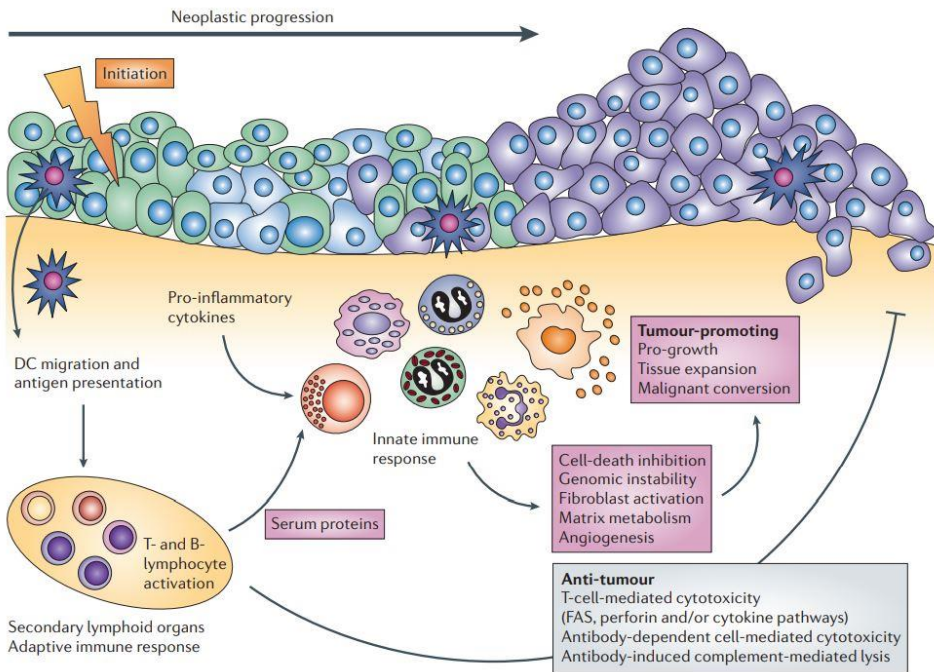


Figure 19: A model of innate and adaptive immune cell functions during inflammation-associated cancer development. Antigens that are present in early neoplastic tissues are transported to lymphoid organs by dendritic cells (DCs) that activate adaptive immune responses, resulting in both tumour-promoting and anti-tumour effects. The pathways that regulate DC trafficking during early cancer development and the exact nature of the antigen(s) remain to be established. Activation of B cells and humoral immune responses results in chronic activation of innate immune cells in neoplastic tissues. Activated innate immune cells, such as

mast cells, granulocytes and macrophages, promote tumour development by the release of potent pro-survival soluble molecules that modulate gene-expression programmes in initiated neoplastic cells, culminating in altered cell-cycle progression and increased survival. Inflammatory cells positively influence tissue remodelling and the development of the angiogenic vasculature by producing proangiogenic mediators and extracellular proteases. Tissues in which these pathways are chronically engaged exhibit an increased risk of tumour development. In contrast, activation of adaptive immunity also elicits anti-tumour responses through T-cell-mediated toxicity (by induction of FAS, perforin and/or cytokine pathways) in addition to antibody-dependent cell-mediated cytotoxicity and antibody-induced complement-mediated lysis. Adapted with permission from²²². Copyright© Springer Nature 2006.

1.5.1 The immune system in colorectal cancer

Over the last few decades, great efforts have been made to investigate how immune response affects progression and prognosis in CRC. Pronounced lymphocytic or inflammatory cell infiltrate in and around the tumour is associated with an improved prognosis in primary resectable CRC^{223, 224} and reduces disease progression and metastatic potential²²⁵. Especially, the T-cell response plays a significant role in this respect^{226, 227}. For example, Galon and co-workers showed that CRC patients with a high number of CD3+ cells (T-cells) and CD45RO+ (Memory T-cells) in tumours had a better prognosis compared to patients with a low number, independent of TNM stage²²⁶. In contrast, chronic inflammation and the presence of anti-inflammatory macrophages favour tumour growth and the spreading of cancer²²⁸. Another study found that low densities of CD68+ (macrophage lineage) and CD57+ (T-cells/natural killer cells) were independent prognostic markers, regardless of stage (stage II–III), in patients with CRC²²⁹.

MSI-high cancers have a better prognosis. However, they also have a distinct histopathological growth pattern and prominent inflammation, with tumour-infiltrating lymphocytes (**Figure 20**)²³⁰. The mechanism for this is believed to be mutations in mismatch repair (MMR) genes, leading to high levels of MSI. This results in a higher mutational burden, which correlates with increased expression of neoantigens on MHC-I molecules, in turn leading to an increased immune response (**Figure 21**)²³¹.

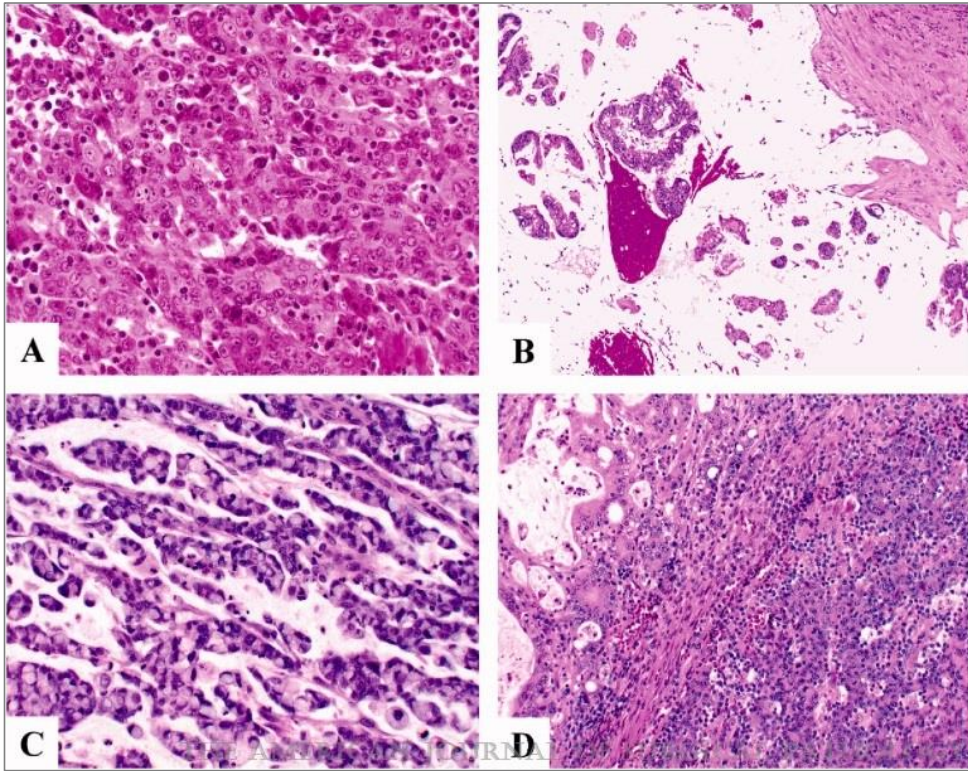


Figure 20: Various morphologic features associated with microsatellite instable cancer (MSI-high). A) Medullary-type carcinoma showing nests and cords of cells with pink cytoplasm, vesicular nuclei, and prominent nucleoli (note apparent tumour infiltrating lymphocytes). B) Mucinous carcinoma with abundant extracellular mucin and free-floating carcinoma cells. C) Signet-ring cells. D) Histologic heterogeneity with a distinct mucinous component abutting a poorly differentiated carcinoma component. Republished with permission from²³⁰. Copyright© Wolters Kluwer Health, Inc 2003.

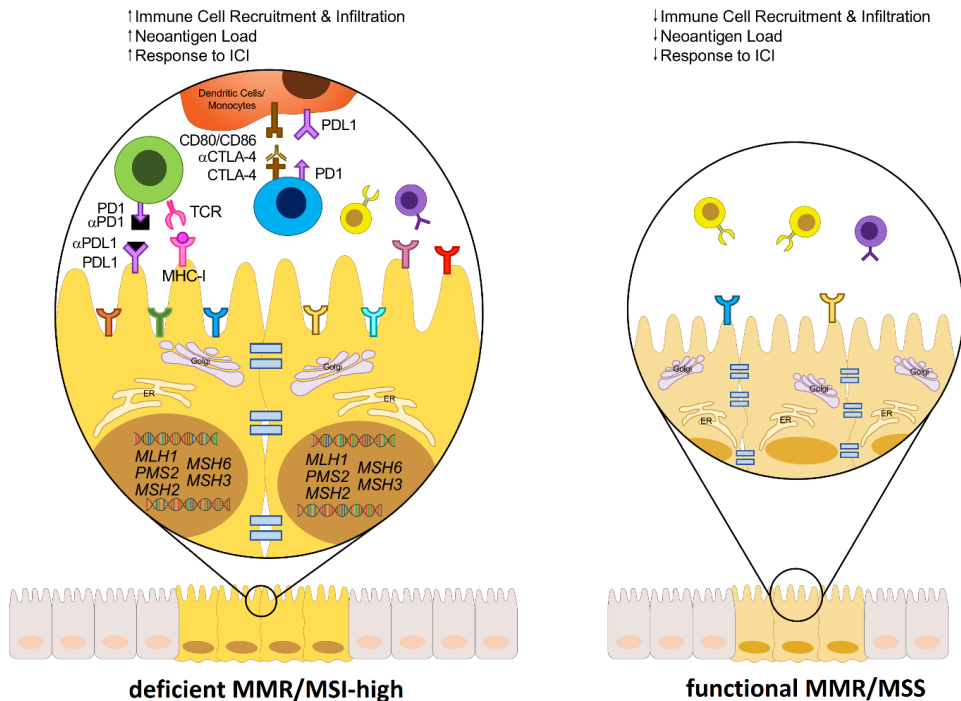


Figure 21. The immune landscape of microsatellite instable (MSI) and microsatellite stable (MSS) cancer. The DNA mismatch repair (MMR) system relies on key genes, such as MLH1, MSH2, MSH6, PMS2 or MSH3, that correct mismatched or wrongly inserted or deleted bases in the DNA. If this machinery fails due to defects in one or more repair genes, these errors are free to be integrated into the DNA permanently, forming microsatellites. Thus, deficient MMR/MSI-high tumours have a defect in one of the major DNA repair genes, resulting in high levels of microsatellites (MSI-high). However, tumours with a functional MMR system result in low or stable levels of microsatellites (MSS). The result of this damaged repair system in deficient MMR/MSI-high tumours is a higher mutational burden, which correlates with a higher expression of neoantigens on MHC-I molecules. Adapted with permission from²³¹ under Creative Commons Attribution (CC BY) licence. Copyright© MDPI 2020.

Immunotherapy

Immunotherapy, particularly ICI, has revolutionized cancer treatment²³². Although the response rate to ICI is only about 10–20% in different cancers, those who respond usually have an enduring response²³³. ICI inhibits negative regulatory receptors on T-cells, such as cytotoxic T lymphocyte antigen 4 and programmed cell death 1. This

results in a boosting of anti-tumour immune responses²¹⁶. Several factors influence tumour response to immune checkpoint inhibitors, for example, mutational load, MHC, tumour infiltrating lymphocytes and regulatory checkpoint receptors²³¹. Tumours with high mutational burdens, such as non-small cell lung cancer and melanomas, respond better to ICI. For stage IV CRC, patients with MSI-high tumours have been shown to benefit from immunotherapy. These cancers have a high mutational burden and respond to ICI²³¹. Thus, so far, not many CRC patients have been eligible for this treatment²³⁴. Although MSS CRC generally does not respond to ICI, some patients may still respond to this therapy²³⁵. Studies have shown that MSS CRC with a high T-cell infiltrate in tumours has a better prognosis^{236, 237}. Further studies are required to determine whether some of these patients are candidates for ICI²³¹.

1.5.2 Immunoscore

In exploring the role of T-cells in CRC as a diagnostic tool for evaluating immune reactions, the Immunoscore was developed by Galon and coworkers²³⁸. Two populations of lymphocytes (either CD3/CD45RO, CD3/CD8 or CD8/CD45RO), in the core of the tumour and at the invasive margin, are visualised using IHC. The slides were analysed by digital pathology. Based on the number of positive cells, a score between 0 and 4 was calculated (**Figure 22**). A high score (I4) equals a strong immune reaction²³⁸. They found that CRC patients with high densities of CD8+ and CD45RO+ T-cells (high Immunoscore) in tumours had a 5-year survival rate of 86.2%. Those with low densities had a 5-year survival rate of only 27.5%²³⁹. The method has been validated for colon cancer in an international consortium (14 centres in 13 different countries), which found that the Immunoscore association with time to recurrence was independent of existing prognostic factors and patient age, sex, T- and N-stage and MSI status²³⁷. Immunoscore is not validated for rectal cancer, but it might be a prognostic tool in patients with rectal cancer treated with primary surgery²³⁶. It has been suggested to implement the Immunoscore in a TNM-Immune

classification system for CRC^{237, 240}. Initially, there was a scoring system of five categories, but in the validation study, this was reduced to three: low, intermediate and high²³⁷. The prognostic value of the Immunoscore might also be relevant in other types of cancer^{241, 242}. The method has been patented and is now commercially available as Immunoscore® (HalioDx, Marseille, France)²³⁷. A validated, non-commercial, method for scoring immune response is therefore lacking.

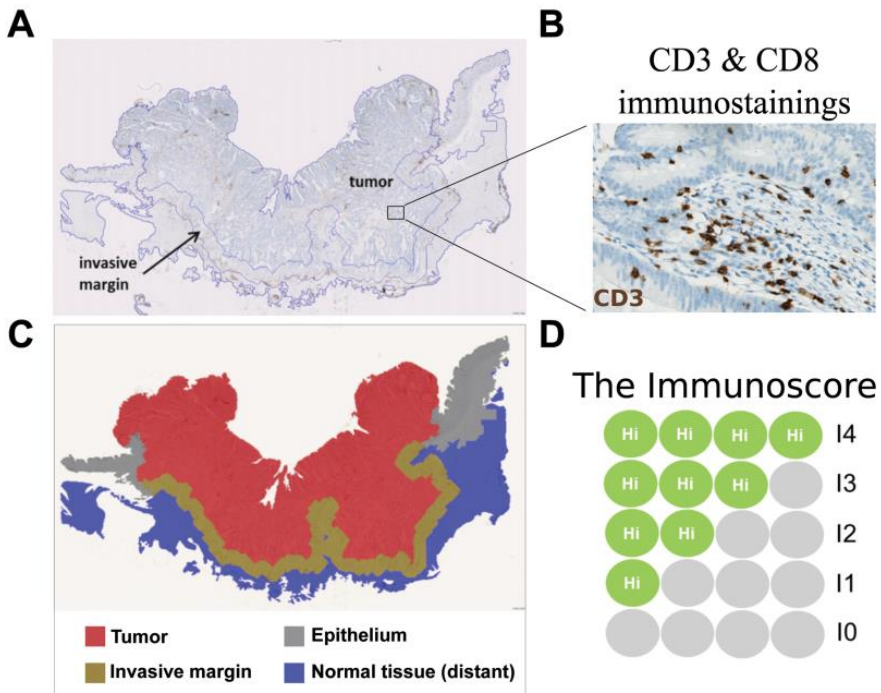


Figure 22: (A) A section of colonic cancer immunostained for CD3, showing the regions of interest (the tumour and the invasive margin). (B) An enlargement showing CD3⁺ cells (stained brown) in the stroma and within the tumour glands (original magnification $\times 300$). (C) The tumour (shown in red) and the invasive margin (shown in brown) were selected to determine the Immunoscore. (D) The Immunoscore is based on the numeration of CD3⁺ and CD8⁺ cells in the tumour and the invasive margin. The densities of the stained cells were determined using an image analysis workstation. According to a predetermined cut-off value, the immune densities are categorized as Hi (high) or Lo (low) in each tumour region. Patients are stratified according to a score ranging from 10 to 14, depending on the total number of high densities observed (the two markers CD3 and CD8 are assessed in the tumour, and the two markers are assessed in the invasive margin). Abbreviations: CD: Cluster of differentiation. Reprinted with permission from²⁴³. Copyright© Oxford University Press 2016.

1.6 Proliferation in cancer cells

Proliferation is the most essential feature of cancer development. The ability of cancer cells to sustain proliferative signalling, evade growth suppressors, resist cell death and enable replicative immortality is evident in the *Hallmarks of cancer*, as mentioned above^{61, 62}. Cell proliferation is a complex and carefully regulated process with an intrinsic quality control system²⁴⁴, dependant on interaction with the surrounding cells/environment and stimulation of growth factors. When this process gets out of control, cells avoid the intrinsic control system in the body, and cancer may develop. Cancer cells often establish autocrine proliferation stimulation as well⁶².

Cell proliferation occurs in a multistep process called the cell cycle, which comprises several phases. The cells' resting phase are called G0. The active part of the cell cycle starts with G1, where the cells grow and prepare for DNA synthesis. The S-phase is when the DNA replication occurs. The S-phase is followed by the G2-phase, where the cells continue to grow and prepare for mitosis, with DNA maintained at double copies. The final phase is mitosis, the M-phase, where the division into two cells occurs. The M-phase is divided into several sub-stages, see **Figure 23**. Together, G1, S and G2 are called the interphase. The interphase constitutes the largest part of the cell cycle²⁴⁵.

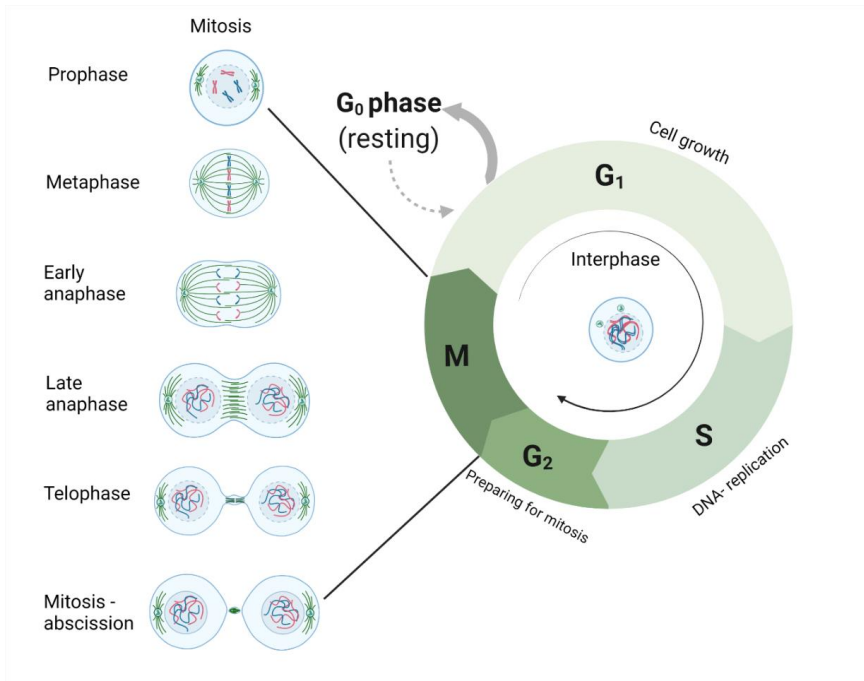


Figure 23: The different phases of the cell cycle. From G₀ (resting phase) to mitosis. The phases in preparation for mitosis are called the G₁, S and G₂, while mitosis (M-phase) is divided into several sub-stages, from prophase to mitosis abscission. Created with BioRender.com.

Proliferation is a prognostic marker in several types of cancer, such as breast cancer, malignant lymphomas, gastrointestinal stromal tumour and NEN^{246, 247}.

1.6.1 Mitotic activity

Tumour growth correlates with mitotic activity, which is one of the main prognostic factors in several types of cancer¹⁹². Mitotic activity can be visualised and counted in the microscope with haematoxylin and eosin (HE) – staining. This is, however, time-consuming. In some cases, it is also difficult to determine whether a cell is mitotic, especially to distinguish it from an apoptotic body (**Figure 24**)¹⁹¹. There are different

ways to determine and score mitotic activity, depending on the cancer type. For NEN, the mitotic count is reported as the number of mitosis pr. 2 mm², counting in a tumour area of 10 mm², which is 50 high-power fields at x40. This usually requires a surgical specimen to ensure enough tumour tissue for evaluation¹¹².

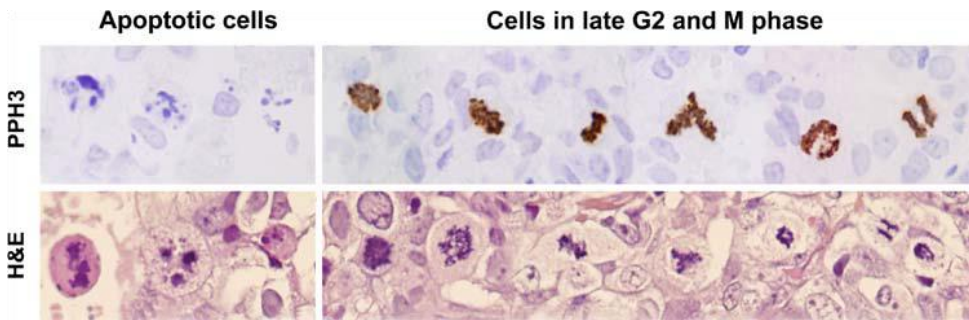


Figure 24: Haematoxylin and eosin (HE) and phosphohistone H3 (PHH3) staining of different sub-stages of mitosis. The examples include cells in prophase, metaphase, anaphase and telophase. Reprinted with permission from¹⁹¹. Copyright © Springer 2008.

1.6.2 Ki67

Ki67 is a nuclear DNA-binding protein expressed in proliferating cells²⁴⁷. Its function has been unclear, but it has been shown to play a role in controlling and timing of cell division²⁴⁸. To visualise Ki67 in pathological specimens, IHC staining with the MIB-1 antibody is the most commonly used and recommended assay²⁴⁹. However, the method has been criticised because of difficulties in standardising Ki67 staining, which affects reliability and reproducibility^{250, 251}. Ki67 can be expressed in apoptotic bodies²⁵², which may overestimate the number of positive cells in a specimen. However, Ki67 correlates with a mitotic count, even though more cells than those in actual mitosis are labelled, and Ki67 is easier to quantify compared to the mitotic count in an HE stain¹⁹³. Consequently, Ki67 is used as a prognostic biomarker in several types of cancers, such as GEP-NENs¹⁹². However, its role as a predictive marker is not yet well established²⁵³.

1.6.3 Phosphohistone H3

Histone H3 is a nuclear core histone protein of DNA chromatin with an important role in chromosome condensation and cell cycle progression during mitosis. Phosphorylation occurs between late G2 and early prophase, while dephosphorylation occurs slowly from late anaphase to early telophase. Therefore, histone H3 is always heavily phosphorylated in the metaphase and positive for phospho-histone H3 (PHH3) IHC. In the interphase, there is no or minimal expression of PHH3, which allows PHH3 to stain only mitotically active cells. Hence, PHH3 is regarded as proliferation-specific and a promising marker of mitotic activity²⁵⁴. In addition, it is a validated prognostic marker in several types of cancer²⁵⁵ and has been identified as a promising marker for predicting disease-free survival and disease-specific survival in pancreatic NEN^{256, 257}. However, its role in GEP-NENs has yet to be determined.

As already mentioned, counting mitosis in an HE stain is challenging because apoptotic bodies can be misinterpreted as mitotic figures^{191, 252}. In contrast to Ki67, which is present in all proliferative phases of the cell cycle and can also be expressed in apoptotic bodies, PHH3 only stains M-phase cells, see **Figure 25**. Thus, with PHH3, mitotic activity can be specifically determined²⁵⁸, and PHH3 may be a better biomarker for mitosis²⁵². Several studies have shown good concordance between the number of mitoses and PHH3^{259, 260}. PHH3 is suggested as an alternative to the Ki67 index in pancreatic NEN²⁵² and is regarded as promising for assessing grading in GEP-NENs in general.

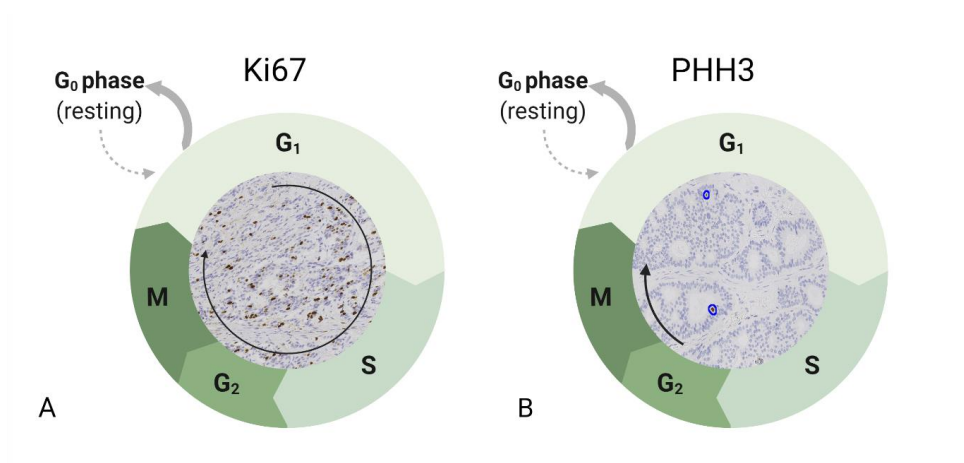


Figure 25: Expression of Ki67 (A) and phosphohistone H3 (PHH3) (B) in the cell cycle. The arrows indicate which phase the immunohistochemical markers are expressed. Created with BioRender.com.

2. Aims of the study

Prognostic and predictive factors are important for treatment decisions in gastrointestinal cancer. In addition, the reproducibility and accuracy of the methods used in the diagnostics are crucial for the optimal clinical management of patients.

The aims of our study were as follows:

- To establish a method for evaluating the immune response in CRC tumours (**Papers I and II**);
- To compare the serologic immune response with the immune response in CRC tumours (**Paper I**);
- To calculate an immune score for colon cancer and see how it corresponds with known histopathological parameters (**Paper II**);
- To improve the prognostic assessment regarding which patients with colon cancer may benefit from additional treatment (**Paper II**);
- To improve the prognostic value of grading using digital image analysis of Ki-67 in GEP-NENs compared to manual evaluation with a light microscope (**Paper III**); and
- To evaluate the proliferation marker phosphohistone-H3 (PHH3) in GEP-NENs to improve prognostic assessment and evaluate the potential advantages or challenges in routine practice (**Paper III**)

3. Methods

3.1 Study population

This thesis involved two different study populations. The patients recruited for the **Papers I and II** were from the ACROBATICC cohort²⁶¹ (clinicaltrials.gov identifier: NCT01762813). This is an ongoing prospective clinical-molecular biomarker outcomes study. ACROBATICC is an abbreviation for ‘Assessment of clinically related outcomes and biomarker analysis for translational integration in colorectal cancer’. The study was approved by the Norwegian Regional Committees for Medical and Health Research Ethics (REK-Vest, #2012/742) and conducted according to national legislation. Written informed consent was obtained from all participants before inclusion in the ACROBATICC project.

Twenty-one patients were recruited for an early pilot feasibility study, resulting in **Paper I**. These patients were recruited for the ACROBATICC cohort between February 2015 and May 2015. Eighteen of them had stage I–III invasive CRC and were included in the analysis. Three patients were excluded due to a final diagnosis of adenoma without an invasive tumour. The second study, culminating in **Paper II**, encompassed a sub-cohort of patients with stage I–III colon cancer that did not undergo neoadjuvant treatment from the initial cohort recruited between January 2013 and May 2014¹⁰⁶.

The second study population, for **Paper III**, was all consecutive patients diagnosed with GEP-NENs and treated at Stavanger University Hospital from 2003 to 2013. This hospital serves as the only hospital for a well-defined Norwegian population of approximately 380,000 people¹⁵³. The study was approved by the Norwegian Regional Committees for Medical and Health Research Ethics (REK -Vest, #2016/1622) and conducted following national legislations. Written informed consent

was obtained from all living participants before they were included in the study. Out of 204 consecutive patients, 35 did not respond or declined their participation.

3.2 Material and data collected

3.2.1 ACROBATICC

ACROBATICC is a translational cancer research project led by the Department of Gastrointestinal Surgery at Stavanger University Hospital. The prospective registration includes all patients with CRC, either primary or metastatic disease²⁶¹. Collaboration between departments and institutions is key to the project. By inclusion, the patients received a unique identifier number in the project. Blood samples were taken before surgery and at follow-up, which is normally about one month after surgery. From the surgical specimen, fresh frozen tissue was sampled from the normal mucosa and the tumour tissue and stored at -80°C . In addition, routine samples were selected for diagnostics as formalin-fixed paraffin-embedded (FFPE) tissue. Minimum three FFPE blocs were sampled from the primary tumour from each patient. The section with the deepest infiltration was used in this study. The same procedures were performed with patients who developed metastatic disease. The database was handled and protected according to the hospital's regulations and current legislation.

3.2.2 GEP-NENs cohort

The GEP-NENs cohort was obtained from the Department of Gastrointestinal Surgery at Stavanger University Hospital, and this department led the inclusion of patients. In addition, FFPE sections were retrieved from archives at the Department of Pathology. All tumours were confirmed as NENs by positive IHC staining for

synaptophysin and/or chromogranin A. NEC was included as grade 3 (high grade). MiNENs were excluded. A patient was excluded due to possible primary pulmonary NEC. Nine patients were excluded due to a lack of tissue for analysis. Thus, 159 (77.9%) patients were included in the study. The material comprised 63 (39.6%) biopsies and 96 (60.4%) surgical specimens. For some patients, there was not enough material to perform IHC for PHH3. In these cases, only IHC for Ki67 was analysed.

Routine evaluation of patients encompassed clinical examination, blood tests, including tumour marker detection (i.e. CgA), and standard oncologic imaging, as recommended in available guidelines^{155, 262-264}. PET imaging was not routinely performed. Transthoracic echocardiography was performed in cases of suspected carcinoid heart disease. Endoscopy, including endoscopic ultrasound (EUS) and video capsule endoscopy, was available if indicated. If a GEP-NEN was incidentally discovered during an unrelated surgery, a clinical evaluation was performed postoperatively.

3.2.3 Enhancing the quality and transparency of health research

The ACROBATICC cohort study is reported according to the STROBE (strengthening of the reporting of observational studies in epidemiology)²⁶⁵ and the REMARK (REporting recommendations of tumour MARKer prognostic studies)²⁶⁶ guidelines for biomarker studies. STROBE is a checklist to improve reports of observational studies developed by methodologists, researchers and journal editors to ensure transparency and good reporting of observational studies²⁶⁷. The checklist is used for both cohort, case-control and cross-sectional studies²⁶⁸. The REMARK guidelines are used to provide relevant information about the study design, preplanned hypotheses, patient and specimen characteristics, assay methods and statistical analysis methods. These guidelines were developed jointly by the US National Cancer Institute (NCI) and the European Organisation for Research and Treatment of Cancer (EORTC)²⁶⁹. The goal of these guidelines is to encourage

transparent and complete reporting so that relevant information is available to others in tumour marker studies²⁶⁹.

3.3 Statistical analysis

IBM SPSS Statistics for Windows, Version 23 or 26.0 (IBM Corporation, Armonk, NY, USA), was used for the statistical calculations.

In **Paper I**, correlation analyses were performed using the non-parametric test Spearman's rank correlation coefficient (ρ), assuming a non-Gaussian distribution of variables. In **Paper II**, associations between categorical variables were tested with Chi-square. In addition, Mann–Whitney U test was used to compare differences in continuous or ordinal variables between groups. All tests were two-tailed, and a p-value <0.050 was determined as statistically significant.

In **Paper III**, quadratically weighted kappa was used to measure the agreement between ordinal variables²⁷⁰ and calculations were aided using VasserStats²⁷¹. The interclass correlation coefficient (ICC) was used to measure the agreement between continuous variables (single rater, absolute agreement). All agreement estimates are presented with 95% confidence intervals (CIs). Values less than 0.50, between 0.50 and 0.75, between 0.75 and 0.90 and greater than 0.90 indicated poor, moderate, good and excellent reliability, respectively²⁷². To plot the difference in pathology Ki67 and digital image analysis Ki67 measurements against the average value, we used a Bland-Altman plot²⁷³.

3.4 Techniques

3.4.1 Flow cytometry

Flow cytometry enables the rapid analysis of numerous cells at a single cell level. Physical characteristics of each cell are registered as it flows in suspension through a detector based on scatter made from laser excitation. Targeted antibodies with fluorescent markers can be used to label whole cells or cellular components, such as organelles, nuclei, DNA, ribonucleic acid (RNA), chromosomes, cytokines, hormone receptors or protein content²⁷⁴. This allows flow cytometry to be used for many purposes, such as antigen detection.

The main principle of this technique is based on the scattering of light and the emission of fluorescence, which occurs when light from an excitation source, usually a laser beam, hits the cells moving in a directed fluid stream^{274, 275}. A flow cytometer comprises several components for the different analytical steps. First, there is a fluidic system that contains the material to be analysed, such as white blood cells. Second, the fluidic system aligns the cells to flow at the same speed and axis through the light source. The light source is usually one or several lasers that focus on the cells. The resulting light scatter is detected through a forward scatter and a side scatter. Forward scatter is proportional to the cell surface area or size and is suitable for detecting particles greater than a given size. Side scatter is a measurement of refracted and reflected light collected at approximately 90° of the laser beam. It is an expression of the granularity/complexity of the cell. Forward scatter and side scatter combined are commonly used for immunophenotyping, as different blood cells are easily separated by size and granularity²⁷⁴. To study specific biomarkers or the complexity of cells, cell components are detected using antibodies with different fluorescent markers and lasers emitting light at different wavelengths. The light signals are converted to voltage by a detection system that comprises photodiodes or

photomultiplier tubes. The photodiodes detect the strong signals sent by forward scatter, while photomultiplier tubes detect the weaker signal generated by side scatter and fluorescence. A converter transforms analogue signals from detectors into digital signals, which are then sent to a computer. The software usually displays the results as a scatter plot or histogram, which can then be analysed (**Figure 26**). Finally, the waste products end up in a collecting waste container to be disposed of²⁷⁵.

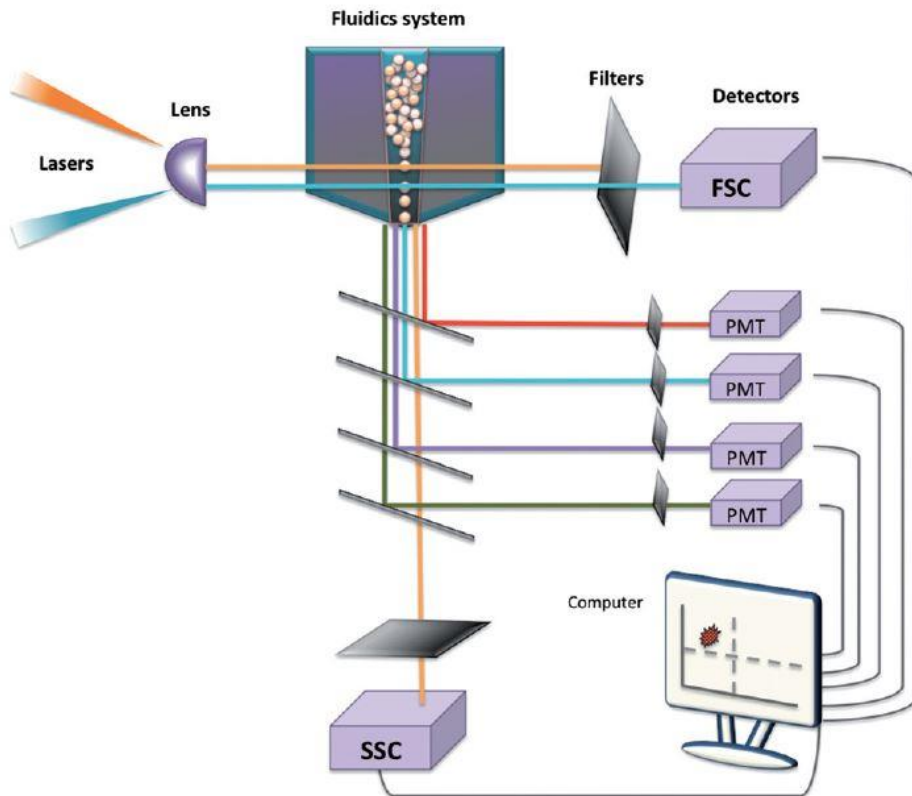


Figure 26: The signalling process of flow cytometry. The fluidics contain particles that go through the light detection system. Here, two types of light scatter occur: forward scatter (FSC) and side scatter (SSC). The light signals are converted to voltage by detectors. There are two types of detectors: photodiodes (FSC) and photomultiplier tubes (PMT). The photodiodes detect signals sent by FSC, while PMT detects signals generated by SSC and fluorescence. The signals from the detectors go to a computer that analyses and displays the results. Adapted with permission from²⁷⁴. Copyright© Taylor & Francis 2017.

In present work, blood samples were run using a two-laser flow cytometer (BD Accuri C6 and Cytotflex, Beckman-Coulter, USA). The flow cytometer was equipped with a blue (588 nm) and red laser (640 nm), two light scatter detectors (forward scatter and side scatter) and four fluorescence detectors. The fluorescence detectors were equipped with optical filters optimized for the detection of fluorescence from fluorescein isothiocyanate (FITC 588/30 nm), phycoerythrin (PE 585/40 nm), peridinin chlorophyll (PER-CP 670 nm) and allophycocyanin (APC 675/25 nm). As described in our paper, we used an antibody kit from BD Biosciences (NJ, USA). White blood cells were marked with CD45+ conjugated to Per-CP, all T-cells were marked with CD3+ linked to FITC and cytotoxic T-cells with CD8 PE. In addition, CD4+ positive T-cells were marked with APC-conjugated antibodies for staining. Using the corresponding software, we calculated the absolute numbers of the different T-cell populations per ml blood²⁷⁶.

3.4.2 Multiplex polymerase chain reaction and fragment analysis

PCR is a method used to examine small segments of DNA or RNA. PCR can be used to detect gene mutations, but it is widely used in forensic medicine²⁷⁷. The method is based on the amplification of small segments of DNA²⁷⁸.

PCR is performed in several stages. First, a DNA template is made. To do this, the tissue of interest is mixed with a buffer before primers, DNA polymerase and nucleotides are added. A primer is a short stretch of DNA, usually 20–30 base pairs, which complement the DNA region to be examined. At least two primers are used. These are forward and reverse primers and ensure that the DNA strands can be read upstream and downstream directions in the region of interest. DNA polymerase is the enzyme that synthesises DNA, and nucleotides are the actual building stones for DNA.

The DNA template was placed in a PCR machine. The machine can change temperature very quickly, and a rapid temperature change is one of the key factors of the method. The process comprises three steps (**Figure 27**). Step 1 is the denaturation of DNA, in which the DNA strands are separated. For this to take place, a high temperature is required. Step 2 involves annealing when the primers bind to the separated DNA strands. Step 3 is elongation, as the primers synthesise DNA strands. These steps were repeated several times, with the resulting amplification of the DNA segments. The process requires specific temperatures at each step.²⁷⁹ When amplification is completed, the product is analysed with electrophoresis. In modern PCR techniques, the fluorescent labelling of primers makes detection by laser possible. In multiplex PCR, several primers are used so that several genes can be examined simultaneously²⁸⁰.

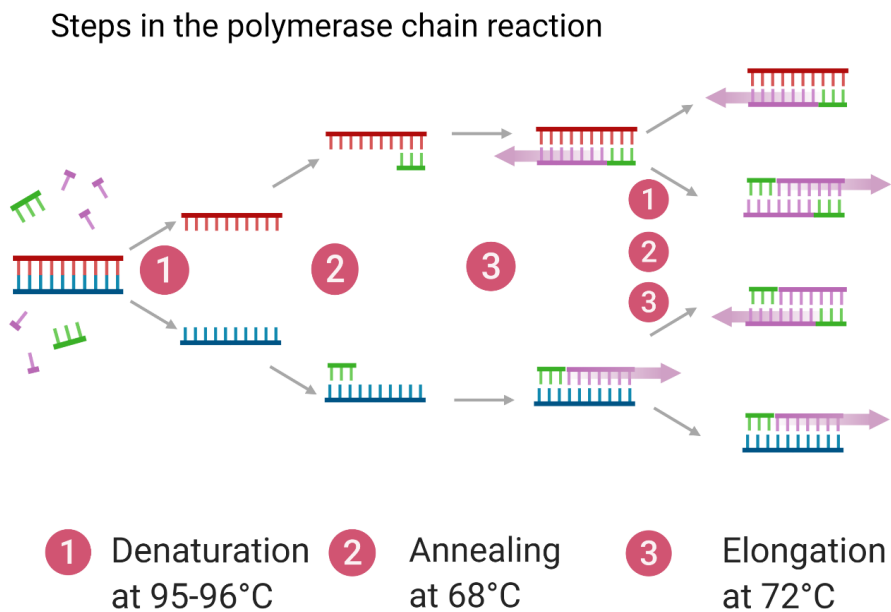


Figure 27: Steps in the polymerase chain reaction. Green = primer. Purple = nucleotides. Red and blue: DNA template strands. Created with BioRender.com

In our case, tissue was extracted from sections of FFPE blocs. Five primers were used for both MSI and EMAST, and two independent multiplex PCR reactions were performed. Detailed descriptions of the procedure and interpretation of the results are given in each paper (**Papers I and II**).

3.4.3 Immunohistochemistry

IHC is used to detect specific proteins in FFPE tissue and has revolutionised diagnostics in pathology²⁸¹. When performing IHC, enzyme-linked antibodies are used to detect tissue antigens. The basic principles of IHC are described in **Figure 28**. The first step is sectioning tissue from the FFPE block onto a slide. Next, the slide is heated in a buffer to unmask the antigen, a process called antigen retrieval. After incubation with the primary antibody, a secondary antibody with a polymer complex (polymer with horseradish peroxidase) binds to the primary antibody. The peroxidase enzymes convert a chromogen substrate solution called 3,3 Diaminobenzidine into a brown precipitate. This occurs close to the location of the antigen and is used to visualise the antibody. Endogenous enzymes are blocked, so they will not interfere with the detection system. Between each step of the procedure, unbound reagents are washed off. The final step is to counterstain the slide with haematoxylin and apply a cover glass before viewing and interpreting the results in a microscope.

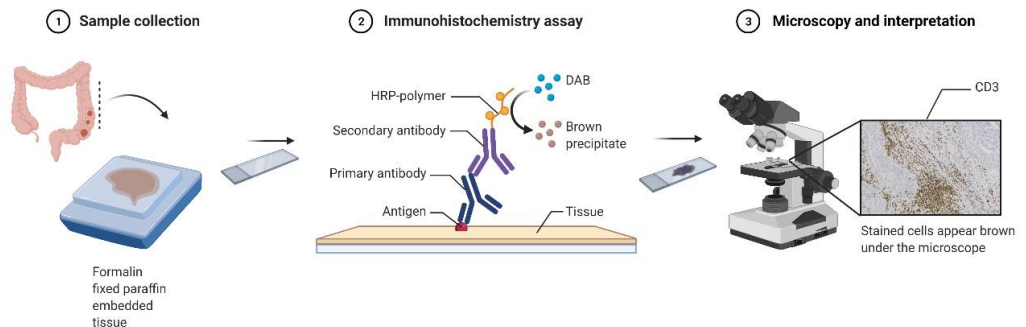


Figure 28: Basic principles of immunohistochemistry. Abbreviations: HPR: horseradish peroxidase, DAB: 3,3 diaminobenzidines, CD: cluster of differentiation. Created with BioRender.com

Over the years, the different steps of IHC have been standardised and automated²⁸¹. This improved the method. However, international standardisation remains insufficient, hampering reproducibility²⁸². Several studies have shown poor intra- and inter-observer reliability^{15, 283}. Numerous factors affect the results: pre-analytical, such as fixation time; analytical, such as detection system; and post-analytical, such as interpretation of results²⁸². Therefore, every step of IHC has to be optimised for the method to be reliable²⁸⁴.

All the IHC stains used in our studies were performed in routine diagnostics at the Department of Pathology, Stavanger University Hospital. The laboratory participates in Nordic immunohistochemical quality control (NordiCQ), a scientific organisation that standardises and recommends protocols for IHC¹⁹⁶. Hence, the method was optimised before our studies. The specific methods for the different IHC antibodies are described in each paper. An automated slide stainer was used, with positive and negative controls in each run.

3.4.4 Digital image analysis

Digital image analysis involves several variables that must be optimised for a successful result. These can be divided into pre-processing, classification and post-processing variables. Pre-processing variables include laboratory routines for fixation, preparation and staining of the surgical specimen or biopsy. The section you want to scan has to be evenly cut and stained. Artefacts from suboptimal processing or staining can hamper the results. Furthermore, the slide has to be clean, without air bubbles or dust under the glass.

The first step in digital image analysis is scanning the sections. Photos taken with a camera can also be used, but usually, a scanner is preferred. The scanner is calibrated and adjusted for focus, white balance, light source, exposure time and colour. To sustain details in the image, scanning at x40 is favourable. The more details you want, the more storage is required. The scanned image is compressed into a digital image file. File format varies depending on the scanner and programme used. Examples of formats are tagged image file format (TIFF) and joint photographic expert group (JPEG). TIFF preserves more details in the image, whereas JPEG is more compressed and results in a smaller file size with less detail. The Leica scanner used in our studies uses scenario (SCN) format, which is comparable to TIFF.

For classification, there are three categories of digital image analysis measuring algorithms⁸:

- Area-based measurements
 - o Pixel-based assessment, where the algorithm quantifies the colour (or intensity of staining) in each pixel
- Cell-based measurements
 - o Morphometry-based assessment where pixels are grouped based on similarity defines structure (e.g. cells or nuclei) profiles that meet certain preselected criteria (e.g. size and shape).
- Object-based counting or assessment of ‘events’
 - o Specialised algorithms are designed to serve a particular need, often the automated identification and/or enumeration of non-cell structures.

Classification, in applications used for digital image analysis, requires a classifier. A classifier aims to create a contrast between the structures you want to examine in the image and other image segments. One aim could be to separate positively stained nuclei from negatively stained nuclei in an image. Several types of classifiers are available, and some will be mentioned here. The simplest classifier is ‘Threshold’. This classifier marks areas of and above a defined pixel value to separate objects from the background²⁸⁵. Although ‘Threshold’ is used in some image analysis

software²⁸⁶, it is not very sensitive to variation in staining intensity, and the optimal 'Threshold' might vary from one image to another. More sophisticated classifiers include 'Bayes classification' and 'K-means clustering'²⁸⁵. These can be unsupervised (K-means clustering) or supervised (Bayes classification), depending on whether pixels relevant for the classification are set or not²¹. K-means clustering does not need a training set to be used for digital image analysis²⁸⁷, while Bayes classification is a probabilistic model that uses training data to find the most probable prediction²⁸⁸. If you teach the classifier to recognise one or several colour pixels in a training set, the classifier will use this knowledge to recognise the same colours in different virtual slides that have not been presented to the classifier before. This knowledge is used to develop an application for digital image analysis. Applications that use more sophisticated classifiers can be trained to group several colour pixel intensities into the same category²⁸⁷. For example, a nucleus positive for 3,3-diaminobenzidine staining can be light brown or dark brown, and the application can be trained to include different shades of brown in the positive category. For haematoxylin (blue) staining, the same applies. This feature is important when the same application is used for several scanned sections, as there will always be some differences between scanned slides from different patients. Lezoray and Cardot found that Bayes classification gave a better segmentation of colour pixels than K-means clustering²⁸⁷. Bayes classification can also be used to assign objects to different groups, depending on the size and shape in a segmentation²⁸⁵. This can be used to separate tumour cells from stroma and lymphocytes in digital image analysis. An example of Bayes classification used in digital image analysis is shown in **Figure 28**.

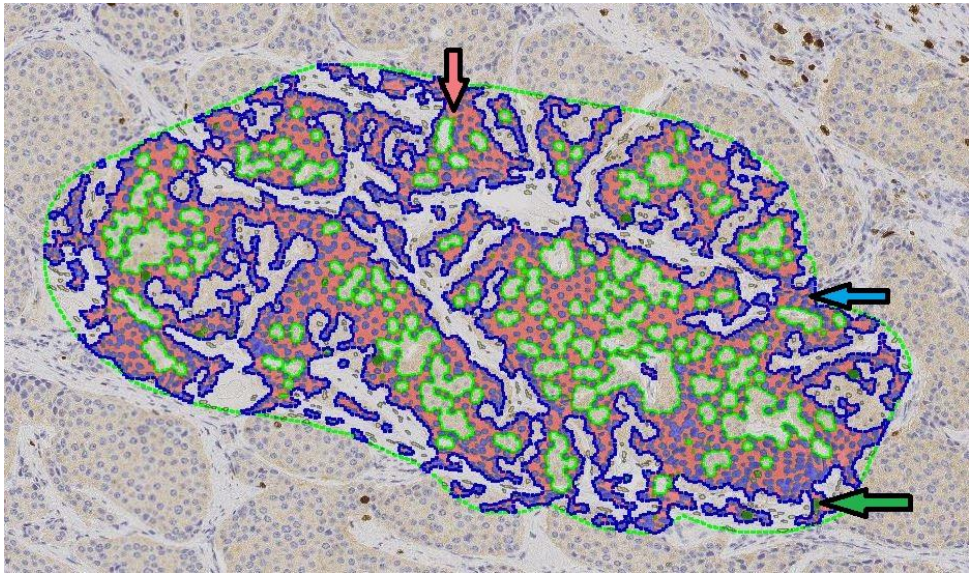


Figure 29: Bayes classification of Ki67 immunohistochemical staining in a neuroendocrine neoplasm. The green dotted line outlines the region of interest. The classifier has separated tumour from stroma (blue line). It has also identified positive tumour cells (green) and negative tumour cells (blue) based on nuclei staining. The red areas are cytoplasm/background, which was excluded from the calculation. The different classified areas are exemplified by the green, blue and red arrows.

An important step in digital image analysis is selecting the region of interest on a virtual slide. The region of interest can be manually selected, or digital image analysis can be used to do this. For example, digital image analysis can identify the region of interest using a heat map that selects a hot spot based on threshold, clustering or other criteria^{285, 289}. The benefit of automation is avoiding selection bias. However, manual selection might be better to avoid tissue that you do not want to include in the analysis. If a technician selects a region of interest, it should always be controlled by a pathologist⁸. Several regions of interest can be selected, and measurements can be performed on several areas simultaneously.

Post-processing involves manual control and adjustment of the image. Examples include the removal of artefacts or the separation of overlapping objects¹. This usually requires some knowledge of histopathology. Digital image analysis measures

pixels, and this must be translated into understandable variables that can be interpreted. This is done by applying definitions to output data. A spreadsheet or other type of software is usually used in this process.

In our studies, we used Bayes classification to develop the different classifiers utilised in applications for digital image analysis. The applications used for digital image analysis were developed based on knowledge from similar studies^{13, 191}. Region of interest and applications used were defined differently in the different papers. In **Paper I**, we used two different applications. The first counted T-cells (CD3 and CD8) in a manually defined region of interest in the tumour centre and the invasive margin. The second separated the epithelium and stroma into a 2 mm circle in the tumour centre and the invasive margin before quantifying the same T-cell populations. In **Paper II**, we used the first application from **Paper I**. In **Paper III**, a manually defined region of interest for hotspot Ki67 was used. 500–2000 cells in the region of interest were counted based on the mean nuclear size. Stroma was excluded from the region of interest if present. The percentage of Ki67-positive nuclei was calculated based on positive and negative nuclei staining. For PHH3, depending on the area available, we had 1 to 4 different manually selected regions of interest in hotspots where the number of PHH3-positive cells was counted in an area of 2mm². Further details and photos are provided in the corresponding papers^{276, 290, 291}. All the annotations of the region of interest, analysis and post-processing were done by a certified pathologist (DL). To avoid selection bias, measurements were done without information about clinicopathological data, such as the stage of the disease or the previous histopathological evaluation.

4. Results

In **Paper I**, (*Hagland, Lea et al., Anticancer Research, 2017*), the relationship between circulating T-cells in blood and intratumoural T-cells in CRC was investigated in a feasibility study. Eighteen patients with stage I–III CRC were included. Using flow cytometry, pre-surgical blood samples were analysed for T-cell type (CD3+, CD4+ and CD8+) and count. Intratumoural T-cells were stained with CD3 and CD8 using IHC and quantified in the invasive margin and tumour centre by digital image analysis, using an automated image analysis software, Visiopharm® (Hoersholm, Denmark). We found that the number of CD3+ and CD4+ T-cells in pre-surgical blood samples correlated with the number of CD3+ T-cells found in the invasive margin (Spearman $\rho = 0.558$, $p < 0.05$ and 0.598 , $p < 0.01$, respectively) and with CD3+ T-cells in the tumour centre ($\rho = 0.496$, $p < 0.05$, and $\rho = 0.637$, $p < 0.01$, respectively). There was a strong correlation between CD4+ T-cells in blood and CD8+ T-cells in the tumour centre and the invasive margin ($\rho = 0.602$ and $\rho = 0.591$, $p < 0.01$). The correlation was strongest for analysis on whole section scans, compared to 2 mm circles in the tumour centre and invasive margin.

In **Paper II** (*Lea, Watson et al., Cancer Immunology Immunotherapy, 2021*), we developed an objective quantification method for T-cells to calculate an immune score for colon cancer. The method was based on one of the digital image analysis applications used in **Paper I** and used automated image analysis software, Visiopharm® (Hoersholm, Denmark). CD3 and CD8 T-cells at the invasive margin and in the tumour centre were quantified. An algorithm template for whole slide assessment generated cell counts per square millimetres (cells/mm²), from which the immune score was calculated using distribution volumes. To confirm its relevance, the immune score was juxtaposed with the clinical and histopathological characteristics. Based on the number of T-cells calculated by digital image analysis, patients were classified into low ($n = 83$, 69.7%), intermediate ($n = 14$, 11.8%) and high ($n = 22$, 18.5%) immune score groups. A high immune score was associated with stage I–II tumours ($p = 0.017$) and a higher prevalence of MSI-high tumours (p

= 0.030). MSI-high tumours had significantly higher numbers of CD3+ T-cells in the invasive margin and significantly higher numbers of CD8+ T-cells in both the tumour centre and the invasive margin than MSS tumours. Our digital template to quantify T-cells is an easy-to-use immune score, corresponding with known clinicopathological features such as stage and MSI in colon cancer.

In **Paper III** (Lea, Gudlaugsson et al., *Applied Immunohistochemistry & Molecular Morphology*, 2021), we evaluated the use of digital image analysis as an objective assessment of proliferation markers in GEP-NENs. The study included 159 patients (57% male) in a consecutive cohort of 204 patients. Automated digital image analysis measurements of Ki67 (*digital image analysis Ki67*) and PHH3 (*digital image analysis PHH3*) on IHC slides were analysed using Visiopharm® image analysis software (Hoersholm, Denmark). The results were compared with the Ki67 index recorded in the corresponding routine pathology reports (*pathology Ki67*). The median *pathology Ki67* was 2.0%. Median *digital image analysis Ki67* was 4.1%. The interclass correlation coefficient of the *digital image analysis Ki67* compared with the *pathology Ki67* showed an excellent agreement of 0.96 (95% confidence interval [CI]: 0.94–0.96). When comparing grades based on the same methods, the observed kappa value was 0.86 (95% CI: 0.81–0.91). PHH3 was measured in 145 (91.2%) tumours. The observed kappa value was 0.74 (95% CI: 0.65–0.83) when comparing grades based on the *digital image analysis PHH3* and the *pathology Ki67*. In conclusion, there was excellent agreement between *digital image analysis Ki67* and *pathology Ki67*. However, *digital image analysis Ki67* tended to upgrade cases from grade 1 to grade 2. The *digital image analysis PHH3* measurements were more diverse and could not replace established methods for grading GEP-NENs.

5. Discussion

There is an ongoing paradigm shift in pathology, where laboratories are going digital and the microscope will eventually become obsolete. There are many benefits to digitalisation, especially concerning patient safety and logistics in the pathology departments. However, one challenge in pathology today is the subjectivity in evaluating and interpreting IHC staining, especially in the quantification of prognostic markers. This leads to intra-and inter-observer variations. By introducing new diagnostic methods, including digital image analysis, some of these obstacles might be solved. In addition, novel prognostic parameters (e.g. a score for immune response) not routinely used today might be introduced.

5.1 Determine immune status in colorectal patients

We aimed to investigate the correlation between T-cells in the blood and T-cells in tumour tissue from patients with CRC (**Paper 1**). Although this was a feasibility study with only 18 patients, we found an interesting relationship between the two. Unfortunately, these findings are not explored further in the cohort at this time. To our knowledge, no other studies with the same methodology have been conducted for CRC. However, a study by Chirca et al. found different levels of CD4⁺ and CD8⁺ in peripheral blood compared with tumours, using flow cytometry for both analyses²⁹². A study by Won et al. found a lower number of circulating mucosal-associated invariant T-cells in mucosa-associated cancers (including colon cancer) compared to healthy controls²⁹³. Sun et al. found that several immune-related genes were upregulated in blood samples from CRC patients compared with healthy controls. Furthermore, the gene protein phosphatase 3 regulatory subunits B α (PPP3R1) was especially associated with poor prognosis²⁹⁴. In this latter study, the CRC patients were significantly older than the healthy controls, which may have influenced the results. The beneficial effect of a local cancer-specific immune reaction in CRC is well documented and has been shown to be related to a better outcome. However, a

lower immune response is associated with a worse prognosis^{226, 237, 295, 296}. Liquid biopsies, especially in the blood, are evolving in other fields of cancer diagnostics for the early detection and tracking of biomarkers²⁹⁷. The role of liquid biopsies for immune cells as prognostic markers in CRC remains unsettled.

5.2 Immune score for colon cancer

In **Papers I and II**, we developed a method for quantifying T-cells in CRC. In **Paper I**, two different digital image analysis methods to quantify T-cells in the tumour were explored. We found that analysis of whole-section scans gave the highest correlation with T-cells in the corresponding blood samples. The method emanates from the constructed principle of Immunoscore® (HalioDx, Marseille, France), which has been validated in a large international cohort series²³⁷. Over the years, there has been a shift in methodology for calculating iImmunoscore, from analysis on tissue micro arrays to analysis on whole section scans^{226, 237}. In addition, the classification of Immunoscore® (HalioDx, Marseille, France) has been changed from five to three categories^{237, 240}. The calculations, including the cut-off values, are largely under wraps²³⁷, complicating the method's reproducibility. In addition, the commercially available Immunoscore® (HalioDx, Marseille, France) is adapted to certain manufacturers of antibodies and autostainer²³⁷, and this may prevent pathology departments from setting up the method with equipment available in their laboratory. Others have developed deep learning methods to analyse tumour-infiltrating lymphocytes in CRC and have found an association with survival^{23, 298}.

Our method for immune score (**Paper II**) may represent an alternative that is adaptable, easy to implement, affordable and objective and provides transparency for reproduction. The latest guidelines from the European Society for Medical Oncology recommend that Immunoscore® (HalioDx, Marseille, France) be considered in conjunction with TNM to refine the estimate of prognosis for early colon cancer patients and assist chemotherapy decision making in stage II and low-risk stage III

patients²⁹⁹. This highlights the necessity of this parameter in clinical practice. However, pathology departments must be able to determine immune scores using the available equipment. Integration with digital software must also be possible, as pathology departments are transitioning to digital pathology. The necessity of an immune score is also highlighted as an indication for immunotherapy becomes more available. Chalabi et al. showed that neoadjuvant immunotherapy decreased primary tumours in MSI-high colon cancer patients. In several cases, the tumour disappeared completely. Some patients with MSS tumours also responded to immunotherapy³⁰⁰, and an immune score might be a tool for selecting these patients²³¹.

5.3 Digital image analysis of proliferation markers in neuroendocrine neoplasms

In **Paper III**, we quantified two different proliferation markers in GEP-NENs, where one of the markers, Ki67, is currently used in diagnostics. Previous studies have shown that digital image analysis or counting on a camera captured/printed image gave the best results for evaluating Ki67 in GEP-NENs^{14, 15}. The same studies found that eyeball estimation had the lowest agreement and reproducibility. In this study (**Paper III**), we found more grade 2 tumours when digital image analysis calculated the Ki67, but when we compared the percentage of *digital image analysis Ki67* with the *pathology Ki67*, we found excellent agreement. We think that an explanation for this finding is that many of these cases had a percentage between 2% and 4%, which is around the cut-off value to separate WHO grade 1 and grade 2 tumours. Another explanation might be that eyeball estimations of Ki67 tend to downgrade more NETs to grade 1 than evaluations by digital image analysis, as found by Kroneman et al.³⁰¹. A study by Owens et al. found that digital image analysis overestimated the Ki67 percentage compared with manual counting, but increasing the hot spot size reduced the difference³⁰². One can discuss whether manual evaluation should be the reference standard^{303, 304} since we believe that many of the diagnostic cases have been evaluated with eyeball estimation, while others have been counted properly. A study by

Hacking et al. did not manage to establish a good concordance between digital image analysis and manual counting, and an explanation might be the program/software used for digital image analysis in their study³⁰⁵. In our routine practice today, we always use quantitative counting if there are Ki67-positive cells in the tumour. This was not the case when the cohort was established. We have not yet established a routine for *digital image analysis Ki67*, but hopefully, we will get more experience with the method when digital pathology is established in our department.

In **Paper III**, we explored PHH3 as a marker in GEP-NENs. The results for PHH3 varied, and agreement with WHO grade was worse than for the *digital image analysis Ki67*. This parallels the results of others^{257, 305, 306}. Villani et al. found this marker to be of prognostic value in pancreatic NEN²⁵⁶ and seven mitosis pr. 10 high power fields differentiated between low-and high-risk patients. We did not explore whether this marker or Ki67 gives prognostic information about disease-free survival or overall survival in this study. The challenge with these comparisons is the limited number of patients in this study and the prognosis varies depending on tumour localisation¹⁷⁵.

5.4 Methodological considerations and limitations

5.4.1 Study population

Two different study populations were included in this study. **Paper I** is a feasibility study with a limited number of patients. The aim of that study was merely to test the hypothesis that there is an association between blood and tumour T-cell count, which we could confirm. In **Paper II**, the total number of patients was 119, which is quite low for analysing disease-free survival and overall survival. In addition, there is no validation cohort. Validation is necessary to demonstrate any predictive or prognostic

impact of our immune score method. However, the ACROBATICC cohort is consecutive and thus should not have an inherent referral bias. This makes our results more robust.

In **Paper III**, 159 patients were included. For GEP-NENs, this is quite a large cohort. In addition, the cohort includes quite an even distribution of WHO grade 1–3. Compared with similar studies, the number of included patients with grade 2 and 3 tumours were high^{14, 15, 252, 303-305}. Like with the ACROBATICC cohort, we lack a validation cohort for the GEP-NENs. A validation of our findings in another cohort will be necessary, with data for disease-free survival and overall survival, to demonstrate the predictive and prognostic impact of digital image analysis methods. A drawback of **Paper III** is that almost 40% of the tumour samples were from biopsies. Therefore, the material was more fragmented, and the sample size was smaller compared to surgical specimens. However, this parallels current routine practice at many centres, as surgical specimens are not achievable for all patients, especially patients with advanced disease¹⁹⁷. A study by Yang et al. showed that the Ki67 staining of core biopsies was reliable for the prognosis of metastatic NETs to the liver, despite tumour heterogeneity³⁰⁷. The same biopsies were compared using different methods in this study; therefore, a small sample size should not affect the comparison. However, PHH3 was omitted for some of the samples.

5.4.2 Reference standard

In **Paper II**, we did not compare our method with the patented Immunoscore® (HalioDx, Marseille, France). Immunoscore® (HalioDx, Marseille, France) is the closest resemblance to a reference standard, but the calculations in this method are different, using intervals of 0%–25%, > 25%–70% and > 70%–100% for mean percentiles²³⁷. However, it would be interesting to see whether our method for an immune score gave similar results. Unfortunately, since our laboratory used different equipment and our immune stains were done with different antibodies/laboratory

equipment, we could not have sent our IHC slides for evaluation either, but we had to send the tumour blocs for an evaluation. This was quite expensive and was not done.

In **Paper III**, the digital image analysis of Ki67 was compared with manual counting from the corresponding pathology report. Several pathologists have been involved in diagnostics, and there might be differences in how they count and grade these tumours. These data are subjective histopathological scores³⁹ and reflect routine practice in different pathology departments. Tumours were graded and staged, and patients underwent follow-up based on these evaluations. Discussions are ongoing regarding whether digital image analysis of Ki67 versus manual counting should be the reference standard^{15, 303, 304}. Digital image analysis is more objective and reproducible than manual counting due to several known cognitive and visual biases hampering human visual evaluation of tissue³⁹. This favours digital image analysis. For breast cancer, several studies have shown superior prognostic information from digital image analysis^{308, 309}. For GEP-NENs, Tang and co-workers demonstrated the best agreement with the digital image analysis of Ki67¹⁵. The same is true for similar studies^{14, 305}, but none of these studies compared their results with disease-free survival or overall survival.

5.4.3 Digital image analysis

Digital image analysis was used in all of our papers to evaluate prognostic and predictive markers. The biggest challenge with digital image analysis in **Papers I and II** was that the same analysis was performed on two different slides. Although slides for IHC CD3 and CD8 were cut immediately following each other, there were small differences between one image and the next. In addition, the orientation of the sectioned tissue was of significance. In **Paper I**, we used two different applications for digital image analysis of the same scanned images. For one of the applications in **Paper I**, tissue orientation on the CD3 and CD8 slides did not matter, as the region of interest was circular. For the other method, using a whole-section scan, the

orientation of the tissue was important for us to mark the same region of interest on both slides. In all of our papers, the region of interest was manually annotated in the scanned images. This process might be biased compared with an automated annotation of the region of interest. For the region of interest shaped as 2 mm circles in **Paper I**, the circles were placed in the centre of the tumour and at the deepest infiltration of the invasive margin. For the whole section scans, a larger region of interest was employed for the analyses, largely avoiding selection bias.

Manual scoring of IHC slides has the inherent possibility of several biases and errors compared to digital image analysis, wherein visual traps/optical illusions are avoided³⁹. With manual scoring, the region of interest was selected by the pathologist. So, although selection bias might be present using digital image analysis with manual annotation, the same bias is present in manual scoring.

Not only does the method used for digital image analysis matter, but the work beforehand must also be optimal and standardised. Several preanalytical variables may affect the results of digital image analysis, such as tissue collection, fixation time, section thickness, morphologic criteria for assessment and the staining processes³¹⁰. In our laboratory, we have procedures for handling the tissue, fixation time, section thickness, etc. to avoid bias from such variables. The same technician was also used to section the samples for the different studies. Furthermore, digital image analysis can be hampered by poor slide quality and a lack of consistency in slide preparation. In addition, the digital image analysis results can be greatly affected by the quality of IHC⁶. As mentioned in the method, our laboratory participates in Nordic immunohistochemical Quality Control (NordiCQ) to ensure standardised and recommended protocols for IHC¹⁹⁶.

In **Papers I and II**, we analysed the number of cells in an area given as $n \text{ cells/mm}^2$. The mean nuclear area of the lymphocyte was the basis for the algorithm. As the image analysis software measured area rather than register entities, the IHC staining intensity of positive cells was important. Although CD3 and CD8 staining of T-cells are similar, there are differences in staining intensity between the slides and from

patient to patient. Therefore, it is of great significance that the algorithm for digital image analysis is trained to recognize different staining intensities to make it more robust²⁸⁵. In our study, we used the Bayes classifier to ensure that the application of digital image analysis could handle different staining intensities. Since we programmed the applications ourselves, we could adjust the different applications until we found the results satisfying to perform digital image analysis.

In **Papers I and III**, we used segmentation to distinguish the stroma from the epithelium and identify negative IHC-stained nuclei (**Paper III**). This process is often difficult in the presence of adjacent or overlapping cells, which can lead to under-segmentation or over-segmentation²⁸⁵. There are several ways to adjust the application for digital image analysis to avoid these issues³¹¹. When developing algorithms for digital image analysis, it is often necessary to prioritise between sensitivity (how likely the algorithm is to capture a weakly stained nucleus or cell), specificity (how well the algorithm rejects artefacts) and contour accuracy (how well the algorithm can approximate the exact shape of the nucleus or cell)¹.

In all our papers, we used a software called Visiopharm® (Hoersholm, Denmark). This is licenced commercial software. The alternative would be an open-source software³¹². Options for adaptations and adjustments are often better in commercial software compared to open-source software¹. The Visiopharm® (Hoersholm, Denmark) offers CE-IVD applications for use in the diagnostic workflow, which means that the programme is approved according to the requirements of the European Union for in vitro diagnostic medical devices³¹³. We did not use these applications in diagnostics but programmed and adjusted the applications according to what we wanted to examine in our studies. To our knowledge, no CE-IVD applications are available for either scoring immune cells or measuring proliferation in NEN. There are, however, applications for CE-IVD Ki67 in breast cancer³¹⁴.

6. Conclusion and future perspectives

We developed a whole slide digital pathology template to quantify immune cells (**Papers I and II**) in CRC using imaging software. In **Paper II**, we established an immune score based on the distribution volumes of CD3 and CD8. We found that immune scores correlate with known clinicopathological parameters, such as MSI status and stage of the disease. In **Paper I**, we found an association between T-cells in the blood and T-cells in the tumour, but this association was not investigated further. Thus, there is a need for large-scale internal and external validation to demonstrate the robustness and adaptability of the immune score for clinical use in CRC. We initiated such validation with a follow-up study encompassing a larger cohort of ACROBATICC patients. We hope that this will provide further information about the predictive and prognostic value of the immune scores we developed.

In **Paper III**, we successfully developed a digital image analysis for grading GEP-NENs based on Ki67 IHC. The method can be integrated with routine diagnostics in pathology departments that are digital. However, because of the heterogeneity of the disease, it is difficult to obtain reliable data regarding disease-free survival and overall survival. Survival rates need to be further evaluated in subsequent studies to gain more information about this method's predictive and prognostic value. PPH3 needs to be further evaluated in a larger cohort to determine whether it can be of any predictive or prognostic value in GEP-NENs patients. It might be of prognostic value in subpopulations of GEP-NENs, such as NET grade 3 versus NEC grade 3 or large-cell or small-cell NEC.

With the implementation of digital pathology, there is a need for validation of both equipment and whole slide imaging, including methods for digital image analysis^{315, 316}, to ensure that the developed methods can be safely used at different laboratories. This requires both national and international collaboration. In Norway, the National Department of Health has appointed a national forum to address equipment issues. This forum will also establish guidelines for standardisation for handling tissue/surgical specimens, macroscopic examination and reporting of results³¹⁷. It is

difficult to predict how this will be implemented and what the ramifications will be. Hopefully, it will enhance quality control and provide results based on more robust and comparable diagnostics across pathology departments. It would be interesting to perform a similar analysis for digital image analysis to what we conducted with open-source software tools. It would be a great advantage if the method could be used in platforms available to pathology departments free of cost. We hope to evaluate immune score on other digital image analysis platforms in close collaboration with researchers within our network.

7. References

1. Aeffner F, Zarella MD, Buchbinder N, et al. Introduction to Digital Image Analysis in Whole-slide Imaging: A White Paper from the Digital Pathology Association. *J Pathol Inform* 2019; 10:9.
2. Weinstein RS, Graham AR, Lian F, et al. Reconciliation of diverse telepathology system designs. Historic issues and implications for emerging markets and new applications. *Apmis* 2012; 120(4):256-75.
3. Griffin J, Treanor D. Digital pathology in clinical use: where are we now and what is holding us back? *Histopathology* 2017; 70(1):134-145.
4. Cheng CL, Azhar R, Sng SH, et al. Enabling digital pathology in the diagnostic setting: navigating through the implementation journey in an academic medical centre. *J Clin Pathol* 2016; 69(9):784-92.
5. Stathonikos N, Veta M, Huisman A, et al. Going fully digital: Perspective of a Dutch academic pathology lab. *J Pathol Inform* 2013; 4:15.
6. Webster JD, Dunstan RW. Whole-slide imaging and automated image analysis: considerations and opportunities in the practice of pathology. *Vet Pathol* 2014; 51(1):211-23.
7. Diller RB, Kellar RS. Validating whole slide digital morphometric analysis as a microscopy tool. *Microsc Microanal* 2015; 21(1):249-55.
8. Aeffner F, Wilson K, Bolon B, et al. Commentary: Roles for Pathologists in a High-throughput Image Analysis Team. *Toxicol Pathol* 2016; 44(6):825-34.
9. Kumar N, Gupta R, Gupta S. Whole Slide Imaging (WSI) in Pathology: Current Perspectives and Future Directions. *J Digit Imaging* 2020; 33(4):1034-1040.
10. Wright AM, Smith D, Dhurandhar B, et al. Digital slide imaging in cervicovaginal cytology: a pilot study. *Arch Pathol Lab Med* 2013; 137(5):618-24.
11. Meijer GA, Beliën JA, van Diest PJ, et al. Origins of ... image analysis in clinical pathology. *J Clin Pathol* 1997; 50(5):365-70.
12. Laurinavicius A, Laurinaviciene A, Dasevicius D, et al. Digital image analysis in pathology: benefits and obligation. *Anal Cell Pathol (Amst)* 2012; 35(2):75-8.
13. Gudlaugsson E, Skaland I, Janssen EA, et al. Comparison of the effect of different techniques for measurement of Ki67 proliferation on reproducibility and prognosis prediction accuracy in breast cancer. *Histopathology* 2012; 61(6):1134-44.
14. Reid MD, Bagci P, Ohike N, et al. Calculation of the Ki67 index in pancreatic neuroendocrine tumors: a comparative analysis of four counting methodologies. *Mod Pathol* 2015; 28(5):686-94.
15. Tang LH, Gonen M, Hedvat C, et al. Objective quantification of the Ki67 proliferative index in neuroendocrine tumors of the gastroenteropancreatic system: a comparison of digital image analysis with manual methods. *Am J Surg Pathol* 2012; 36(12):1761-70.
16. Wolff AC, Hammond MEH, Allison KH, et al. Human Epidermal Growth Factor Receptor 2 Testing in Breast Cancer: American Society of Clinical

-
- Oncology/College of American Pathologists Clinical Practice Guideline Focused Update. *Arch Pathol Lab Med* 2018; 142(11):1364-1382.
17. Bui MM, Riben MW, Allison KH, et al. Quantitative Image Analysis of Human Epidermal Growth Factor Receptor 2 Immunohistochemistry for Breast Cancer: Guideline From the College of American Pathologists. *Arch Pathol Lab Med* 2019; 143(10):1180-1195.
 18. Cui M, Zhang DY. Artificial intelligence and computational pathology. *Laboratory Investigation* 2021; 101(4):412-422.
 19. Bini SA. Artificial Intelligence, Machine Learning, Deep Learning, and Cognitive Computing: What Do These Terms Mean and How Will They Impact Health Care? *J Arthroplasty* 2018; 33(8):2358-2361.
 20. Komura D, Ishikawa S. Machine Learning Methods for Histopathological Image Analysis. *Comput Struct Biotechnol J* 2018; 16:34-42.
 21. Abels E, Pantanowitz L, Aeffner F, et al. Computational pathology definitions, best practices, and recommendations for regulatory guidance: a white paper from the Digital Pathology Association. *J Pathol* 2019; 249(3):286-294.
 22. Levine AB, Schlosser C, Grewal J, et al. Rise of the Machines: Advances in Deep Learning for Cancer Diagnosis. *Trends Cancer* 2019; 5(3):157-169.
 23. Skrede OJ, De Raedt S, Kleppe A, et al. Deep learning for prediction of colorectal cancer outcome: a discovery and validation study. *Lancet* 2020; 395(10221):350-360.
 24. Korbar B, Olofson AM, Miraflor AP, et al. Deep Learning for Classification of Colorectal Polyps on Whole-slide Images. *J Pathol Inform* 2017; 8:30.
 25. Pagni F, Bono F, Di Bella C, et al. Virtual surgical pathology in underdeveloped countries: The Zambia Project. *Arch Pathol Lab Med* 2011; 135(2):215-9.
 26. Hitchcock CL. The future of telepathology for the developing world. *Arch Pathol Lab Med* 2011; 135(2):211-4.
 27. Nordrum I, Engum B, Rinde E, et al. Remote frozen section service: a telepathology project in northern Norway. *Hum Pathol* 1991; 22(6):514-8.
 28. Graham AR, Bhattacharyya AK, Scott KM, et al. Virtual slide telepathology for an academic teaching hospital surgical pathology quality assurance program. *Hum Pathol* 2009; 40(8):1129-36.
 29. Chan HP, Samala RK, Hadjiiski LM, et al. Deep Learning in Medical Image Analysis. *Adv Exp Med Biol* 2020; 1213:3-21.
 30. Jara-Lazaro AR, Thamboo TP, Teh M, et al. Digital pathology: exploring its applications in diagnostic surgical pathology practice. *Pathology* 2010; 42(6):512-8.
 31. Nakhleh RE, Idowu MO, Souers RJ, et al. Mislabeling of cases, specimens, blocks, and slides: a college of american pathologists study of 136 institutions. *Arch Pathol Lab Med* 2011; 135(8):969-74.
 32. Zarbo RJ, D'Angelo R. The Henry ford production system: effective reduction of process defects and waste in surgical pathology. *Am J Clin Pathol* 2007; 128(6):1015-22.
 33. Nakhleh RE. Role of Informatics in Patient Safety and Quality Assurance. *Surg Pathol Clin* 2015; 8(2):301-7.

34. Williams BJ, DaCosta P, Goacher E, et al. A Systematic Analysis of Discordant Diagnoses in Digital Pathology Compared With Light Microscopy. *Arch Pathol Lab Med* 2017; 141(12):1712-1718.
35. Lashen A, Ibrahim A, Katayama A, et al. Visual assessment of mitotic figures in breast cancer: a comparative study between light microscopy and whole slide images. *Histopathology* 2021.
36. Tomić S, Mrklić I, Razumović JJ, et al. Inter-laboratory comparison of Ki-67 proliferating index detected by visual assessment and automated digital image analysis. *Breast Dis* 2019; 38(2):73-79.
37. Rawlins SR, El-Zammar O, Zinkievich JM, et al. Digital quantification is more precise than traditional semiquantitation of hepatic steatosis: correlation with fibrosis in 220 treatment-naïve patients with chronic hepatitis C. *Dig Dis Sci* 2010; 55(7):2049-57.
38. Jahn SW, Plass M, Moïnfar F. Digital Pathology: Advantages, Limitations and Emerging Perspectives. *Journal of Clinical Medicine* 2020; 9(11):3697.
39. Aeffner F, Wilson K, Martin NT, et al. The Gold Standard Paradox in Digital Image Analysis: Manual Versus Automated Scoring as Ground Truth. *Arch Pathol Lab Med* 2017; 141(9):1267-1275.
40. Pannucci CJ, Wilkins EG. Identifying and avoiding bias in research. *Plast Reconstr Surg* 2010; 126(2):619-625.
41. Whiting P, Rutjes AW, Reitsma JB, et al. Sources of variation and bias in studies of diagnostic accuracy: a systematic review. *Ann Intern Med* 2004; 140(3):189-202.
42. Conway C, Dobson L, O'Grady A, et al. Virtual microscopy as an enabler of automated/quantitative assessment of protein expression in TMAs. *Histochem Cell Biol* 2008; 130(3):447-63.
43. Raffone A, Srinivasan N, van Leeuwen C. The interplay of attention and consciousness in visual search, attentional blink and working memory consolidation. *Philos Trans R Soc Lond B Biol Sci* 2014; 369(1641):20130215.
44. Memmert D. The effects of eye movements, age, and expertise on inattentive blindness. *Conscious Cogn* 2006; 15(3):620-7.
45. Potchen EJ. Measuring observer performance in chest radiology: some experiences. *J Am Coll Radiol* 2006; 3(6):423-32.
46. Perales E, Martínez-Verdú FM, Linhares JM, et al. Number of discernible colors for color-deficient observers estimated from the MacAdam limits. *J Opt Soc Am A Opt Image Sci Vis* 2010; 27(10):2106-14.
47. Kay EW, O'Dowd J, Thomas R, et al. Mild abnormalities in liver histology associated with chronic hepatitis: distinction from normal liver histology. *J Clin Pathol* 1997; 50(11):929-31.
48. Thavarajah S, White WB, Mansoor GA. Terminal digit bias in a specialty hypertension faculty practice. *J Hum Hypertens* 2003; 17(12):819-22.
49. Wen SW, Kramer MS, Hoey J, et al. Terminal digit preference, random error, and bias in routine clinical measurement of blood pressure. *J Clin Epidemiol* 1993; 46(10):1187-93.

-
50. Berbaum KS, Scharzt KM, Caldwell RT, et al. Satisfaction of search from detection of pulmonary nodules in computed tomography of the chest. *Acad Radiol* 2013; 20(2):194-201.
 51. Nickerson RS. Confirmation Bias: A Ubiquitous Phenomenon in Many Guises. *Review of General Psychology* 1998; 2(2):175-220.
 52. Witt JK. Awareness Is Not a Necessary Characteristic of a Perceptual Effect: Commentary on Firestone (2013). *Perspect Psychol Sci* 2015; 10(6):865-72.
 53. Cancer 2018, 12. September. Available at: <https://www.who.int/news-room/fact-sheets/detail/cancer>.
 54. Cancer in Norway 2020. Cancer Registry of Norway, Institute of Population-based Cancer Research 2021.
 55. Knudson AG. Two genetic hits (more or less) to cancer. *Nat Rev Cancer* 2001; 1(2):157-62.
 56. Croce CM. Oncogenes and cancer. *N Engl J Med* 2008; 358(5):502-11.
 57. Dupont C, Armant DR, Brenner CA. Epigenetics: definition, mechanisms and clinical perspective. *Seminars in reproductive medicine* 2009; 27(5):351-357.
 58. Greenman C, Stephens P, Smith R, et al. Patterns of somatic mutation in human cancer genomes. *Nature* 2007; 446(7132):153-8.
 59. Sun W, Yang J. Functional mechanisms for human tumor suppressors. *J Cancer* 2010; 1:136-40.
 60. Wang LH, Wu CF, Rajasekaran N, et al. Loss of Tumor Suppressor Gene Function in Human Cancer: An Overview. *Cell Physiol Biochem* 2018; 51(6):2647-2693.
 61. Hanahan D, Weinberg RA. The hallmarks of cancer. *Cell* 2000; 100(1):57-70.
 62. Hanahan D, Weinberg RA. Hallmarks of cancer: the next generation. *Cell* 2011; 144(5):646-74.
 63. Messerschmidt JL, Prendergast GC, Messerschmidt GL. How Cancers Escape Immune Destruction and Mechanisms of Action for the New Significantly Active Immune Therapies: Helping Nonimmunologists Decipher Recent Advances. *Oncologist* 2016; 21(2):233-43.
 64. Artandi SE, DePinho RA. Telomeres and telomerase in cancer. *Carcinogenesis* 2010; 31(1):9-18.
 65. Gunter MJ, Alhomoud S, Arnold M, et al. Meeting report from the joint IARC-NCI international cancer seminar series: a focus on colorectal cancer. *Ann Oncol* 2019; 30(4):510-519.
 66. Bray F, Ferlay J, Soerjomataram I, et al. Global cancer statistics 2018: GLOBOCAN estimates of incidence and mortality worldwide for 36 cancers in 185 countries. *CA Cancer J Clin* 2018; 68(6):394-424.
 67. Erratum: Global cancer statistics 2018: GLOBOCAN estimates of incidence and mortality worldwide for 36 cancers in 185 countries. *CA Cancer J Clin* 2020; 70(4):313.
 68. Nedrebø BS, Søreide K, Eriksen MT, et al. Survival effect of implementing national treatment strategies for curatively resected colonic and rectal cancer. *Br J Surg* 2011; 98(5):716-23.
 69. The global, regional, and national burden of colorectal cancer and its attributable risk factors in 195 countries and territories, 1990-2017: a

- systematic analysis for the Global Burden of Disease Study 2017. *Lancet Gastroenterol Hepatol* 2019; 4(12):913-933.
70. Ferlay J, Soerjomataram I, Dikshit R, et al. Cancer incidence and mortality worldwide: sources, methods and major patterns in GLOBOCAN 2012. *Int J Cancer* 2015; 136(5):E359-86.
 71. Cancer Today - IARC 2020. Available at: https://gco.iarc.fr/today/online-analysis-map?v=2020&mode=population&mode_population=continents&population=900&populations=900&key=asr&sex=0&cancer=39&type=0&statistic=5&prev_alence=0&population_group=0&ages_group%5B%5D=0&ages_group%5B%5D=17&nb_items=10&group_cancer=1&include_nmssc=1&include_nmssc_oth er=1&projection=natural-earth&color_palette=default&map_scale=quantile&map_nb_colors=5&continent=0&rotate=%255B10%252C0%255D. Accessed 2021, 5. February.
 72. Arnold M, Sierra MS, Laversanne M, et al. Global patterns and trends in colorectal cancer incidence and mortality. *Gut* 2017; 66(4):683-691.
 73. Kingham TP, Alatise OI, Vanderpuye V, et al. Treatment of cancer in sub-Saharan Africa. *Lancet Oncol* 2013; 14(4):e158-67.
 74. Schreuders EH, Ruco A, Rabeneck L, et al. Colorectal cancer screening: a global overview of existing programmes. *Gut* 2015; 64(10):1637-49.
 75. Cardoso R, Guo F, Heisser T, et al. Colorectal cancer incidence, mortality, and stage distribution in European countries in the colorectal cancer screening era: an international population-based study. *Lancet Oncol* 2021.
 76. Krefregisteret. Tarmscreening blir tilbud til alle 55- åringer. Available at: <https://krefttforeningen.no/forebygging/screening-og-masseundersokelser/tarmscreeningprogrammet/>. Accessed 18. September, 2021.
 77. Dekker E, Tanis PJ, Vleugels JLA, et al. Colorectal cancer. *Lancet* 2019; 394(10207):1467-1480.
 78. Schoen RE, Razzak A, Yu KJ, et al. Incidence and mortality of colorectal cancer in individuals with a family history of colorectal cancer. *Gastroenterology* 2015; 149(6):1438-1445.e1.
 79. Syngal S, Brand RE, Church JM, et al. ACG clinical guideline: Genetic testing and management of hereditary gastrointestinal cancer syndromes. *Am J Gastroenterol* 2015; 110(2):223-62; quiz 263.
 80. Lung MS, Trainer AH, Campbell I, et al. Familial colorectal cancer. *Intern Med J* 2015; 45(5):482-91.
 81. Baglietto L, Jenkins MA, Severi G, et al. Measures of familial aggregation depend on definition of family history: meta-analysis for colorectal cancer. *J Clin Epidemiol* 2006; 59(2):114-24.
 82. Vogelstein B, Fearon ER, Hamilton SR, et al. Genetic alterations during colorectal-tumor development. *N Engl J Med* 1988; 319(9):525-32.
 83. Fearon ER, Vogelstein B. A genetic model for colorectal tumorigenesis. *Cell* 1990; 61(5):759-67.

84. Robles AI, Traverso G, Zhang M, et al. Whole-Exome Sequencing Analyses of Inflammatory Bowel Disease–Associated Colorectal Cancers. *Gastroenterology* 2016; 150(4):931-943.
85. Richard GF, Kerrest A, Dujon B. Comparative genomics and molecular dynamics of DNA repeats in eukaryotes. *Microbiol Mol Biol Rev* 2008; 72(4):686-727.
86. Vilar E, Gruber SB. Microsatellite instability in colorectal cancer—the stable evidence. *Nat Rev Clin Oncol* 2010; 7(3):153-62.
87. Lander ES, Linton LM, Birren B, et al. Initial sequencing and analysis of the human genome. *Nature* 2001; 409(6822):860-921.
88. Brinkmann B, Klintschar M, Neuhuber F, et al. Mutation rate in human microsatellites: influence of the structure and length of the tandem repeat. *Am J Hum Genet* 1998; 62(6):1408-15.
89. Aaltonen LA, Peltomäki P, Leach FS, et al. Clues to the pathogenesis of familial colorectal cancer. *Science* 1993; 260(5109):812-6.
90. Thibodeau SN, Bren G, Schaid D. Microsatellite instability in cancer of the proximal colon. *Science* 1993; 260(5109):816-9.
91. Ionov Y, Peinado MA, Malkhosyan S, et al. Ubiquitous somatic mutations in simple repeated sequences reveal a new mechanism for colonic carcinogenesis. *Nature* 1993; 363(6429):558-61.
92. Hampel H, Frankel WL, Martin E, et al. Screening for the Lynch syndrome (hereditary nonpolyposis colorectal cancer). *N Engl J Med* 2005; 352(18):1851-60.
93. Guastadisegni C, Colafranceschi M, Ottini L, et al. Microsatellite instability as a marker of prognosis and response to therapy: a meta-analysis of colorectal cancer survival data. *Eur J Cancer* 2010; 46(15):2788-98.
94. Aaltonen LA, Salovaara R, Kristo P, et al. Incidence of hereditary nonpolyposis colorectal cancer and the feasibility of molecular screening for the disease. *N Engl J Med* 1998; 338(21):1481-7.
95. Salovaara R, Loukola A, Kristo P, et al. Population-based molecular detection of hereditary nonpolyposis colorectal cancer. *J Clin Oncol* 2000; 18(11):2193-200.
96. Boland CR, Thibodeau SN, Hamilton SR, et al. A National Cancer Institute Workshop on Microsatellite Instability for cancer detection and familial predisposition: development of international criteria for the determination of microsatellite instability in colorectal cancer. *Cancer Res* 1998; 58(22):5248-57.
97. Leach FS, Polyak K, Burrell M, et al. Expression of the human mismatch repair gene hMSH2 in normal and neoplastic tissues. *Cancer Res* 1996; 56(2):235-40.
98. Beamer LC, Grant ML, Espenschied CR, et al. Reflex immunohistochemistry and microsatellite instability testing of colorectal tumors for Lynch syndrome among US cancer programs and follow-up of abnormal results. *J Clin Oncol* 2012; 30(10):1058-63.
99. Luchini C, Bibeau F, Ligtenberg MJL, et al. ESMO recommendations on microsatellite instability testing for immunotherapy in cancer, and its

- relationship with PD-1/PD-L1 expression and tumour mutational burden: a systematic review-based approach. *Ann Oncol* 2019; 30(8):1232-1243.
100. Loughrey MB, McGrath J, Coleman HG, et al. Identifying mismatch repair-deficient colon cancer: near-perfect concordance between immunohistochemistry and microsatellite instability testing in a large, population-based series. *Histopathology* 2021; 78(3):401-413.
 101. McCarthy AJ, Capo-Chichi JM, Spence T, et al. Heterogenous loss of mismatch repair (MMR) protein expression: a challenge for immunohistochemical interpretation and microsatellite instability (MSI) evaluation. *J Pathol Clin Res* 2019; 5(2):115-129.
 102. Nasjonalt handlingsprogram med retningslinjer for diagnostikk, behandling og oppfølging av kreft i tykktarm og endetarm 2021, 12. January. Available at: <https://helsedirektoratet.no/retningslinjer/nasjonalt-handlingsprogram-med-retningslinjer-for-diagnostikk-behandling-og-oppfolging-av-kreft-i-tykktarm-og-endetarm>.
 103. Vasen HF, Blanco I, Aktan-Collan K, et al. Revised guidelines for the clinical management of Lynch syndrome (HNPCC): recommendations by a group of European experts. *Gut* 2013; 62(6):812-23.
 104. Watson MM, Berg M, Soreide K. Prevalence and implications of elevated microsatellite alterations at selected tetranucleotides in cancer. *Br J Cancer* 2014; 111(5):823-7.
 105. Koi M, Tseng-Rogenski SS, Carethers JM. Inflammation-associated microsatellite alterations: Mechanisms and significance in the prognosis of patients with colorectal cancer. *World Journal of Gastrointestinal Oncology* 2018; 10(1):1-14.
 106. Watson MM, Kanani A, Lea D, et al. Elevated Microsatellite Alterations at Selected Tetranucleotides (EMAST) in Colorectal Cancer is Associated with an Elderly, Frail Phenotype and Improved Recurrence-Free Survival. *Ann Surg Oncol* 2020; 27(4):1058-1067.
 107. Hazewinkel Y, Dekker E. Colonoscopy: basic principles and novel techniques. *Nature Reviews Gastroenterology & Hepatology* 2011; 8(10):554-564.
 108. Becerra AZ, Probst CP, Tejani MA, et al. Evaluating the Prognostic Role of Elevated Preoperative Carcinoembryonic Antigen Levels in Colon Cancer Patients: Results from the National Cancer Database. *Ann Surg Oncol* 2016; 23(5):1554-61.
 109. Körner H, Söreide K, Stokkeland PJ, et al. Diagnostic Accuracy of Serum-Carcinoembryonic Antigen in Recurrent Colorectal Cancer: A Receiver Operating Characteristic Curve Analysis. *Annals of Surgical Oncology* 2007; 14(2):417-423.
 110. AJCC Cancer Staging Manual. 8 ed. Cham, Switzerland: Springer International Publishing AG, 2017.
 111. Weiser MR. AJCC 8th Edition: Colorectal Cancer. *Ann Surg Oncol* 2018; 25(6):1454-1455.
 112. WHO Classification of Tumours, Digestive System Tumours. 5 ed. Vol. 1: IARC Publications, 2019.

113. Cho SJ, Kakar S. Tumor Budding in Colorectal Carcinoma: Translating a Morphologic Score Into Clinically Meaningful Results. *Arch Pathol Lab Med* 2018; 142(8):952-957.
114. Lugli A, Kirsch R, Ajioka Y, et al. Recommendations for reporting tumor budding in colorectal cancer based on the International Tumor Budding Consensus Conference (ITBCC) 2016. *Mod Pathol* 2017; 30(9):1299-1311.
115. Williams ST, Beart RW, Jr. Staging of colorectal cancer. *Semin Surg Oncol* 1992; 8(2):89-93.
116. Hashiguchi Y, Hase K, Kotake K, et al. Evaluation of the seventh edition of the tumour, node, metastasis (TNM) classification for colon cancer in two nationwide registries of the United States and Japan. *Colorectal Dis* 2012; 14(9):1065-74.
117. Lea D, Haland S, Hagland HR, et al. Accuracy of TNM staging in colorectal cancer: a review of current culprits, the modern role of morphology and stepping-stones for improvements in the molecular era. *Scand J Gastroenterol* 2014; 49(10):1153-63.
118. Cascinu S, Staccioli MP, Gasparini G, et al. Expression of vascular endothelial growth factor can predict event-free survival in stage II colon cancer. *Clin Cancer Res* 2000; 6(7):2803-7.
119. Auclin E, Zaanan A, Vernerey D, et al. Subgroups and prognostication in stage III colon cancer: future perspectives for adjuvant therapy. *Ann Oncol* 2017; 28(5):958-968.
120. Nagtegaal ID, Quirke P, Schmol HJ. Has the new TNM classification for colorectal cancer improved care? *Nat Rev Clin Oncol* 2012; 9(2):119-23.
121. Puppa G, Sonzogni A, Colombari R, et al. TNM staging system of colorectal carcinoma: a critical appraisal of challenging issues. *Arch Pathol Lab Med* 2010; 134(6):837-52.
122. Lin Y, Chappell R, Gonen M. A systematic selection method for the development of cancer staging systems. *Stat Methods Med Res* 2013.
123. Nagtegaal ID, Tot T, Jayne DG, et al. Lymph nodes, tumor deposits, and TNM: are we getting better? *J Clin Oncol* 2011; 29(18):2487-92.
124. Lan YT, Yang SH, Chang SC, et al. Analysis of the seventh edition of American Joint Committee on colon cancer staging. *Int J Colorectal Dis* 2012; 27(5):657-63.
125. Quirke P, Cuvelier C, Ensari A, et al. Evidence-based medicine: the time has come to set standards for staging. *J Pathol* 2010; 221(4):357-60.
126. Ueno H, Mochizuki H, Akagi Y, et al. Optimal colorectal cancer staging criteria in TNM classification. *J Clin Oncol* 2012; 30(13):1519-26.
127. Bosetti C, Levi F, Rosato V, et al. Recent trends in colorectal cancer mortality in Europe. *Int J Cancer* 2011; 129(1):180-91.
128. Edwards BK, Ward E, Kohler BA, et al. Annual report to the nation on the status of cancer, 1975-2006, featuring colorectal cancer trends and impact of interventions (risk factors, screening, and treatment) to reduce future rates. *Cancer* 2010; 116(3):544-73.
129. Schubbert S, Shannon K, Bollag G. Hyperactive Ras in developmental disorders and cancer. *Nat Rev Cancer* 2007; 7(4):295-308.

130. Douillard JY, Oliner KS, Siena S, et al. Panitumumab-FOLFOX4 treatment and RAS mutations in colorectal cancer. *N Engl J Med* 2013; 369(11):1023-34.
131. Cremolini C, Loupakis F, Antoniotti C, et al. FOLFOXIRI plus bevacizumab versus FOLFIRI plus bevacizumab as first-line treatment of patients with metastatic colorectal cancer: updated overall survival and molecular subgroup analyses of the open-label, phase 3 TRIBE study. *Lancet Oncol* 2015; 16(13):1306-15.
132. Modest DP, Ricard I, Heinemann V, et al. Outcome according to KRAS-, NRAS- and BRAF-mutation as well as KRAS mutation variants: pooled analysis of five randomized trials in metastatic colorectal cancer by the AIO colorectal cancer study group. *Ann Oncol* 2016; 27(9):1746-53.
133. Hu Y, Tao SY, Deng JM, et al. Prognostic Value of NRAS Gene for Survival of Colorectal Cancer Patients: A Systematic Review and Meta-Analysis. *Asian Pac J Cancer Prev* 2018; 19(11):3001-3008.
134. Ducreux M, Chamseddine A, Laurent-Puig P, et al. Molecular targeted therapy of BRAF-mutant colorectal cancer. *Ther Adv Med Oncol* 2019; 11:1758835919856494.
135. Le DT, Uram JN, Wang H, et al. PD-1 Blockade in Tumors with Mismatch-Repair Deficiency. *N Engl J Med* 2015; 372(26):2509-20.
136. Popat S, Hubner R, Houlston RS. Systematic review of microsatellite instability and colorectal cancer prognosis. *J Clin Oncol* 2005; 23(3):609-18.
137. Dudley JC, Lin MT, Le DT, et al. Microsatellite Instability as a Biomarker for PD-1 Blockade. *Clin Cancer Res* 2016; 22(4):813-20.
138. Kim CG, Ahn JB, Jung M, et al. Effects of microsatellite instability on recurrence patterns and outcomes in colorectal cancers. *Br J Cancer* 2016; 115(1):25-33.
139. Carethers JM, Chauhan DP, Fink D, et al. Mismatch repair proficiency and in vitro response to 5-fluorouracil. *Gastroenterology* 1999; 117(1):123-31.
140. Kim GP, Colangelo LH, Wieand HS, et al. Prognostic and predictive roles of high-degree microsatellite instability in colon cancer: a National Cancer Institute-National Surgical Adjuvant Breast and Bowel Project Collaborative Study. *J Clin Oncol* 2007; 25(7):767-72.
141. Deng G, Bell I, Crawley S, et al. BRAF mutation is frequently present in sporadic colorectal cancer with methylated hMLH1, but not in hereditary nonpolyposis colorectal cancer. *Clin Cancer Res* 2004; 10(1 Pt 1):191-5.
142. Aasebø K, Dragomir A, Sundström M, et al. Consequences of a high incidence of microsatellite instability and BRAF-mutated tumors: A population-based cohort of metastatic colorectal cancer patients. *Cancer Med* 2019; 8(7):3623-3635.
143. Yaghoubi N, Soltani A, Ghazvini K, et al. PD-1/ PD-L1 blockade as a novel treatment for colorectal cancer. *Biomed Pharmacother* 2019; 110:312-318.
144. Overman MJ, Lonardi S, Wong KYM, et al. Durable Clinical Benefit With Nivolumab Plus Ipilimumab in DNA Mismatch Repair-Deficient/Microsatellite Instability-High Metastatic Colorectal Cancer. *J Clin Oncol* 2018; 36(8):773-779.

145. Boyar Cetinkaya R, Aagnes B, Myklebust T, et al. Survival in neuroendocrine neoplasms; A report from a large Norwegian population-based study. *Int J Cancer* 2018; 142(6):1139-1147.
146. Schimmack S, Svejda B, Lawrence B, et al. The diversity and commonalities of gastroenteropancreatic neuroendocrine tumors. *Langenbecks Arch Surg* 2011; 396(3):273-98.
147. Turaga KK, Kvols LK. Recent progress in the understanding, diagnosis, and treatment of gastroenteropancreatic neuroendocrine tumors. *CA Cancer J Clin* 2011; 61(2):113-32.
148. Cives M, Strosberg JR. Gastroenteropancreatic Neuroendocrine Tumors. *CA Cancer J Clin* 2018; 68(6):471-487.
149. Dasari A, Shen C, Halperin D, et al. Trends in the Incidence, Prevalence, and Survival Outcomes in Patients With Neuroendocrine Tumors in the United States. *JAMA Oncol* 2017; 3(10):1335-1342.
150. Boyar Cetinkaya R, Aagnes B, Myklebust TA, et al. Survival in neuroendocrine neoplasms; A report from a large Norwegian population-based study. *Int J Cancer* 2018; 142(6):1139-1147.
151. Zhong Q, Chen QY, Xie JW, et al. Incidence trend and conditional survival estimates of gastroenteropancreatic neuroendocrine tumors: A large population-based study. *Cancer Med* 2018.
152. Merola E, Rinzivillo M, Cicchese N, et al. Digestive neuroendocrine neoplasms: A 2016 overview. *Dig Liver Dis* 2016.
153. Sandvik OM, Søreide K, Gudlaugsson E, et al. Epidemiology and classification of gastroenteropancreatic neuroendocrine neoplasms using current coding criteria. *Br J Surg* 2016; 103(3):226-32.
154. Lee MR, Harris C, Baeg KJ, et al. Incidence Trends of Gastroenteropancreatic Neuroendocrine Tumors in the United States. *Clin Gastroenterol Hepatol* 2019; 17(11):2212-2217 e1.
155. Janson ET, Sørbye H, Welin S, et al. Nordic Guidelines 2010 for diagnosis and treatment of gastroenteropancreatic neuroendocrine tumours. *Acta Oncol* 2010; 49(6):740-56.
156. Modlin IM, Lye KD, Kidd M. A 5-decade analysis of 13,715 carcinoid tumors. *Cancer* 2003; 97(4):934-59.
157. Maggard MA, O'Connell JB, Ko CY. Updated population-based review of carcinoid tumors. *Ann Surg* 2004; 240(1):117-22.
158. Zheng Z, Chen C, Jiang L, et al. Incidence and risk factors of gastrointestinal neuroendocrine neoplasm metastasis in liver, lung, bone, and brain: A population-based study. *Cancer Med* 2019; 8(17):7288-7298.
159. Cai W, Tan Y, Ge W, et al. Pattern and risk factors for distant metastases in gastrointestinal neuroendocrine neoplasms: a population-based study. *Cancer Med* 2018; 7(6):2699-2709.
160. Modlin IM, Oberg K, Chung DC, et al. Gastroenteropancreatic neuroendocrine tumours. *Lancet Oncol* 2008; 9(1):61-72.
161. Kidambi TD, Pedley C, Blanco A, et al. Lower gastrointestinal neuroendocrine neoplasms associated with hereditary cancer syndromes: a case series. *Fam Cancer* 2017; 16(4):537-543.

162. Lewis MA. Hereditary Syndromes in Neuroendocrine Tumors. *Curr Treat Options Oncol* 2020; 21(6):50.
163. Modlin IM, Shapiro MD, Kidd M. Siegfried Oberndorfer: origins and perspectives of carcinoid tumors. *Hum Pathol* 2004; 35(12):1440-51.
164. Gluckman CR, Metz DC. Gastric Neuroendocrine Tumors (Carcinoids). *Curr Gastroenterol Rep* 2019; 21(4):13.
165. Vortmeyer AO, Huang S, Lubensky I, et al. Non-islet origin of pancreatic islet cell tumors. *J Clin Endocrinol Metab* 2004; 89(4):1934-8.
166. Scarpa A, Chang DK, Nones K, et al. Whole-genome landscape of pancreatic neuroendocrine tumours. *Nature* 2017; 543(7643):65-71.
167. Jiao Y, Shi C, Edil BH, et al. DAXX/ATRX, MEN1, and mTOR pathway genes are frequently altered in pancreatic neuroendocrine tumors. *Science* 2011; 331(6021):1199-203.
168. Oberg K, Casanovas O, Castaño JP, et al. Molecular pathogenesis of neuroendocrine tumors: implications for current and future therapeutic approaches. *Clin Cancer Res* 2013; 19(11):2842-9.
169. Missiaglia E, Dalai I, Barbi S, et al. Pancreatic endocrine tumors: expression profiling evidences a role for AKT-mTOR pathway. *J Clin Oncol* 2010; 28(2):245-55.
170. Terris B, Scoazec JY, Rubbia L, et al. Expression of vascular endothelial growth factor in digestive neuroendocrine tumours. *Histopathology* 1998; 32(2):133-8.
171. Faivre S, Niccoli P, Castellano D, et al. Sunitinib in pancreatic neuroendocrine tumors: updated progression-free survival and final overall survival from a phase III randomized study. *Annals of Oncology* 2017; 28(2):339-343.
172. Raymond E, Dahan L, Raoul J-L, et al. Sunitinib Malate for the Treatment of Pancreatic Neuroendocrine Tumors. *New England Journal of Medicine* 2011; 364(6):501-513.
173. Clement D, Ramage J, Srirajaskanthan R. Update on Pathophysiology, Treatment, and Complications of Carcinoid Syndrome. *J Oncol* 2020; 2020:8341426.
174. Garcia-Carbonero R, Capdevila J, Crespo-Herrero G, et al. Incidence, patterns of care and prognostic factors for outcome of gastroenteropancreatic neuroendocrine tumors (GEP-NETs): results from the National Cancer Registry of Spain (RGETNE). *Ann Oncol* 2010; 21(9):1794-1803.
175. Janson ET, Knigge U, Dam G, et al. Nordic guidelines 2021 for diagnosis and treatment of gastroenteropancreatic neuroendocrine neoplasms. *Acta Oncol* 2021:1-11.
176. Papantoniou D, Grönberg M, Landerholm K, et al. Assessment of hormonal levels as prognostic markers and of their optimal cut-offs in small intestinal neuroendocrine tumours grade 2. *Endocrine* 2021; 72(3):893-904.
177. Jensen KH, Hilsted L, Jensen C, et al. Chromogranin A is a sensitive marker of progression or regression in ileo-cecal neuroendocrine tumors. *Scand J Gastroenterol* 2013; 48(1):70-7.
178. Pollard J, McNeely P, Menda Y. Nuclear Imaging of Neuroendocrine Tumors. *Surg Oncol Clin N Am* 2020; 29(2):209-221.

179. Putzer D, Schullian P, Jaschke W, et al. NEN: Advancement in Diagnosis and Minimally Invasive Therapy. *Rofo* 2020; 192(5):422-430.
180. Mohamed A, Strosberg JR. Medical Management of Gastroenteropancreatic Neuroendocrine Tumors: Current Strategies and Future Advances. *J Nucl Med* 2019; 60(6):721-727.
181. Hu Y, Ye Z, Wang F, et al. Role of Somatostatin Receptor in Pancreatic Neuroendocrine Tumor Development, Diagnosis, and Therapy. *Front Endocrinol (Lausanne)* 2021; 12:679000.
182. Patel N, Barbieri A, Gibson J. Neuroendocrine Tumors of the Gastrointestinal Tract and Pancreas. *Surg Pathol Clin* 2019; 12(4):1021-1044.
183. Klöppel G. Tumour biology and histopathology of neuroendocrine tumours. *Best Pract Res Clin Endocrinol Metab* 2007; 21(1):15-31.
184. Saeger W, Schnabel PA, Komminoth P. [Grading of neuroendocrine tumors]. *Pathologe* 2016; 37(4):304-13.
185. Pathology and Genetics of Tumours of the Digestive System 3ed. Vol. 2: IARC Publications, 2000.
186. Rindi G, Klöppel G, Alhman H, et al. TNM staging of foregut (neuro)endocrine tumors: a consensus proposal including a grading system. *Virchows Arch* 2006; 449(4):395-401.
187. Nagtegaal ID, Odze RD, Klimstra D, et al. The 2019 WHO classification of tumours of the digestive system. *Histopathology* 2020; 76(2):182-188.
188. McCall CM, Shi C, Cornish TC, et al. Grading of well-differentiated pancreatic neuroendocrine tumors is improved by the inclusion of both Ki67 proliferative index and mitotic rate. *Am J Surg Pathol* 2013; 37(11):1671-7.
189. Elvebakken H, Perren A, Scoazec JY, et al. A consensus developed morphological re-evaluation of 196 high-grade gastroenteropancreatic neuroendocrine neoplasms and its clinical correlations. *Neuroendocrinology* 2020.
190. Tang LH, Basturk O, Sue JJ, et al. A Practical Approach to the Classification of WHO Grade 3 (G3) Well-differentiated Neuroendocrine Tumor (WD-NET) and Poorly Differentiated Neuroendocrine Carcinoma (PD-NEC) of the Pancreas. *Am J Surg Pathol* 2016; 40(9):1192-202.
191. Skaland I, Janssen EA, Gudlaugsson E, et al. Validating the prognostic value of proliferation measured by Phosphohistone H3 (PPH3) in invasive lymph node-negative breast cancer patients less than 71 years of age. *Breast Cancer Res Treat* 2009; 114(1):39-45.
192. Klöppel G, La Rosa S. Ki67 labeling index: assessment and prognostic role in gastroenteropancreatic neuroendocrine neoplasms. *Virchows Arch* 2018; 472(3):341-349.
193. Guadagno E, D'Avella E, Cappabianca P, et al. Ki67 in endocrine neoplasms: to count or not to count, this is the question! A systematic review from the English language literature. *J Endocrinol Invest* 2020; 43(10):1429-1445.
194. Sorbye H, Baudin E, Perren A. The Problem of High-Grade Gastroenteropancreatic Neuroendocrine Neoplasms: Well-Differentiated Neuroendocrine Tumors, Neuroendocrine Carcinomas, and Beyond. *Endocrinol Metab Clin North Am* 2018; 47(3):683-698.

195. Blank A, Wehweck L, Marinoni I, et al. Interlaboratory variability of MIB1 staining in well-differentiated pancreatic neuroendocrine tumors. *Virchows Arch* 2015; 467(5):543-50.
196. NordiCQ 2021. Available at: <https://www.nordiqc.org/index.php>. Accessed 22. June, 2021.
197. Søreide JA, Kvaløy JT, Lea D, et al. The overriding role of surgery and tumor grade for long-term survival in patients with gastroenteropancreatic neuroendocrine neoplasms: A population-based cohort study. *Cancer Rep (Hoboken)* 2021:e1462.
198. Panzuto F, Nasoni S, Falconi M, et al. Prognostic factors and survival in endocrine tumor patients: comparison between gastrointestinal and pancreatic localization. *Endocr Relat Cancer* 2005; 12(4):1083-92.
199. Rindi G, Klöppel G, Couvelard A, et al. TNM staging of midgut and hindgut (neuro) endocrine tumors: a consensus proposal including a grading system. *Virchows Arch* 2007; 451(4):757-62.
200. Frilling A, Åkerström G, Falconi M, et al. Neuroendocrine tumor disease: an evolving landscape. *Endocr Relat Cancer* 2012; 19(5):R163-85.
201. Sakin A, Tambas M, Secmeler S, et al. Factors Affecting Survival in Neuroendocrine Tumors: A 15-Year Single Center Experience. *Asian Pac J Cancer Prev* 2018; 19(12):3597-3603.
202. Zhai H, Li D, Feng Q, et al. Pancreatic neuroendocrine tumours: Grade is superior to T, N, or M status in predicting outcome and selecting patients for chemotherapy:A retrospective cohort study in the SEER database. *Int J Surg* 2019; 66:103-109.
203. Coriat R, Walter T, Terris B, et al. Gastroenteropancreatic Well-Differentiated Grade 3 Neuroendocrine Tumors: Review and Position Statement. *Oncologist* 2016; 21(10):1191-1199.
204. Fuksiewicz M, Kowalska M, Kolaszińska-Ćwikła A, et al. Prognostic value of chromogranin A in patients with GET/NEN in the pancreas and the small intestine. *Endocr Connect* 2018; 7(6):803-810.
205. Marotta V, Zatelli MC, Sciammarella C, et al. Chromogranin A as circulating marker for diagnosis and management of neuroendocrine neoplasms: more flaws than fame. *Endocr Relat Cancer* 2018; 25(1):R11-r29.
206. Ali AS, Langer SW, Federspiel B, et al. PD-L1 expression in gastroenteropancreatic neuroendocrine neoplasms grade 3. *PLoS One* 2020; 15(12):e0243900.
207. Shao C, Li G, Huang L, et al. Prevalence of High Tumor Mutational Burden and Association With Survival in Patients With Less Common Solid Tumors. *JAMA Netw Open* 2020; 3(10):e2025109.
208. Malczewska A, Kos-Kudła B, Kidd M, et al. The clinical applications of a multigene liquid biopsy (NETest) in neuroendocrine tumors. *Adv Med Sci* 2020; 65(1):18-29.
209. Balkwill F, Mantovani A. Inflammation and cancer: back to Virchow? *Lancet* 2001; 357(9255):539-45.

-
210. Colotta F, Allavena P, Sica A, et al. Cancer-related inflammation, the seventh hallmark of cancer: links to genetic instability. *Carcinogenesis* 2009; 30(7):1073-81.
 211. Hussain SP, Harris CC. Inflammation and cancer: an ancient link with novel potentials. *Int J Cancer* 2007; 121(11):2373-80.
 212. de Martel C, Georges D, Bray F, et al. Global burden of cancer attributable to infections in 2018: a worldwide incidence analysis. *Lancet Glob Health* 2020; 8(2):e180-e190.
 213. Ekblom A, Helmick C, Zack M, et al. Ulcerative colitis and colorectal cancer. A population-based study. *N Engl J Med* 1990; 323(18):1228-33.
 214. Gulumian M. The role of oxidative stress in diseases caused by mineral dusts and fibres: current status and future of prophylaxis and treatment. *Mol Cell Biochem* 1999; 196(1-2):69-77.
 215. Miller JF. Immunological function of the thymus. *Lancet* 1961; 2(7205):748-9.
 216. Sharma P, Allison JP. The future of immune checkpoint therapy. *Science* 2015; 348(6230):56-61.
 217. LeBien TW, Tedder TF. B lymphocytes: how they develop and function. *Blood* 2008; 112(5):1570-80.
 218. Sarvaria A, Madrigal JA, Saudemont A. B cell regulation in cancer and anti-tumor immunity. *Cell Mol Immunol* 2017; 14(8):662-674.
 219. Bonam SR, Partidos CD, Halmuthur SKM, et al. An Overview of Novel Adjuvants Designed for Improving Vaccine Efficacy. *Trends Pharmacol Sci* 2017; 38(9):771-793.
 220. Foster DS, Jones RE, Ransom RC, et al. The evolving relationship of wound healing and tumor stroma. *JCI Insight* 2018; 3(18).
 221. Hinshaw DC, Shevde LA. The Tumor Microenvironment Innately Modulates Cancer Progression. *Cancer Res* 2019; 79(18):4557-4566.
 222. de Visser KE, Eichten A, Coussens LM. Paradoxical roles of the immune system during cancer development. *Nat Rev Cancer* 2006; 6(1):24-37.
 223. Di Caro G, Bergomas F, Grizzi F, et al. Occurrence of tertiary lymphoid tissue is associated with T-cell infiltration and predicts better prognosis in early-stage colorectal cancers. *Clin Cancer Res* 2014; 20(8):2147-58.
 224. Roxburgh CS, McMillan DC. The role of the in situ local inflammatory response in predicting recurrence and survival in patients with primary operable colorectal cancer. *Cancer treatment reviews* 2012; 38(5):451-66.
 225. Curtis NJ, Primrose JN, Thomas GJ, et al. The adaptive immune response to colorectal cancer: from the laboratory to clinical practice. *European journal of surgical oncology : the journal of the European Society of Surgical Oncology and the British Association of Surgical Oncology* 2012; 38(10):889-96.
 226. Galon J, Costes A, Sanchez-Cabo F, et al. Type, density, and location of immune cells within human colorectal tumors predict clinical outcome. *Science* 2006; 313(5795):1960-4.
 227. Mlecnik B, Tosolini M, Kirilovsky A, et al. Histopathologic-based prognostic factors of colorectal cancers are associated with the state of the local immune reaction. *J Clin Oncol* 2011; 29(6):610-8.

-
228. Mantovani A, Allavena P, Sica A, et al. Cancer-related inflammation. *Nature* 2008; 454(7203):436-44.
 229. Chaput N, Svrcek M, Auperin A, et al. Tumour-infiltrating CD68+ and CD57+ cells predict patient outcome in stage II-III colorectal cancer. *Br J Cancer* 2013; 109(4):1013-22.
 230. Shia J, Ellis NA, Paty PB, et al. Value of histopathology in predicting microsatellite instability in hereditary nonpolyposis colorectal cancer and sporadic colorectal cancer. *Am J Surg Pathol* 2003; 27(11):1407-17.
 231. Lichtenstern CR, Ngu RK, Shalapour S, et al. Immunotherapy, Inflammation and Colorectal Cancer. *Cells* 2020; 9(3):618.
 232. Couzin-Frankel J. Cancer Immunotherapy. *Science* 2013; 342(6165):1432-1433.
 233. Zugazagoitia J, Guedes C, Ponce S, et al. Current Challenges in Cancer Treatment. *Clin Ther* 2016; 38(7):1551-66.
 234. Franke AJ, Skelton WP, Starr JS, et al. Immunotherapy for Colorectal Cancer: A Review of Current and Novel Therapeutic Approaches. *J Natl Cancer Inst* 2019; 111(11):1131-1141.
 235. André T, Shiu KK, Kim TW, et al. Pembrolizumab in Microsatellite-Instability-High Advanced Colorectal Cancer. *N Engl J Med* 2020; 383(23):2207-2218.
 236. Anitei MG, Zeitoun G, Mlecnik B, et al. Prognostic and predictive values of the immunoscore in patients with rectal cancer. *Clin Cancer Res* 2014; 20(7):1891-9.
 237. Pages F, Mlecnik B, Marliot F, et al. International validation of the consensus Immunoscore for the classification of colon cancer: a prognostic and accuracy study. *Lancet* 2018; 391(10135):2128-2139.
 238. Galon J, Franck P, Marincola FM, et al. Cancer classification using the Immunoscore: a worldwide task force. *Journal of translational medicine* 2012; 10(1):205.
 239. Pagès F, Kirilovsky A, Mlecnik B, et al. In situ cytotoxic and memory T cells predict outcome in patients with early-stage colorectal cancer. *J Clin Oncol* 2009; 27(35):5944-51.
 240. Galon J, Mlecnik B, Bindea G, et al. Towards the introduction of the 'Immunoscore' in the classification of malignant tumours. *J Pathol* 2014; 232(2):199-209.
 241. Selvi I, Demirci U, Bozdogan N, et al. The prognostic effect of immunoscore in patients with clear cell renal cell carcinoma: preliminary results. *Int Urol Nephrol* 2020; 52(1):21-34.
 242. Petrizzo A, Buonaguro L. Application of the Immunoscore as prognostic tool for hepatocellular carcinoma. *J Immunother Cancer* 2016; 4:71.
 243. Kirilovsky A, Marliot F, El Sissy C, et al. Rational bases for the use of the Immunoscore in routine clinical settings as a prognostic and predictive biomarker in cancer patients. *Int Immunol* 2016; 28(8):373-82.
 244. Sclafani RA, Holzen TM. Cell cycle regulation of DNA replication. *Annu Rev Genet* 2007; 41:237-80.

-
245. Mercadante AA, Kasi A. Genetics, Cancer Cell Cycle Phases. StatPearls. Treasure Island (FL): StatPearls Publishing LLC. Copyright © 2021.; 2021.
 246. Menon SS, Guruvayoorappan C, Sakthivel KM, et al. Ki-67 protein as a tumour proliferation marker. *Clin Chim Acta* 2019; 491:39-45.
 247. Sobiecki M, Mrouj K, Colinge J, et al. Cell-Cycle Regulation Accounts for Variability in Ki-67 Expression Levels. *Cancer Res* 2017; 77(10):2722-2734.
 248. Sun X, Kaufman PD. Ki-67: more than a proliferation marker. *Chromosoma* 2018; 127(2):175-186.
 249. Pavel M, Öberg K, Falconi M, et al. Gastroenteropancreatic neuroendocrine neoplasms: ESMO Clinical Practice Guidelines for diagnosis, treatment and follow-up. *Ann Oncol* 2020; 31(7):844-860.
 250. Raap M, Ließem S, Rüschoff J, et al. Quality assurance trials for Ki67 assessment in pathology. *Virchows Arch* 2017; 471(4):501-508.
 251. Polley MY, Leung SC, McShane LM, et al. An international Ki67 reproducibility study. *J Natl Cancer Inst* 2013; 105(24):1897-906.
 252. Tracht J, Zhang K, Peker D. Grading and Prognostication of Neuroendocrine Tumors of the Pancreas: A Comparison Study of Ki67 and PHH3. *J Histochem Cytochem* 2017; 65(7):399-405.
 253. Chan DL, Clarke SJ, Diakos CI, et al. Prognostic and predictive biomarkers in neuroendocrine tumours. *Crit Rev Oncol Hematol* 2017; 113:268-282.
 254. Lee LH, Yang H, Bigras G. Current breast cancer proliferative markers correlate variably based on decoupled duration of cell cycle phases. *Sci Rep* 2014; 4:5122.
 255. Kim JY, Jeong HS, Chung T, et al. The value of phosphohistone H3 as a proliferation marker for evaluating invasive breast cancers: A comparative study with Ki67. *Oncotarget* 2017; 8(39):65064-65076.
 256. Villani V, Mahadevan KK, Ligorio M, et al. Phosphorylated Histone H3 (PHH3) Is a Superior Proliferation Marker for Prognosis of Pancreatic Neuroendocrine Tumors. *Ann Surg Oncol* 2016; 23(Suppl 5):609-617.
 257. Ozturk Sari S, Taskin OC, Gundogdu G, et al. The Impact of Phosphohistone-H3-Assisted Mitotic Count and Ki67 Score in the Determination of Tumor Grade and Prediction of Distant Metastasis in Well-Differentiated Pancreatic Neuroendocrine Tumors. *Endocr Pathol* 2016; 27(2):162-70.
 258. Sun A, Zhou W, Lunceford J, et al. Level of phosphohistone H3 among various types of human cancers. *BMJ Open* 2012; 2(5).
 259. Bossard C, Jarry A, Colombeix C, et al. Phosphohistone H3 labelling for histoprognostic grading of breast adenocarcinomas and computer-assisted determination of mitotic index. *J Clin Pathol* 2006; 59(7):706-10.
 260. Ribalta T, McCutcheon IE, Aldape KD, et al. The mitosis-specific antibody anti-phosphohistone-H3 (PHH3) facilitates rapid reliable grading of meningiomas according to WHO 2000 criteria. *Am J Surg Pathol* 2004; 28(11):1532-6.
 261. Soreide K, Watson MM, Lea D, et al. Assessment of clinically related outcomes and biomarker analysis for translational integration in colorectal cancer (ACROBATICC): study protocol for a population-based, consecutive

- cohort of surgically treated colorectal cancers and resected colorectal liver metastasis. *J Transl Med* 2016; 14(1):192.
262. Åkerström G, Falconi M, Kianmanesh R, et al. ENETS Consensus Guidelines for the Standards of Care in Neuroendocrine Tumors: pre- and perioperative therapy in patients with neuroendocrine tumors. *Neuroendocrinology* 2009; 90(2):203-8.
 263. Sundin A, Vullierme MP, Kaltsas G, et al. ENETS Consensus Guidelines for the Standards of Care in Neuroendocrine Tumors: radiological examinations. *Neuroendocrinology* 2009; 90(2):167-83.
 264. Collaborative. Neuroendokrine tumorer. En veiledning til diagnostikk og behandling(in Norwegian). Norwegian Neuroendocrine Tumor Group – 2003.
 265. Elm Ev, Altman DG, Egger M, et al. Strengthening the Reporting of Observational Studies in Epidemiology (STROBE) statement: guidelines for reporting observational studies. *BMJ (Clinical research ed.)* 2007; 335(7624):806–808.
 266. McShane LM, Altman DG, Sauerbrei W, et al. REporting recommendations for tumour MARKer prognostic studies (REMARK). *British journal of cancer* 2005; 93(4):387-391.
 267. von Elm E, Altman DG, Egger M, et al. Strengthening the Reporting of Observational Studies in Epidemiology (STROBE) statement: guidelines for reporting observational studies. *Bmj* 2007; 335(7624):806-8.
 268. von Elm E, Altman DG, Egger M, et al. The Strengthening the Reporting of Observational Studies in Epidemiology (STROBE) statement: guidelines for reporting observational studies. *J Clin Epidemiol* 2008; 61(4):344-9.
 269. McShane LM, Altman DG, Sauerbrei W, et al. REporting recommendations for tumour MARKer prognostic studies (REMARK). *Br J Cancer* 2005; 93(4):387-91.
 270. Cohen J. Weighted kappa: nominal scale agreement with provision for scaled disagreement or partial credit. *Psychol Bull* 1968; 70(4):213-20.
 271. Lowry R. Kappa as a Measure of Concordance in Categorical Sorting 2021. Available at: <http://vassarstats.net/kappa.html>. Accessed 18. September, 2021.
 272. Koo TK, Li MY. A Guideline of Selecting and Reporting Intraclass Correlation Coefficients for Reliability Research. *J Chiropr Med* 2016; 15(2):155-63.
 273. Bland JM, Altman DG. Comparing methods of measurement: why plotting difference against standard method is misleading. *Lancet* 1995; 346(8982):1085-7.
 274. Adan A, Alizada G, Kiraz Y, et al. Flow cytometry: basic principles and applications. *Crit Rev Biotechnol* 2017; 37(2):163-176.
 275. Wilkerson MJ. Principles and applications of flow cytometry and cell sorting in companion animal medicine. *Vet Clin North Am Small Anim Pract* 2012; 42(1):53-71.
 276. Hagland HR, Lea D, Watson MM, et al. Correlation of Blood T-Cells to Intratumoural Density and Location of CD3(+) and CD8(+) T-Cells in Colorectal Cancer. *Anticancer Res* 2017; 37(2):675-683.

-
277. Decorte R, Cassiman JJ. Forensic medicine and the polymerase chain reaction technique. *J Med Genet* 1993; 30(8):625-33.
 278. Templeton NS. The polymerase chain reaction. History, methods, and applications. *Diagn Mol Pathol* 1992; 1(1):58-72.
 279. Green MR, Sambrook J. Polymerase Chain Reaction. *Cold Spring Harb Protoc* 2019; 2019(6).
 280. Arya M, Shergill IS, Williamson M, et al. Basic principles of real-time quantitative PCR. *Expert Review of Molecular Diagnostics* 2005; 5(2):209-219.
 281. Prichard JW. Overview of automated immunohistochemistry. *Arch Pathol Lab Med* 2014; 138(12):1578-82.
 282. Leong AS, Leong TY. Standardization in immunohistology. *Methods Mol Biol* 2011; 724:37-68.
 283. Zlobec I, Steele R, Michel RP, et al. Scoring of p53, VEGF, Bcl-2 and APAF-1 immunohistochemistry and interobserver reliability in colorectal cancer. *Modern Pathology* 2006; 19(9):1236-1242.
 284. True LD. Methodological requirements for valid tissue-based biomarker studies that can be used in clinical practice. *Virchows Arch* 2014; 464(3):257-63.
 285. Irshad H, Veillard A, Roux L, et al. Methods for nuclei detection, segmentation, and classification in digital histopathology: a review-current status and future potential. *IEEE Rev Biomed Eng* 2014; 7:97-114.
 286. Sertel O, Catalyurek UV, Shimada H, et al. Computer-aided prognosis of neuroblastoma: detection of mitosis and karyorrhexis cells in digitized histological images. *Annu Int Conf IEEE Eng Med Biol Soc* 2009; 2009:1433-6.
 287. Lezoray O, Cardot H. Cooperation of color pixel classification schemes and color watershed: A study for microscopic images. *IEEE transactions on image processing : a publication of the IEEE Signal Processing Society* 2002; 11:783-9.
 288. Bayes T. An Essay towards solving a Problem in the Doctrine of Chances. *Philosophical Transactions* 1763; 53:370-418.
 289. Watson MM, Lea D, Hagland HR, et al. Elevated Microsatellite Alterations at Selected Tetranucleotides (EMAST) Is Not Attributed to MSH3 Loss in Stage I-III Colon cancer: An Automated, Digitalized Assessment by Immunohistochemistry of Whole Slides and Hot Spots. *Transl Oncol* 2019; 12(12):1583-1588.
 290. Lea D, Gudlaugsson EG, Skaland I, et al. Digital Image Analysis of the Proliferation Markers Ki67 and Phosphohistone H3 in Gastroenteropancreatic Neuroendocrine Neoplasms: Accuracy of Grading Compared With Routine Manual Hot Spot Evaluation of the Ki67 Index. *Appl Immunohistochem Mol Morphol* 2021.
 291. Lea D, Watson M, Skaland I, et al. A template to quantify the location and density of CD3 + and CD8 + tumor-infiltrating lymphocytes in colon cancer by digital pathology on whole slides for an objective, standardized immune score assessment. *Cancer Immunol Immunother* 2021; 70(7):2049-2057.

292. Chirica M, Le Bourhis L, Lehmann-Che J, et al. Phenotypic analysis of T cells infiltrating colon cancers: Correlations with oncogenetic status. *Oncoimmunology* 2015; 4(8):e1016698.
293. Won EJ, Ju JK, Cho YN, et al. Clinical relevance of circulating mucosal-associated invariant T cell levels and their anti-cancer activity in patients with mucosal-associated cancer. *Oncotarget* 2016; 7(46):76274-76290.
294. Sun Z, Xia W, Lyu Y, et al. Immune-related gene expression signatures in colorectal cancer. *Oncol Lett* 2021; 22(1):543.
295. Mlecnik B, Bindea G, Kirilovsky A, et al. The tumor microenvironment and Immunoscore are critical determinants of dissemination to distant metastasis. *Sci Transl Med* 2016; 8(327):327ra26.
296. Mlecnik B, Bindea G, Angell HK, et al. Functional network pipeline reveals genetic determinants associated with in situ lymphocyte proliferation and survival of cancer patients. *Sci Transl Med* 2014; 6(228):228ra37.
297. Herrera M, Galindo-Pumariño C, García-Barberán V, et al. A Snapshot of The Tumor Microenvironment in Colorectal Cancer: The Liquid Biopsy. *Int J Mol Sci* 2019; 20(23).
298. Saltz J, Gupta R, Hou L, et al. Spatial Organization and Molecular Correlation of Tumor-Infiltrating Lymphocytes Using Deep Learning on Pathology Images. *Cell Rep* 2018; 23(1):181-193.e7.
299. Argilés G, Taberero J, Labianca R, et al. Localised colon cancer: ESMO Clinical Practice Guidelines for diagnosis, treatment and follow-up. *Ann Oncol* 2020; 31(10):1291-1305.
300. Chalabi M, Fanchi LF, Dijkstra KK, et al. Neoadjuvant immunotherapy leads to pathological responses in MMR-proficient and MMR-deficient early-stage colon cancers. *Nature Medicine* 2020; 26(4):566-576.
301. Kroneman TN, Voss JS, Lohse CM, et al. Comparison of Three Ki-67 Index Quantification Methods and Clinical Significance in Pancreatic Neuroendocrine Tumors. *Endocr Pathol* 2015; 26(3):255-62.
302. Owens R, Gilmore E, Bingham V, et al. Comparison of different anti-Ki67 antibody clones and hot-spot sizes for assessing proliferative index and grading in pancreatic neuroendocrine tumours using manual and image analysis. *Histopathology* 2020; 77(4):646-658.
303. Dhall D, Mertens R, Breesee C, et al. Ki-67 proliferative index predicts progression-free survival of patients with well-differentiated ileal neuroendocrine tumors. *Hum Pathol* 2012; 43(4):489-95.
304. Goodell PP, Krasinskas AM, Davison JM, et al. Comparison of methods for proliferative index analysis for grading pancreatic well-differentiated neuroendocrine tumors. *Am J Clin Pathol* 2012; 137(4):576-82.
305. Hacking SM, Sajjan S, Lee L, et al. Potential Pitfalls in Diagnostic Digital Image Analysis: Experience with Ki-67 and PHH3 in Gastrointestinal Neuroendocrine Tumors. *Pathol Res Pract* 2020; 216(3):152753.
306. Kim MJ, Kwon MJ, Kang HS, et al. Identification of Phosphohistone H3 Cutoff Values Corresponding to Original WHO Grades but Distinguishable in Well-Differentiated Gastrointestinal Neuroendocrine Tumors. *Biomed Res Int* 2018; 2018:1013640.

-
307. Yang Z, Tang LH, Klimstra DS. Effect of tumor heterogeneity on the assessment of Ki67 labeling index in well-differentiated neuroendocrine tumors metastatic to the liver: implications for prognostic stratification. *Am J Surg Pathol* 2011; 35(6):853-60.
 308. Stålhammar G, Robertson S, Wedlund L, et al. Digital image analysis of Ki67 in hot spots is superior to both manual Ki67 and mitotic counts in breast cancer. *Histopathology* 2018; 72(6):974-989.
 309. Klauschen F, Wienert S, Schmitt WD, et al. Standardized Ki67 Diagnostics Using Automated Scoring—Clinical Validation in the GeparTrio Breast Cancer Study. *Clinical Cancer Research* 2015; 21(16):3651-3657.
 310. Dunstan RW, Wharton KA, Jr., Quigley C, et al. The use of immunohistochemistry for biomarker assessment--can it compete with other technologies? *Toxicol Pathol* 2011; 39(6):988-1002.
 311. Qi X, Xing F, Foran DJ, et al. Robust segmentation of overlapping cells in histopathology specimens using parallel seed detection and repulsive level set. *IEEE Trans Biomed Eng* 2012; 59(3):754-65.
 312. Varghese F, Bukhari AB, Malhotra R, et al. IHC Profiler: an open source plugin for the quantitative evaluation and automated scoring of immunohistochemistry images of human tissue samples. *PLoS One* 2014; 9(5):e96801.
 313. CE IVD 2021. Available at: https://www.gpc.center/ce_ivd_/585. Accessed 7. July, 2021.
 314. APPsolute image analysis 2021. Available at: <https://visiopharm.com/app-center/?cat=40>. Accessed 7. July, 2021.
 315. Pantanowitz L, Sinard JH, Henricks WH, et al. Validating whole slide imaging for diagnostic purposes in pathology: guideline from the College of American Pathologists Pathology and Laboratory Quality Center. *Arch Pathol Lab Med* 2013; 137(12):1710-22.
 316. Thrall MJ, Wimmer JL, Schwartz MR. Validation of multiple whole slide imaging scanners based on the guideline from the College of American Pathologists Pathology and Laboratory Quality Center. *Arch Pathol Lab Med* 2015; 139(5):656-64.
 317. Nasjonalt forum for digital patologi 2020. Available at: <https://spesialisthelsetjenesten.no/seksjon/ikt/Sider/Nasjonalt-forum-for-digital-patologi.aspx>. Accessed 7. july, 2021.

8. Figure credits

Figure 1: The figure was made by D. Lea.

Figure 2: The figure was made by D. Lea.

Figure 3: Reprinted with permission from MDPI. Journal of Clinical Medicine 2020;9(11):3697. Digital Pathology: Advantages, Limitations and Emerging Perspectives by Jahn SW et al. ©2020.

Figure 4: Reprinted with permission from Sage. Philosophical Transactions of the Royal Society B London Biological Sciences 2014;369(1641):20130215. The interplay of attention and consciousness in visual search, attentional blink and working memory consolidation by Raffone A et al. ©2015.

Figure 5: Adapted with permission from Elsevier Inc. Cell 2011;144(5):646-74. Hallmarks of cancer: the next generation by Hanahan D and Weinberg RA. ©2011.

Figure 6: Reprinted with permission from the International Agency for Research on Cancer IARC. ©2020.

Figure 7: Reprinted with permission from Elsevier Ltd. Lancet 2019;394(10207):1467-1480. Colorectal cancer by Dekker E et al. ©2019

Figure 8: Adapted with permission from Cell Press. Cell 1990;61(5):759-67. Genetic model for colorectal tumorigenesis by Fearon ER and Vogelstein B. ©1990. The figure was created using BioRender.com with publication licence.

Figure 9: Reprinted with permission from Elsevier Ltd. Lancet 2019;394(10207):1467-1480. Colorectal cancer by Dekker E et al. ©2019

Figure 10: Used with permission of the American College of Surgeons, Chicago, Illinois. The original source for this information is the AJCC Cancer Staging System (2020). ©2020. The figure was created with BioRender.com with publication licence.

Figure 11: Used with permission of the American College of Surgeons, Chicago, Illinois. The original source for this information is the AJCC Cancer Staging System (2020). ©2020. The figure was created with BioRender.com with publication licence.

Figure 12: The figure was made by D. Lea

Figure 13: Republished with permission from American Association for Cancer Research. *Clinical Cancer Research* 2013;19(11):2842-9. Molecular pathogenesis of neuroendocrine tumors: implications for current and future therapeutic approaches by Oberg K et al. ©2013.

Figure 14: The figure was made by D. Lea.

Figure 15: The figure was made by D. Lea

Figure 16: Republished with permission from Elsevier Science & Technology Journals. *Endocrinology and Metabolism Clinics of North America* 2018;47(3):683-698. The Problem of High-Grade Gastroenteropancreatic Neuroendocrine Neoplasms: Well-Differentiated Neuroendocrine Tumors, Neuroendocrine Carcinomas, and Beyond by Sorbye et al. ©2018.

Figure 17: Adapted with permission from Cell Press. *Trends in Pharmacological Sciences* 2017;38(9):771-793. An Overview of Novel Adjuvants Designed for Improving Vaccine Efficacy by Bonam et al. ©2017

Figure 18: Adapted with permission from Elsevier Inc. *Cell* 2011;144(5):646-74. Hallmarks of cancer: the next generation by Hanahan D and Weinberg RA. ©2011.

Figure 19: Adapted with permission from Springer Nature. *Nature Reviews Cancer* 2006;6(1):24-37. Paradoxical roles of the immune system during cancer development by de Visser KE et al. ©2006.

Figure 20: Republished with permission from Wolters Kluwer Health, Inc. *American Journal of Surgical Pathology* 2003;27(11):1407-17. Value of histopathology in

predicting microsatellite instability in hereditary nonpolyposis colorectal cancer and sporadic colorectal cancer by Shia J et al. ©2003.

Figure 21: Adapted with permission from MDPI under Creative Commons Attribution (CC BY 4.0) license. Cells 2020;9(3):618. Immunotherapy, Inflammation and CRC by Lichtenstern CR et al. ©2020.

Figure 22: Reprinted with permission from Oxford University Press. International Immunology 2016;28(8):373-82. Rational bases for the use of the Immunoscore in routine clinical settings as a prognostic and predictive biomarker in cancer patients by Kirilovsky A et al. ©2016.

Figure 23: The figure was created using BioRender.com with publication licence.

Figure 24: Reprinted with permission from Springer. Breast Cancer Research and Treatment 2009;114(1):39-45. Validating the prognostic value of proliferation measured by Phosphohistone H3 (PPH3) in invasive lymph node-negative breast cancer patients less than 71 years of age by Skaland I et al. ©2009.

Figure 25: The figure was created using BioRender.com with publication licence.

Figure 26: Adapted with permission from Taylor & Francis. Critical Reviews Biotechnology 2017;37(2):163-176. Flow cytometry: basic principles and applications by Adan A ©2017

Figure 27: The figure was created using BioRender.com with publication licence.

Figure 28: The figure was created using BioRender.com with publication licence.

Figure 29: The figure was made by D. Lea

9. Errata

In **Paper I**, the terminology ‘invasive front’ is used in the published paper. The terminology has changed to ‘invasive margin’ in the international literature, so ‘invasive margin’ is used as terminology in the PhD thesis.

10. Papers I – III



A template to quantify the location and density of CD3 + and CD8 + tumor-infiltrating lymphocytes in colon cancer by digital pathology on whole slides for an objective, standardized immune score assessment

Dordi Lea^{1,2,3} · Martin Watson^{1,2,5} · Ivar Skaland³ · Hanne R. Hagland^{1,4} · Melinda Lillesand³ · Einar Gudlaugsson³ · Kjetil Søreide^{1,2,5}

Received: 30 September 2020 / Accepted: 15 December 2020 / Published online: 13 January 2021
© The Author(s) 2021

Abstract

Background In colon cancer, the location and density of tumor-infiltrating lymphocytes (TILs) can classify patients into low and high-risk groups for prognostication. While a commercially available ‘Immunoscore[®]’ exists, the incurred expenses and copyrights may prevent universal use. The aim of this study was to develop a robust and objective quantification method of TILs in colon cancer.

Methods A consecutive, unselected series of specimens from patients with colon cancer were available for immunohistochemistry and assessment of TILs by automated digital pathology. CD3 + and CD8 + cells at the invasive margin and in tumor center were assessed on consecutive sections using automated digital pathology and image analysis software (Visiopharm[®]). An algorithm template for whole slide assessment, generated cell counts per square millimeters (cells/mm²), from which the immune score was calculated using distribution volumes. Furthermore, immune score was compared with clinical and histopathological characteristics to confirm its relevance.

Results Based on the quantified TILs numbers by digital image analyses, patients were classified into low ($n = 83$, 69.7%), intermediate ($n = 14$, 11.8%) and high ($n = 22$, 18.5%) immune score groups. High immune score was associated with stage I–II tumors ($p = 0.017$) and a higher prevalence of microsatellite instable (MSI) tumors ($p = 0.030$). MSI tumors had a significantly higher numbers of CD3 + TILs in the invasive margin and CD8 + TILs in both tumor center and invasive margin, compared to microsatellite stable (MSS) tumors.

Conclusion A digital template to quantify an easy-to-use immune score corresponds with clinicopathological features and MSI in colon cancer.

Keywords Colorectal cancer · Immune response · Tumor-infiltrating lymphocytes · Tumor center · Tumor-invasive margin · Digital image analysis

Supplementary Information The online version contains supplementary material available at <https://doi.org/10.1007/s00262-020-02834-y>.

✉ Kjetil Søreide
ksoreide@mac.com

¹ Gastrointestinal Translational Research Unit, Molecular Laboratory, Hillevåg, Stavanger University Hospital, Stavanger, Norway

² Department of Clinical Medicine, University of Bergen, Bergen, Norway

³ Department of Pathology, Stavanger University Hospital, Stavanger, Norway

⁴ Department of Chemistry, Bioscience and Environmental Engineering, Faculty of Science and Technology, University of Stavanger, Stavanger, Norway

⁵ Department of Gastrointestinal Surgery, Stavanger University Hospital, Stavanger, Norway

Introduction

Colorectal cancer (CRC) is a leading cause to the cancer burden and cancer deaths worldwide. Despite improvements in surgical and oncological management over the last decade [1], about half of all patients will develop metastasis and eventually die from disseminated disease [2]. The Tumor–node–metastases system (TNM classification) used for staging and prognostication is imperfect in its ability to correctly guide treatment and define appropriate subgroups beyond surgical treatment [3]. The TNM system largely dependent on using the node status to guide further adjuvant treatment, and as a consequence there is ongoing risk for under- and overtreatment of patients, based on the current guidelines for adjuvant chemotherapy [4, 5].

Of note, emerging data suggest the role of molecular subtypes with distinct features and associated outcomes [6, 7]. Among the suggested consensus molecular subtypes is the “immunogenic” type, which is associated with hypermutation, microsatellite instability (MSI) and a favorable prognosis. Abundant immune cells are found in the vicinity of such tumors and the type, density and location of the immune cells within tumor samples strongly influence the evolution of CRCs [8, 9] with impact on prognosis reported in large, multicenter studies [10–12]. This adaptive immune response of T-cells in tumor has been quantified as a measure called “Immunoscore[®]” (HaliDx, Marseille, France) [11, 13], and is available commercially as a test [14]. However, the costs implied with the commercially available assay may be prohibitive in a public health care setting and/or may currently not be reimbursed for clinical routine use. More widespread use of immune scoring could be available if easy, accessible and low-cost methods would allow for stratification of immunogenic tumors. Moreover, manual and subjective assessment such as counting cells, is increasingly being replaced by digital pathology in routine practice in departments of pathology [15, 16]. The benefits of digital pathology include objective measurement on regular slides [17] with a quantitative read of how many cells of interest are present in an area using immunostained sample slides. The highly objectivity and quantitative approach makes it easier to compare high number of tissue slides from patients and correlate to disease outcome.

The aim of this study was to establish an objective and highly reproducible quantification method for tumor-infiltrating lymphocytes (TILs) in colon cancer and to correlate immune score to clinicopathological characteristics and MSI status.

Methods

Study design

Patients were recruited from an ongoing prospective, clinical-molecular biomarker outcomes study, the ACROBAT-ICC project [18] (clinicaltrials.gov ID: NCT01762813). This cohort study is reported according to the STROBE [19] and the REMARK [20] guidelines for biomarker studies.

Compliance with ethical standards

The study is conducted in accordance to national regulations and approved by the Norwegian Regional Ethics Committee (REK Helse Vest, #2012/742). All procedures performed in studies involving human participants were in accordance with the ethical standards of the institutional and/or national research committee and with the 1964 Helsinki Declaration and its later amendments or comparable ethical standards.

Informed consent

Written informed consent was obtained from all participants prior to inclusion in the study.

Study population

All patients were diagnosed, managed and followed-up at Stavanger University Hospital (SUH), a public-funded university hospital within the universal health care system of Norway. The protocol [18] and study cohort have been described in further detail elsewhere [21, 22]. The current study is based on patients with stage I–III colon cancer from the initial cohort recruited between January 2013 and May 2014 [21] that did not undergo neoadjuvant treatment. Of 132 consecutive stage I–III colon cancers, 119 were included in the study. Patients with two or more invasive colon carcinomas at time of surgery were excluded from the study, as these tumors might have a different biology [23]. When multiple tumor blocks were present, the tumor block that included invasive margin and most immune cells was selected for analysis [24].

Histopathology

All specimens were staged (AJCC 8th edition) [25, 26] by board certified pathologists using a standardized gross

pathology and microscopic histopathology template for reporting.

Immunohistochemistry

Antigen retrieval and antibody dilution were optimized prior to the study onset. Adjacent to the hematoxylin–eosin (H&E) stained sections, consecutive 2 μm paraffin sections were cut and mounted onto Superfrost Plus slides (Menzel, Braunschweig, Germany), along the principles suggest previously [27]. The CD3 and CD8 slides were incubated at 60 °C for 1 h and then placed in the autostainer (Dako Omnis), where they were subject to an automated protocol as per manufacturer instructions, with a pretreatment at 97 °C in 30 min. CD3 (Dako Clone F7.2.38) was diluted with Dako Antibody

diluent by 1:75 and CD8 (Dako Clone C8/144B) by 1:50. A peroxidase detection kit (Envision substrate working solution, Dako, Glostrup, Denmark) visualized the immune complex for all the antibodies. Sections were then counterstained with hematoxylin in the Dako Omnis stainer. Afterwards, the slides were dehydrated and mounted manually.

Digital pathology assessment

CD3- and CD8-stained slides were scanned at 40 \times magnification using Leica SCN400 slide scanner (Leica Microsystems, Wetzlar, Germany) and uploaded to image analysis software, Visiopharm[®] (Hoersholm, Denmark). The region of tumor center (TC) and invasive margin (IM) were marked manually on whole slides in Visiopharm[®]

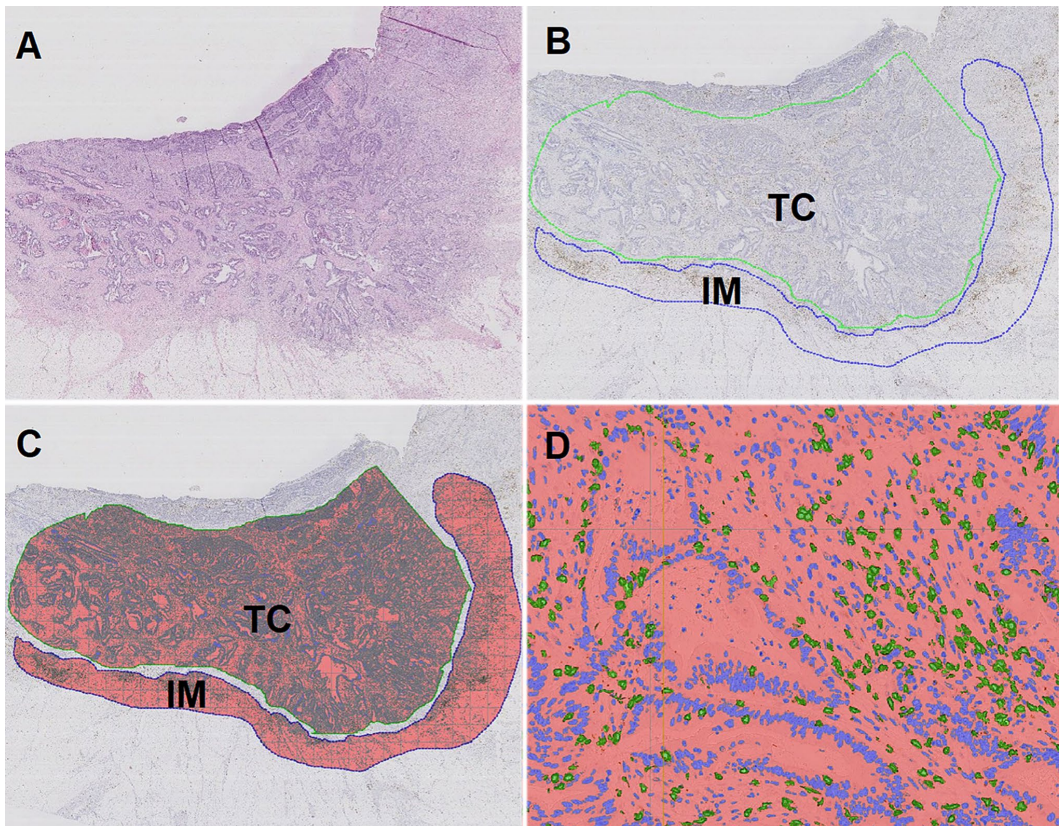


Fig. 1 **a** Hematoxylin–eosin staining of tumor. **b** Immunohistochemical staining of CD3 (brown) in the same tumor with marking of tumor center/TC (blue) and invasive margin/IM (green). **c** Digital image analysis measured the CD3+ tumor-infiltrating lymphocytes (TILs) in TC and IM. The number of positive TILs was calculated per

mm^2 . The same tumor area was analyzed for CD3 and CD8 for each patient. **d** Close-up view that shows positive TILs marked with green. Negative nuclei are marked blue and surrounding stroma is marked red

and these regions (region of interest, ROI) were used for CD3+ and CD8+ cell quantification (Fig. 1). Visiopharm® identified and measured the area of positive cells (µm) using digital image analysis (DIA). After DIA, the area of positive cells were transformed into number of positive TILs based on the estimation of mean area of a lymphocyte (60 µm²). The number of positive CD3+ and CD8+ TILs was calculated per square millimeters (n cells/mm²) [28], further represented as density of cells.

Unspecified stains and artefacts were removed manually using the image software. Application in the image software was adjusted for detection of different immune stain intensity.

Immune response was calculated based on mean densities of CD3+ and CD8+ in TC and IM in all of the patients in the study. The calculated mean density was used to divide the individual cases into “high” or “low” immune response. Cases with mean density ≥ 75-percentile were regarded as “high” immune response. Patients were stratified from I0 to I4 according to the “Immunoscore®”, based on the total number of observed high densities (CD3+ TILs and CD8+ TILs in TC and IM) [11, 13]. The final immune score was categorized based on mean percentiles for all four markers, and divided into immune score “low”, “intermediate” and “high” based on the number of markers (0–4) ≥ 75th percentile (Fig. 2).

Histopathological parameters

Histopathological parameters were registered from the pathology report including mucinous component, lymphovascular infiltration and lymph node status. In addition, tumor budding was registered in the HE section with deepest infiltration according to recommended guidelines [29, 30].

Analysis of microsatellite instability

Analysis of MSI has been described previously [31, 32]. Briefly, FFPE blocks were selected by an experienced pathologist (DL) and 4 × 10 µm sections were cut at a microtome. Automated DNA extraction was carried out using AllPrep DNA/RNA FFPE kit (Qiagen, Hilden, Germany) on a QiaCUBE instrument (Qiagen) according to manufacturer’s instructions. Nucleic acid concentration and purity were measured on a NanoDrop 2000 (ThermoFischer scientific, Waltham, USA). Multiplex PCR reactions (one for each MSI) were set up for tumor and normal DNA in each patient. TypeIT microsatellite (Qiagen) master mix, together with a blending of 5 × 5′-fluorescently labelled primer pairs was used for each reaction. PCR conditions were as follows: 5′ at 95 °C (initial denaturation and enzyme activation), followed by 37 cycles of 30″ at 95 °C (denaturation), 90″ at 55 (MSI) and 30″ at 72 °C (extension). A final extension step for 30′ at 60 °C. The primers for MSI were specific for

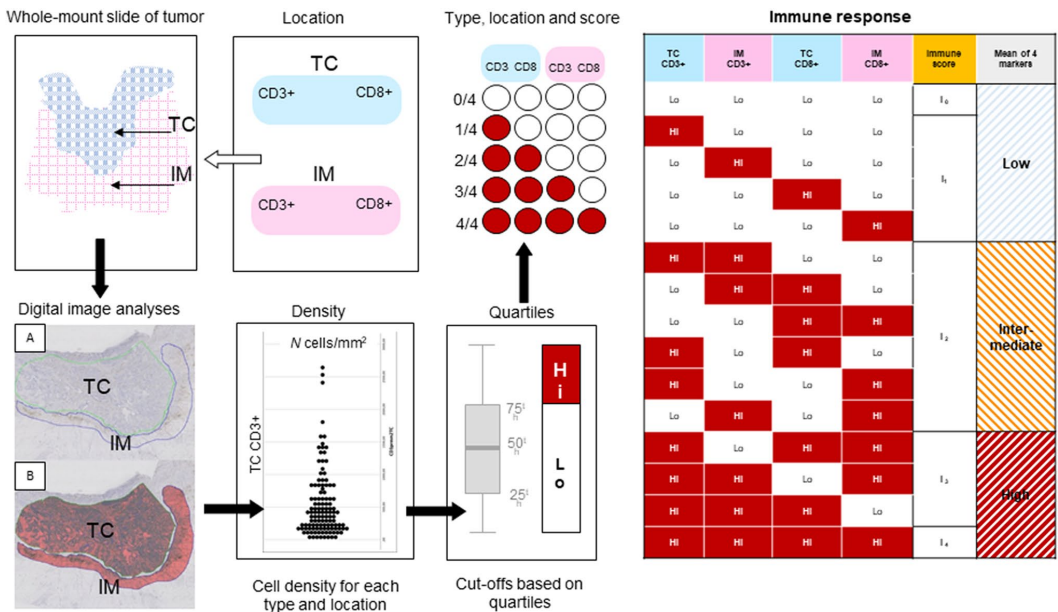


Fig. 2 Flowchart for calculating immune response based on mean densities of CD3+ and CD8+ in tumor center (TC) and invasive margin (IM)

BAT-25, BAT-26, NR-21, NR-24 and NR-27 [33, 34], which are all quasimonomorphic mononucleotide repeats with a high fidelity to high-frequency MSI, as shown previously [32]. To define a tumor as MSI, at least 2/5 markers needed to be unstable in their panels.

Statistics

IBM SPSS Statistics for Windows, Version 26.0 (IBM Corporation, Armonk, NY, USA) was used for statistical analysis. Associations between categorical variables were tested with Chi-square. Mann–Whitney *U* test was used to compare differences in continuous or ordinal variables between groups. All tests were two-tailed and a *p* value < 0.050 was determined as statistically significant.

Results

The study cohort included 119 stage I–III colon cancer patients that underwent surgery with curative intent. Patient characteristics is presented in Supplement Table 1. According to the TNM classification, the distribution between stage I–III were approximately equal (31%, 36% and 32%, respectively). Slightly more women were noted in the cohort, otherwise the distributions were as expected for a consecutive cohort of colon cancer, with lymph node status, tumor size, histological type and grade, and overall age.

Distribution of the number of CD3+ and CD8+ TILs in TC and IM is presented in Fig. 3. The number of TILs

Table 1 Density (cells/mm²) cut-off values based on highest quartiles (75th percentile)

	Tumor center		Invasive margin	
	CD3+	CD8+	CD3+	CD8+
	cells/mm ²	cells/mm ²	cells/mm ²	cells/mm ²
Median	393	220	858	513
Percentiles	25th	187	452	277
	50th	393	220	858
	75th	760	466	1390

was higher in IM compared with TC, both for CD3+ and CD8+ cells. Percentiles for evaluating immune response based on density (cells/mm²) of CD3 and CD8 is presented in Table 1. The total numbers of cells/mm² counted in the upper range (75th percentile) were almost double in the invasive margin compared to tumor center, for both CD3+ and CD8+ cells, respectively. Table 2 shows distribution of cases with high immune response (≥ 75th percentile) in the different regions. These results were summarized to calculate immune score, which is presented in Table 3. According to the immune score set up (Table 3), there number of patients in the immune score groups of low, intermediate and high was 83 (69.7%), 14 (11.8%) and 22 (18.5%), respectively. Hence, two-thirds of the colon cancers were deemed immune-low, with the immune-high cases split even between a three of four and four of four regions marked as immune high.

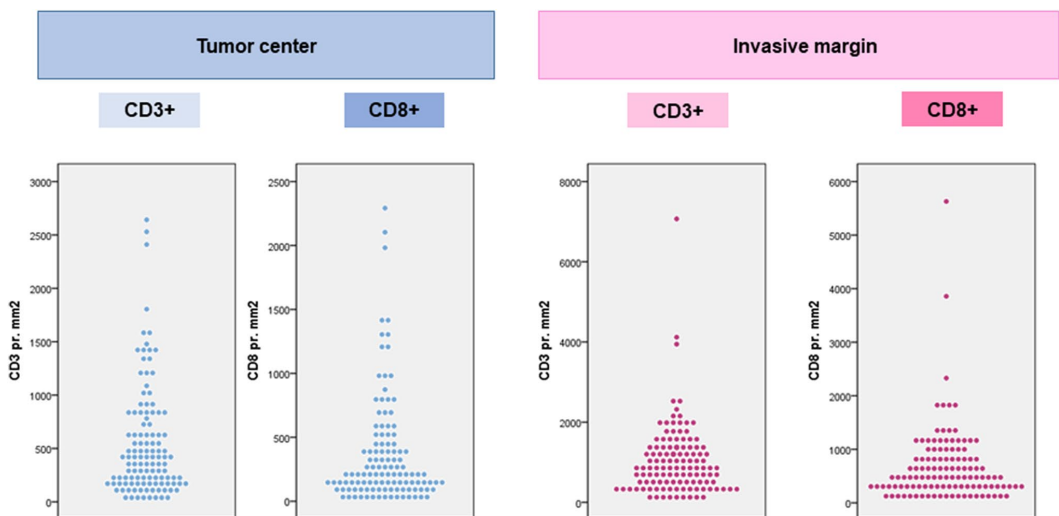


Fig. 3 Distribution of number of CD3+ and CD8+ TILs in tumor center (TC) and invasive margin (IM)

Table 2 Distribution of patients (*n*) with high immune response (≥ 75 th percentile) in different regions

	Tumor center				Invasive margin			
	CD3 Low	CD3 High	CD8 Low	CD8 High	CD3 Low	CD3 High	CD8 Low	CD8 High
0 of 4	69	0	69	0	69	0	69	0
1 of 4	13	1	12	2	9	5	8	6
2 of 4	5	9	5	9	8	6	10	4
3 of 4	3	8	3	8	3	8	2	9
4 of 4	0	11	0	11	0	11	0	11
Total	90	29	89	30	89	30	89	30

Table 3 Immune score based on high tumor density of CD3 and CD8 in different regions

Number of regions	Patients (<i>n</i>)	Means of markers
0 of 4	69	Low
1 of 4	14	Intermediate
2 of 4	14	
3 of 4	11	
4 of 4	11	High
Total	119	

Higher immune scores were associated with a higher frequency of stage I–II tumors ($p=0.017$) and a higher prevalence of MSI tumors ($p=0.030$), compared with tumors from intermediate and low immune score. Three of 22 patients with high immune score had stage III disease, whereas for stage I and II the number was 12 and 7, respectively. For patients with low immune score, 19 were stage I, 34 stage II and 30 stage III. For intermediate immune score, the corresponding number of patients were 6 stage I, 2 stage II and 6 stage III. Twelve of 42 MSI tumors (28.6%) had high immune score and 10 of 77 microsatellite stable (MSS) tumors (13.0%) had a high immune score, responding to twofold increase of immune-high cases in the MSI colon cancers.

Tumors with MSI had a significantly higher number of CD3+ TILs in IM and CD8+ TILs in both TC and IM (Fig. 4). There was no significant association between high immune score and sex, median age, localization, grade, tumor size, N-status, tumor budding, lymphovascular or perineural infiltration.

Discussion

In this study, we present an objective automated, digital quantification method of CD3+ and CD8+ lymphocytes at IM and in TC in colon cancer. The resultant immune score is strongly associated with TNM stage and microsatellite instability, two well-documented and very strong prognostic factors in colon cancer. The immune score allowed to stratify

patients into low, intermediate and high immune response groups. The quantification should be easy to use by other digital pathology laboratories and represent a robust and objective approach to immune cell quantification in colon cancer specimens.

The method is based on the construct principle of the “Immunoscore”, which has been validated in a large international cohort series [11]. However, this commercially available Immunoscore® (HaliDx, Marseille, France) is adapted to certain manufactures of antibodies and autostainer [11], and may prevent laboratories from setting up the method with available equipment in the laboratory. Widespread evaluation and dissemination may thus be hampered. Hence, the current quantification may represent an alternative measurement that is adoptable, easy to implement, affordable and objective, yet provides transparency for reproduction.

We found that the number of TILs is significantly higher at the IM than in TC, corresponding to a previously reported study [35]. Furthermore, our study showed that patients with high immune score were associated with an earlier stage of the disease, which might explain why high immune score is associated with better prognosis. Several studies show that TILs play a significant role for prognosis in colon cancer. Mlecnik et al. found that a high density of CD8+ TILs is associated with reduced risk of relapse [35], whereas Angell and co-workers [36] found that tumors with reduced numbers of CD8+ had a higher risk of metastasis. A recent meta-analysis of 22 studies including 5108 patients by Zhao and co-workers, found that high CD3+ infiltrates in colon cancer correlated with improved cancer-specific survival and overall survival. Furthermore, the same study found that high density of CD3+ in IM indicated increased disease-free survival (DFS) and high CD8+ in TC was associated with improved DFS [37]. The abovementioned studies all support that scoring TILs in colon cancer can give valuable prognostic information.

In the NICHE study [38], the investigators explored the safety and efficiency of neoadjuvant immunotherapy (ipilimumab and nivolumab) in operable colon cancers. Despite being a small phase I/II study with over half being MSI cancer, a remarkable response was found (pathological response in 20/20 MSI patients; 19 had major pathological

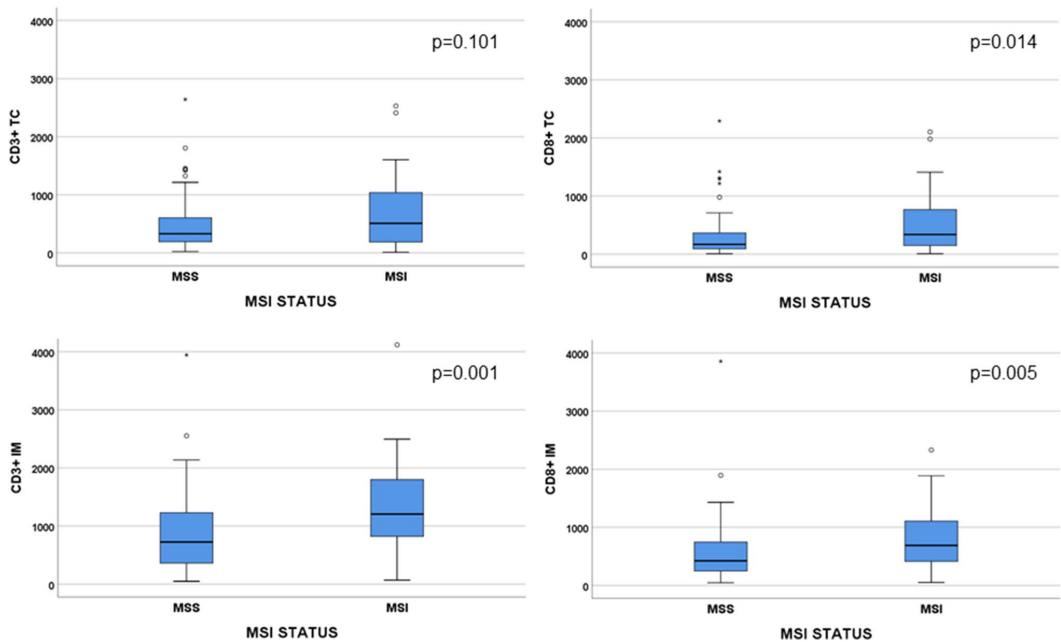


Fig. 4 Comparison of number of CD3+ and CD8+ tumor-infiltrating lymphocytes (TILs) of MSS and MSI tumors in tumor center (TC) and invasive margin (IM). Extreme values >4000 cells is not shown in figure

response and 12 had complete pathological response. Even in tumors with MSS, 4 of 15 had response [38]. As density of immune cells were related to response, a pre-treatment biopsy may become important. While not investigated in the NICHE study, the current template for immune score by digital pathology may become essential to select the patients who would benefit from such treatment in the future. Of note, half the patients in the NICHE study had MSI tumors, suggesting a selection of the included patients. The current rate of 35% MSI is high, but reflect that only colon (and no rectal) cancers were selected for the cohort and, is in line with previously reported data for such cohorts [39].

So far, and to the best of our knowledge, no biomarkers based on digital image analysis (DIA), has been used in pathological classification of colon cancer [24], despite digital pathology now being steadily introduced in routine diagnostic practice at several pathology departments. While there is a lack of consensus biomarkers for use, the implementation and spread in use makes it easier to use DIA in diagnostic setting and to perform prognostic scoring. For immune score to become an international recognized standard, it is important that it is available through affordable software and that the method is transparent. Others have applied deep learning methods to analyze TILs in HE sections [40, 41] and have found association with survival.

The added time and cost to stain and score relies on a couple of assumptions. One, a digital platform needs to be in place. We recognize that not all pathology labs may have this readily available, but increasingly this is being rolled out as the way forward to standardize scoring in quantitative pathology. Second, the time taken for a technician or bioengineer to cut slides and prepare counts from the template is time efficient. If standardized and introduced into the routine pathway of clinical work, the estimated extra time for a bioengineer to cut, stain and prep for digital analysis would be in the range of 15–20 min; the pathologist's time to mark the area for digital analyses would be part of the routine clinical work and add a maximum of 30 min, but probably less. Hence, the use of this score should not be labor intensive nor require extensive human hours of labor.

The cost implied (given that digital pathology instruments are available in a given pathology lab) amounts to reagents for immunohistochemistry markers. These are usually available already in most labs, and in general inexpensive (estimated at around 10 Euros per slide), but with variable costs between countries. Taken together, we believe that the template for an automated immune score presented here would be both time efficient and cost containing.

Our study has some limitations to address, with one being the size of the cohort. A larger cohort size might have

demonstrated more differences between the clinicopathological parameters in the patients to the high immune score versus the patients with intermediate and low immune score. Furthermore, the DIA method is not validated against manual pathology evaluation using a microscope and counting cells. This is near impossible (from a time and labour perspective implied) due to the high number of positive cells found in each tissue slide. However, the less time-consuming and labour-efficient results obtained by DIA exemplifies the strength of using automated digital pathology to this extent. The international effort of validating the “Immunoscore[®]” as a prognostic marker demonstrated value of the commercial test [11]. Future studies using easy-to-use, available, objective and reproducible methods to assess TILs in colon cancer may facilitate its wider dissemination and clinical implementation. With further validation, internally and externally, the role of the current template-based immune score should arrive at clinically relevant use and be able to designate appropriate subgroups of patients stratified to their relevant therapy decisions.

Conclusion

A whole slide, digital pathology template using imaging software was developed to quantify immune score. Known clinicopathological features like MSI status correlated with a higher immune infiltrate, exemplified by a greater immune score. Large-scale internal and external validation to demonstrate robustness and generalizability for clinical use is ongoing.

Author contributions DL, MMW, HRH, IS, EG and KS contributed to the study conception and design. Data collection and material preparation was performed by DL, MMW and ML. Data analyses was performed by DL, MMW, EG and KS. Technical supervision was provided by IS and KS. The first draft of the manuscript was written by DL and all authors commented on previous versions of the manuscript. All authors read and approved the final manuscript.

Funding Open Access funding provided by University of Bergen (incl Haukeland University Hospital). This study was funded by Folke Hermansen Cancer Fund.

Compliance with ethical standards

Conflict of interest The authors declare no conflict of interest.

Ethical approval Approved by ethics committee.

Informed consent Informed consent given by patients.

Open Access This article is licensed under a Creative Commons Attribution 4.0 International License, which permits use, sharing, adaptation, distribution and reproduction in any medium or format, as long as you give appropriate credit to the original author(s) and the source,

provide a link to the Creative Commons licence, and indicate if changes were made. The images or other third party material in this article are included in the article's Creative Commons licence, unless indicated otherwise in a credit line to the material. If material is not included in the article's Creative Commons licence and your intended use is not permitted by statutory regulation or exceeds the permitted use, you will need to obtain permission directly from the copyright holder. To view a copy of this licence, visit <http://creativecommons.org/licenses/by/4.0/>.

References

- Nedrebø BS, Søreide K, Eriksen MT, Dørum LM, Kvaloy JT, Søreide JA et al (2011) Survival effect of implementing national treatment strategies for curatively resected colonic and rectal cancer. *Br J Surg* 98(5):716–723. <https://doi.org/10.1002/bjs.7426>
- Safiri S, Sepanlou SG, Ikuta KS, Bisignano C, Salimzadeh H, Delavari A, Ansari R, Roshandel G, Merat S, Fitzmaurice C, Force LM (2019) The global, regional, and national burden of colorectal cancer and its attributable risk factors in 195 countries and territories, 1990–2017: a systematic analysis for the Global Burden of Disease Study 2017. *Lancet Gastroenterol Hepatol* 4(12):913–933. [https://doi.org/10.1016/s2468-1253\(19\)30345-0](https://doi.org/10.1016/s2468-1253(19)30345-0)
- Lea D, Håland S, Hagland HR, Søreide K (2014) Accuracy of TNM staging in colorectal cancer: a review of current culprits, the modern role of morphology and stepping-stones for improvements in the molecular era. *Scand J Gastroenterol* 49(10):1153–1163. <https://doi.org/10.3109/00365521.2014.950692>
- Nagtegaal ID, Quirke P, Schmol HJ (2012) Has the new TNM classification for colorectal cancer improved care? *Nat Rev Clin Oncol* 9(2):119–123. <https://doi.org/10.1038/nrclinonc.2011.157>
- Puppa G, Sonzogni A, Colombari R, Pelosi G (2010) TNM staging system of colorectal carcinoma: a critical appraisal of challenging issues. *Arch Pathol Lab Med* 134(6):837–852. <https://doi.org/10.1043/1543-2165-134.6.837>
- Dienstmann R, Vermeulen L, Guinney J, Kopetz S, Tejpar S, Tabernero J (2017) Consensus molecular subtypes and the evolution of precision medicine in colorectal cancer. *Nat Rev Cancer* 17(2):79–92. <https://doi.org/10.1038/nrc.2016.126>
- Wang W, Kandimalla R, Huang H, Zhu L, Li Y, Gao F et al (2019) Molecular subtyping of colorectal cancer: recent progress, new challenges and emerging opportunities. *Semin Cancer Biol* 55:37–52. <https://doi.org/10.1016/j.semcancer.2018.05.002>
- Galon J, Costes A, Sanchez-Cabo F, Kirilovsky A, Mlecnik B, Lagorce-Pages C et al (2006) Type, density, and location of immune cells within human colorectal tumors predict clinical outcome. *Science* 313(5795):1960–1964. <https://doi.org/10.1126/science.1129139>
- Pages F, Berger A, Camus M, Sanchez-Cabo F, Costes A, Molitor R et al (2005) Effector memory T cells, early metastasis, and survival in colorectal cancer. *N Engl J Med* 353(25):2654–2666. <https://doi.org/10.1056/NEJMoa051424>
- Ferris RL, Galon J (2016) Additional Support for the Introduction of Immune Cell Quantification in Colorectal Cancer Classification. *J Natl Cancer Inst*. <https://doi.org/10.1093/jnci/djw033>
- Pagès F, Mlecnik B, Marliot F, Bindea G, Ou FS, Bifulco C et al (2018) International validation of the consensus Immunoscore for the classification of colon cancer: a prognostic and accuracy study. *Lancet* 391(10135):2128–2139. [https://doi.org/10.1016/s0140-6736\(18\)30789-x](https://doi.org/10.1016/s0140-6736(18)30789-x)
- Sun G, Dong X, Tang X, Qu H, Zhang H, Zhao E (2019) The prognostic value of immunoscore in patients with colorectal cancer: a systematic review and meta-analysis. *Cancer Med* 8(1):182–189. <https://doi.org/10.1002/cam4.1921>

13. Galon J, Mlecnik B, Bindea G, Angell HK, Berger A, Lagorce C et al (2014) Towards the introduction of the “Immunoscore” in the classification of malignant tumours. *J Pathol* 232(2):199–209. <https://doi.org/10.1002/path.4287>
14. Blair HA (2020) Immunoscore®: a diagnostic assay for clinical management of colon cancer. *Mol Diagn Ther* 24(3):365–370. <https://doi.org/10.1007/s40291-020-00459-6>
15. Thorstenson S, Molin J, Lundstrom C (2014) Implementation of large-scale routine diagnostics using whole slide imaging in Sweden: digital pathology experiences 2006–2013. *J Pathol Inf* 5(1):14. <https://doi.org/10.4103/2153-3539.129452>
16. Cheng CL, Azhar R, Sng SH, Chua YQ, Hwang JS, Chin JP et al (2016) Enabling digital pathology in the diagnostic setting: navigating through the implementation journey in an academic medical centre. *J Clin Pathol* 69(9):784–792. <https://doi.org/10.1136/jclinpath-2015-203600>
17. Veta M, van Diest PJ, Willems SM, Wang H, Madabhushi A, Cruz-Roa A et al (2015) Assessment of algorithms for mitosis detection in breast cancer histopathology images. *Med Image Anal* 20(1):237–248. <https://doi.org/10.1016/j.media.2014.11.010>
18. Søreide K, Watson MM, Lea D, Nordgård O, Søreide JA, Hagland HR (2016) Assessment of clinically related outcomes and biomarker analysis for translational integration in colorectal cancer (ACROBATICC): study protocol for a population-based, consecutive cohort of surgically treated colorectal cancers and resected colorectal liver metastasis. *J Transl Med* 14(1):192. <https://doi.org/10.1186/s12967-016-0951-4>
19. Ev E, Altman DG, Egger M, Pocock SJ, Götzsche PC, Vandembroucke JP (2007) Strengthening the Reporting of Observational Studies in Epidemiology (STROBE) statement: guidelines for reporting observational studies. *BMJ (Clin Res ed.)* 335(7624):806–808. <https://doi.org/10.1136/bmj.39335.541782.AD>
20. McShane LM, Altman DG, Sauerbrei W, Taube SE, Gion M, Clark GM et al (2005) Reporting recommendations for tumour MARKer prognostic studies (REMARK). *Br J Cancer* 93(4):387–391. <https://doi.org/10.1038/sj.bjc.6602678>
21. Watson MM, Kanani A, Lea D, Khajavi RB, Søreide JA, Kørner H et al (2020) Elevated microsatellite alterations at selected tetranucleotides (EMAST) in colorectal cancer is associated with an elderly, frail phenotype and improved recurrence-free survival. *Ann Surg Oncol* 27(4):1058–1067. <https://doi.org/10.1245/s10434-019-08048-6>
22. Watson MM, Lea D, Gudlaugsson E, Skaland I, Hagland HR, Søreide K (2020) Prevalence of PD-L1 expression is associated with EMAST, density of peritumoral T-cells and recurrence-free survival in operable non-metastatic colorectal cancer. *Cancer Immunol Immunother* 69(8):1627–1637. <https://doi.org/10.1007/s00262-020-02573-0>
23. Konecny RJ, King TC, Schechter S, McLean SF, Lodowsky C, Wanebo HJ (1996) Synchronous colon carcinomas: molecular-genetic evidence for multicentricity. *Ann Surg Oncol* 3(2):136–143. <https://doi.org/10.1007/bf022305792>
24. Angell HK, Bruni D, Barrett JC, Herbst R, Galon J (2020) The immunoscore: colon cancer and beyond. *Clin Cancer Res* 26(2):332–339. <https://doi.org/10.1158/1078-0432.Ccr-18-1851>
25. AJCC Cancer Staging Manual, 8 ed. Springer International Publishing AG, Switzerland; 2017
26. WHO Classification of Tumours, Digestive System Tumours, 5 ed. IARC Publications; 2019
27. Hermitte F (2016) Biomarkers immune monitoring technology primer: Immunoscore®(R) Colon. *J Immunother Cancer* 4:57. <https://doi.org/10.1186/s40425-016-0161-x>
28. Hagland HR, Lea D, Watson MM, Søreide K (2017) Correlation of blood T-cells to intratumoural density and location of CD3+ and CD8+ T-cells in colorectal cancer. *Anticancer Res* 37(2):675–683. <https://doi.org/10.21873/anticancer.11363>
29. Cho SJ, Kakar S (2018) Tumor budding in colorectal carcinoma: translating a morphologic score into clinically meaningful results. *Arch Pathol Lab Med* 142(8):952–957. <https://doi.org/10.5858/arpa.2018-0082-RA>
30. Lugli A, Kirsch R, Ajioka Y, Bosman F, Cathomas G, Dawson H et al (2017) Recommendations for reporting tumor budding in colorectal cancer based on the International Tumor Budding Consensus Conference (ITBCC) 2016. *Modern Pathol Off J USA Can Acad Pathol* 30(9):1299–1311. <https://doi.org/10.1038/modpathol.2017.46>
31. Watson MM, Kanani A, Lea D, Khajavi RB, Søreide JA, Kørner H et al (2019) Elevated microsatellite alterations at selected tetranucleotides (EMAST) in colorectal cancer is associated with an elderly, frail phenotype and improved recurrence-free survival. *Ann Surg Oncol* 27(4):1058–1067
32. Søreide K (2011) High-fidelity of five quasimonomorphic mononucleotide repeats to high-frequency microsatellite instability distribution in early-stage adenocarcinoma of the colon. *Anticancer Res* 31(3):967–971
33. Buhard O, Suraweera N, Lectard A, Duval A, Hamelin R (2004) Quasimonomorphic mononucleotide repeats for high-level microsatellite instability analysis. *Dis Markers* 20(4–5):251–257. <https://doi.org/10.1155/2004/159347>
34. Suraweera N, Duval A, Reperant M, Vaury C, Furlan D, Leroy K et al (2002) Evaluation of tumor microsatellite instability using five quasimonomorphic mononucleotide repeats and pentaplex PCR. *Gastroenterology* 123(6):1804–1811. <https://doi.org/10.1053/gast.2002.37070>
35. Mlecnik B, Tosolini M, Kirilovsky A, Berger A, Bindea G, Meatchi T et al (2011) Histopathologic-based prognostic factors of colorectal cancers are associated with the state of the local immune reaction. *J Clin Oncol* 29(6):610–618. <https://doi.org/10.1200/jco.2010.30.5425>
36. Angell HK, Gray N, Womack C, Pritchard DI, Wilkinson RW, Cumberbatch M (2013) Digital pattern recognition-based image analysis quantifies immune infiltrates in distinct tissue regions of colorectal cancer and identifies a metastatic phenotype. *Br J Cancer* 109(6):1618–1624. <https://doi.org/10.1038/bjc.2013.487>
37. Zhao Y, Ge X, He J, Cheng Y, Wang Z, Wang J et al (2019) The prognostic value of tumor-infiltrating lymphocytes in colorectal cancer differs by anatomical subsite: a systematic review and meta-analysis. *World J Surg Oncol* 17(1):85. <https://doi.org/10.1186/s12957-019-1621-9>
38. Chalabi M, Fanchi LF, Dijkstra KK, Van den Berg JG, Aalbers AG, Sikorska K et al (2020) Neoadjuvant immunotherapy leads to pathological responses in MMR-proficient and MMR-deficient early-stage colon cancers. *Nat Med* 26(4):566–576. <https://doi.org/10.1038/s41591-020-0805-8>
39. Guastadisegni C, Colafranceschi M, Ottini L, Dogliotti E (2010) Microsatellite instability as a marker of prognosis and response to therapy: a meta-analysis of colorectal cancer survival data. *Eur J Cancer* 46(15):2788–2798. <https://doi.org/10.1016/j.ejca.2010.05.009>
40. Sultz J, Gupta R, Hou L, Kurc T, Singh P, Nguyen V et al (2018) Spatial organization and molecular correlation of tumor-infiltrating lymphocytes using deep learning on pathology images. *Cell Rep* 23(1):181–93.e7. <https://doi.org/10.1016/j.celrep.2018.03.086>
41. Skrede OJ, De Raedt S, Kleppe A, Hveem TS, Liestol K, Maddison J et al (2020) Deep learning for prediction of colorectal cancer outcome: a discovery and validation study. *Lancet (London, England)* 395(10221):350–360. [https://doi.org/10.1016/s0140-6736\(19\)32998-8](https://doi.org/10.1016/s0140-6736(19)32998-8)

Publisher's Note Springer Nature remains neutral with regard to jurisdictional claims in published maps and institutional affiliations.

Digital Image Analysis of the Proliferation Markers Ki67 and Phosphohistone H3 in Gastroenteropancreatic Neuroendocrine Neoplasms: Accuracy of Grading Compared With Routine Manual Hot Spot Evaluation of the Ki67 Index

Dordi Lea, MD,*†‡ Einar G. Gudlaugsson, MD, PhD,* Ivar Skaland, PhD,*
Melinda Lillesand, MSc,* Kjetil Søreide, MD, PhD, FACS, FRCSEd,†‡§
and Jon A. Søreide, MD, PhD, FACS, FISS†§

Abstract: Gastroenteropancreatic neuroendocrine neoplasms (GEP-NENs) are rare epithelial neoplasms. Grading is based on mitotic activity or the percentage of Ki67-positive cells in a hot spot. Routine methods have poor intraobserver and interobserver consistency, and objective measurements are lacking. This study aimed to evaluate digital image analysis (DIA) as an objective assessment of proliferation markers in GEP-NENs. A consecutive cohort of patients with automated DIA measurement of Ki67 (DIA Ki67) and phosphohistone H3 (DIA PHH3) on immunohistochemical slides was analyzed using Visiopharm image analysis software (Hoersholm, Denmark). The results were compared with the Ki67 index from routine pathology reports (pathology Ki67). The study included 159 patients (57% males). The median pathology Ki67 was 2.0% and DIA Ki67 was 4.1%. The interclass correlation coefficient of the DIA Ki67 compared with the pathology Ki67 showed an excellent agreement of 0.96 [95% confidence interval (CI): 0.94-0.96]. The observed kappa value was 0.86 (95% CI: 0.81-0.91) when comparing grades based on the same methods. PHH3 was measured in 145 (91.2%) cases. The observed kappa value was 0.74. (95% CI: 0.65-0.83) when comparing grade based on the

DIA PHH3 and the pathology Ki67. The DIA Ki67 shows excellent agreement with the pathology Ki67. The DIA PHH3 measurements were more varied and cannot replace other methods for grading GEP-NENs.

Key Words: neuroendocrine tumor, neuroendocrine carcinoma, proliferation, digital image analysis, immunohistochemistry

(*Appl Immunohistochem Mol Morphol* 2021;29:499–505)

Gastroenteropancreatic neuroendocrine neoplasms (GEP-NENs) comprise a heterogeneous group of rare, benign, or malignant epithelial tumors (carcinoids) originating from the pancreas (PNENs) or gastrointestinal tract (GI-NETs). The reported annual incidence varies between 2.39 and 5.83 per 100,000 inhabitants according to international literature,^{1,2} with an estimated prevalence of 35 per 100,000 because of the long survival times. The 5-year survival rates vary between 40% and 100% and are associated with the primary tumor site, tumor grade, and stage of disease at the time of diagnosis.^{3–5} Moreover, GEP-NENs classified as functional tumors (which secrete hormones or peptides to cause clinical symptoms or syndromes) show a different biological behavior from those classified as nonfunctional GEP-NENs,⁶ and tumor behavior is also associated with the histopathologic pattern, including the features of an adenocarcinoma.⁷ The diagnostic criteria of neuroendocrine tumors are based on morphology and the positive staining of the neuroendocrine markers synaptophysin and/or chromogranin A by immunohistochemistry (IHC).⁸

According to the World Health Organization (WHO) criteria, the grading of GEP-NENs is based on the evaluation of mitotic activity, either by counting mitosis, the so-called “mitotic activity index” (MAI), on hematoxylin and eosin (HE)-stained slides or by calculating the percentage of Ki67-positive cells in a hot spot (Table 1).^{9,10} The highest grade should apply if any discordance between the MAI and Ki67 index assessment occurs.¹⁰ The Ki67 index predicts prognosis better than MAI.¹¹

Received for publication November 23, 2020; accepted February 22, 2021.

From the Departments of *Pathology; †Gastrointestinal Surgery; ‡Gastrointestinal Translational Research Unit, Molecular Laboratory, Hillevåg, Stavanger University Hospital, Stavanger; and †Department of Clinical Medicine, University of Bergen, Bergen, Norway.

This study was financially supported in part by an unrestricted research grant provided by the CarciNor, which is the Norwegian patient advocacy association for patients with neuroendocrine tumors.

The authors declare no conflict of interest.

Reprints: Dordi Lea, MD, Department of Pathology, Stavanger University Hospital, Pb 8100, Stavanger N-4068, Norway (e-mail: dordilea@gmail.com).

Copyright © 2021 The Author(s). Published by Wolters Kluwer Health, Inc. This is an open access article distributed under the terms of the Creative Commons Attribution-Non Commercial-No Derivatives License 4.0 (CCBY-NC-ND), where it is permissible to download and share the work provided it is properly cited. The work cannot be changed in any way or used commercially without permission from the journal.

TABLE 1. WHO Grading of Neuroendocrine Tumors (WHO 2019)

	Grade	Mitotic Activity, Per 2 mm ² *	Ki67%*
NET Grade 1	Low	1	<3
NET Grade 2	Intermediate	2-20	3-20
NET Grade 3	High	> 20	> 20
LCNEC	High†	> 20	> 20
SCNEC	High†	> 20	> 20
MiNEN	Variable	Variable	Variable

*Mitotic rates are expressed as the number of mitoses/2 mm² as determined by counting in 50 fields of 0.2 mm² (ie, in a total area of 10 mm²); the Ki67 proliferation index value is determined by counting at least 500 cells in the regions of highest labeling (hot spots), which are identified at scanning magnification.

†Poorly differentiated NECs are not formally graded but are considered high-grade by definition.

LCNEC indicates large-cell neuroendocrine carcinoma; MiNEN, mixed neuroendocrine–non-neuroendocrine neoplasm; NEC, neuroendocrine carcinoma; NET, neuroendocrine tumor; SCNEC, small-cell neuroendocrine carcinoma; WHO, World Health Organization.

One of the challenges related to the current routine grading procedure is the time-consuming counting of > 500 cells by a pathologist, which may lead to an eyeball estimation as a short-cut in a busy routine practice. Moreover, the identification of “hot spots” in a section may be difficult,¹² which may partly explain the reported poor intraobserver and interobserver reliability.¹³ Consequently, objective measurements, including digital image analysis (DIA), are warranted for accurate grade reporting.

The heterogeneous biological behavior of GEP-NENs has encouraged a search for better prognostic markers. Phosphohistone H3 (PHH3) has been identified as a promising marker for the prediction of disease-free survival and disease-specific survival in PNENs.^{14,15} In contrast to Ki67, which is present in cell nuclei in the G1, S, G2, and M phases of the cell cycle, PHH3 stains mitotic cells (M phase). Thus, with PHH3, mitotic activity can be specifically determined;¹⁶ therefore, PHH3 has been suggested as an alternative to the Ki67 index in PNENs.¹⁷ Furthermore, counting MAI is challenging because apoptotic figures can be misidentified as mitotic figures.^{17,18} PHH3 does not stain apoptotic cells and can therefore be a better biomarker for mitosis than MAI. Several studies have shown good concordance between the number of mitoses and PHH3.^{19,20} Accordingly, PHH3 is regarded as promising for the assessment of grading in GEP-NENs in general.

In this study, we evaluated and compared the DIA Ki67 with the routine procedure for the Ki67 index assessment (pathology Ki67). In addition, we applied DIA for PHH3 assessment (DIA PHH3) to explore possible associations between PHH3 and the Ki67 index to evaluate the potential advantages or challenges of PHH3 as a proliferation marker in routine practice.

MATERIALS AND METHODS

Ethical Approval

All procedures performed in studies involving human participants were per the ethical standards of the institutional and/or National Research Committee and the 1964 Helsinki Declaration and its later amendments or comparable ethical

standards. This project was approved by the Regional Ethics Committee of the Western Health Authority (REK 2016/1622). Patients still alive have signed a written consent form to participate.

Materials

We identified all consecutive patients diagnosed with GEP-NENs and treated at Stavanger University Hospital from 2003 to 2013. The hospital serves as the only hospital for a well-defined Norwegian population of ~380,000 people.² Of 204 consecutive patients during that period, 35 declined to participate. In addition, 1 patient was excluded because of the possibility of primary pulmonary neuroendocrine carcinoma, and 9 patients were excluded because of a lack of tissue for analysis. Thus, 159 (77.9%) patients were included.

Archived formalin-fixed paraffin-embedded tissue from the hospital's diagnostic biobank was obtained. The current WHO criteria for neuroendocrine tumors¹⁰ were used, and pathologic tumor-node-metastasis (TNM) staging was performed according to the American Joint Committee on Cancer (AJCC) 8th edition.²¹ For Ki67, 500 to 2000 tumor cells were assessed in hot spots by microscopic evaluation.²¹ The Ki67 index was retrieved from the original routine pathology reports, and cases without available information were re-evaluated to complete pertinent information on all patients, as reported in our previous study.²

All tumors were confirmed as NENs by positive IHC staining for synaptophysin and/or chromogranin A. Neuroendocrine carcinoma was included as grade 3 (high grade). Mixed neuroendocrine–non-neuroendocrine neoplasms were excluded. The sample included 63 (39.6%) biopsies and 96 (60.4%) surgical specimens. MAI was not evaluated because of the high number of biopsies with an area <10 mm².

Methods

IHC

Ki67. The MIB-1 clone (Dako, Glostrup, Denmark) was used for routine staining at the Department of Pathology. The method has had minor changes in processing from 2003 to 2013, but the MIB-1 clone has been the same. The MIB-1 clone is validated for GEP-NEN grading.^{22,23}

PHH3. Antigen retrieval and antibody dilution were optimized before study onset. Paraffin sections adjacent to the HE sections were cut into 2- μ m-thick sections and mounted on Superfrost Plus slides. The slides were incubated at 60°C for 1 hour and stained using a Dako Omnis immunostainer. PHH3 (nr. 06-570; Merck Group, Darmstadt, Germany) was used at a dilution of 1:5000. The Dako EnVision Flex+ (Dako GV80011-2) detection system was used in line with the recommendations of the manufacturer.

DIA

IHC staining of Ki67 was already performed, and the available archived sections were retrieved from the hospital's archive. HE sections, Ki67, and PHH3 were scanned at \times 40 magnification using a Leica SCN400 slide

scanner (Leica Biosystems, Wetzlar, Germany) and uploaded to the image analysis software (Visiopharm, Hoersholm, Denmark). The person responsible for the DIA evaluation (D.L.) was blinded to the previously reported routine Ki67 index results and other parameters when DIA was performed. Patients were excluded from the DIA if there was insufficient tumor material for analysis (< 500 tumor cells). If a biopsy material and not a surgical specimen was used for the original routine Ki67 evaluation, DIA was also performed on the biopsy sample, given that sufficient materials were available.

For Ki67, the percentage of positive tumor cells was measured in the hot spot of the tumor in an area that includes 500 to 2000 tumor cells with the Visiopharm program (Fig. 1). The software program identified positive nuclei (label 1) and negative nuclei (label 2) within a manually selected area named the region of interest (ROI). Stroma and stromal cells were excluded from the ROI by the software program so that only the tumor cells were evaluated, similar to our DIA Ki67 method described for breast cancer.¹² The percentage of tumor cells was calculated. If the hot spot was ill-defined on a slide, the measurement was repeated in different areas, and the area with the highest positivity was counted. The program measured the areas of positive and negative nuclei, and based on the size of the nuclei in each tumor, an estimate of tumor cells was calculated. A percentage was calculated from ~2000 tumor cells. If there were <2000 cells but > 500 cells, a percentage was given based on the available cells in the section. This value was compared with the pathology Ki67 (regarded as the gold standard).

The number of PHH3-positive cells was calculated in 4 different ROIs of 2 mm² (ROI: 1 to 4) (Fig. 2). The different ROIs were chosen subjectively from the visual identification of areas with the highest number of PHH3-positive cells. The number of PHH3-positive cells within each ROI was calculated. If there was insufficient material for 4 ROIs, fewer ROIs were chosen for measurement. For PHH3, Visiopharm was programmed to detect IHC-stained mitotic cells as described by others.²⁴ Cells in all 4 substages of mitosis, prophase, metaphase, anaphase, and telophase, were regarded as positive.²⁵ Objects smaller than mitotic figures were removed by a size filter. The remaining objects were dilated to fuse the chromatin structures of cells in anaphase or telophase into 1 object. All remaining objects were counted, and the number of objects per 2 mm² was calculated. The counted objects were encircled in the original image, allowing a visual inspection of the counted mitotic cells. Apart from the manual selection of the 4 different ROIs, the DIA procedure and all calculations were fully automated.

Statistics

IBM SPSS Statistics for Windows, Version 26.0 (IBM Corporation, Armonk, NY) was used for statistical calculations. The quadratically weighted kappa was used to measure the agreement between ordinal variables.²⁶ The interclass correlation coefficient was used to measure the agreement between continuous variables (single rater, absolute agreement). All agreement estimates are presented with 95% con-

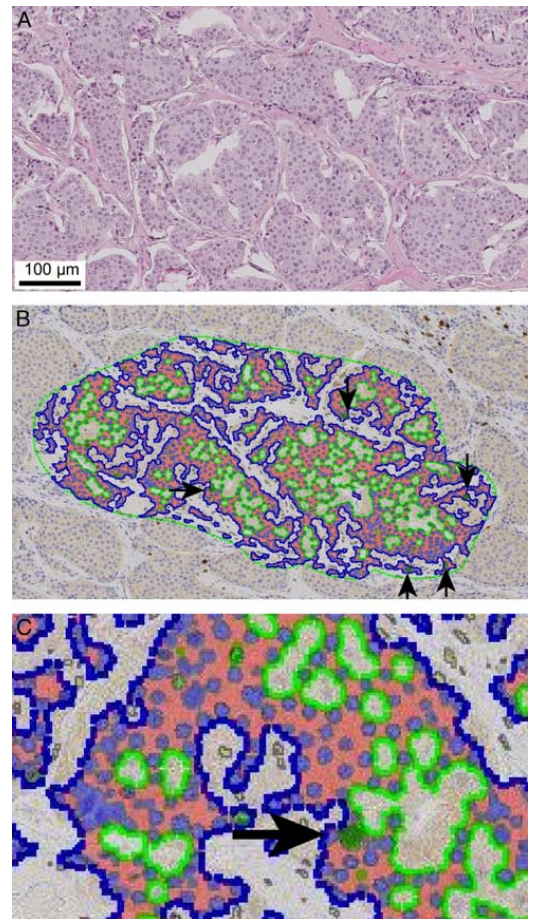


FIGURE 1. A, Hematoxylin and eosin staining of a grade 2 neuroendocrine tumor. B and C Immunohistochemical staining of Ki67 with digital image analyses performed on the same tumor. Black arrows point to some of the positive cells.

fidence intervals (CIs). Values <0.50, between 0.50 and 0.75, between 0.75 and 0.90, and > 0.90 indicated poor, moderate, good, and excellent reliability, respectively.²⁷ To plot the difference in pathology Ki67 and DIA Ki67 measurement against average value, we used a Bland-Altman plot.²⁸

RESULTS

The clinicopathologic characteristics of the patients are shown in Table 2. The distribution of grading based on the DIA Ki67, DIA PHH3, and pathology Ki67 are shown in Figure 3. This figure shows that different methods influence grading, with more grade 2 tumors and fewer grade 1 tumors with the methods based on DIA than with the pathology Ki67. The median pathology Ki67 was 2.0% (range: 1.0% to 100%). The median DIA Ki67 value was 4.1% (range: 0.0%

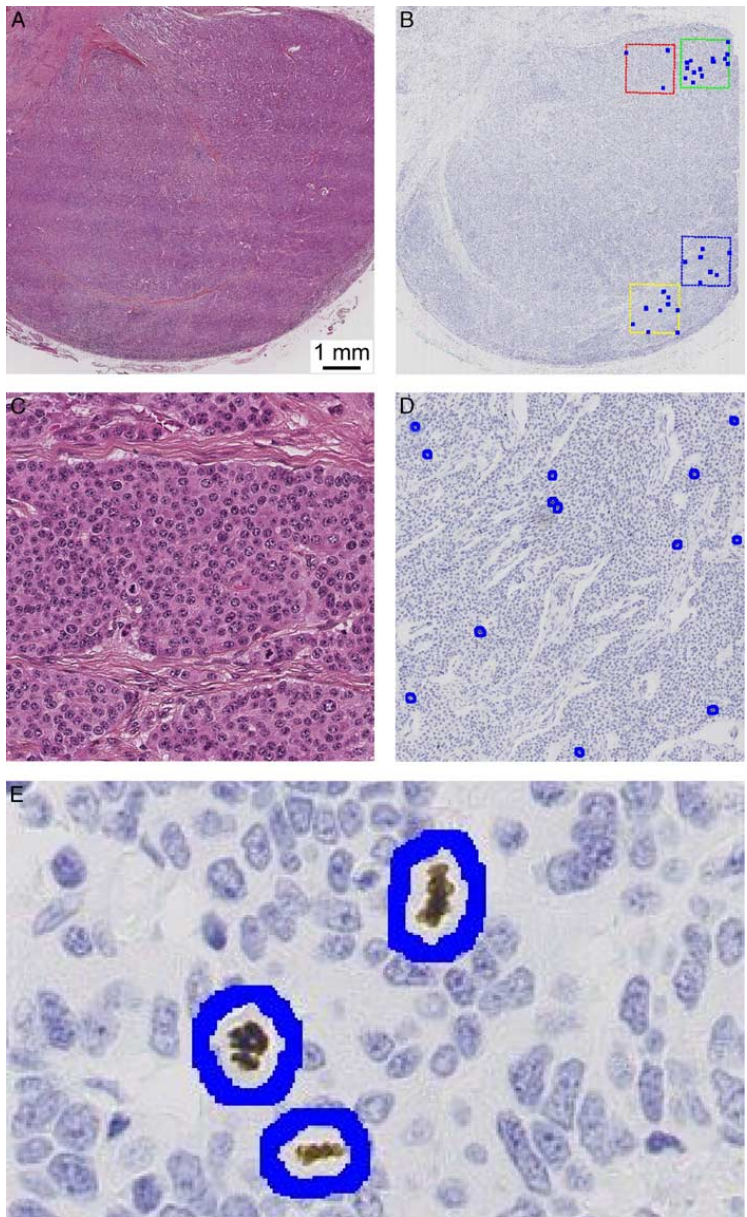


FIGURE 2. A, Hematoxylin and eosin staining of a grade 2 neuroendocrine tumor. B, Digital image measurement of immunohistochemically stained phosphohistone H3 in 4 different regions of interest. C, Close-up image of hematoxylin and eosin staining with marking of mitosis. D and E, Close-up image of the measurement of phosphohistone H3 in the regions of interest with the highest mitotic activity.

to 99.9%). The interclass correlation coefficient of the DIA Ki67 and pathology Ki67 showed an excellent agreement of 0.96 (95% CI: 0.94-0.98). Figure 4A shows a scatter plot of

the distribution of the DIA Ki67 and pathology Ki67. The observed kappa between grading based on the DIA Ki67 and the pathology Ki67 was 0.86 (95% CI: 0.81-0.91).

TABLE 2. Demographics and Clinical Characteristics of the Patients

Characteristics	Value
Age, median (range), y	61.8 (12.5-94.2)
Sex, n (%)	
Male	91 (57.2)
Female	68 (42.8)
Tumor size, median* (range), cm	1.7 (0.1-13.8)
Localization of tumor, n (%)	
esophagus	2 (1.3)
Stomach	9 (5.7)
Duodenum	5 (3.1)
Small intestine	54 (34.0)
Meckel	1 (0.6)
Appendix	31 (19.5)
Pancreas	21 (13.2)
Colon	15 (9.4)
Rectum	14 (8.8)
Metastasis liver/unknown primary	7 (4.4)
WHO grade, n (%)	
1	85 (53.5)
2	38 (23.9)
3	36 (22.6)
T classification*, n (%)	
T1	51 (37.5)
T2	21 (15.4)
T3	50 (36.8)
T4	14 (10.3)
N classification*, n (%)	
N0	69 (44.5)
N1	86 (55.5)
M classification*, n (%)	
M0	95 (61.3)
M1	60 (38.7)
AJCC stage*, n (%)	
I	51 (32.4)
II	12 (7.6)
III	34 (21.6)
IV	60 (38.2)

*Numbers may not add up because of missing data: n=18 for tumor size, n=23 for T-stage, n=4 for N-stage and M-stage and n=2 for AJCC stage. AJCC indicates American Joint Committee on Cancer; WHO, World Health Organization.

A Bland-Altman plot was created to visualize the difference in agreement against average value of pathology Ki67 and DIA Ki67 (Fig. 5).

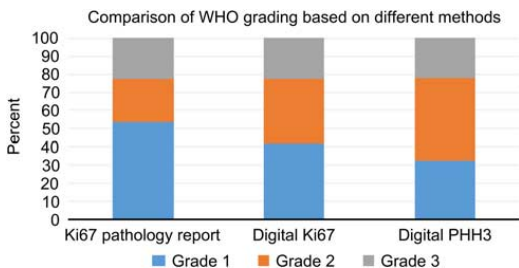


FIGURE 3. Comparison of World Health Organization (WHO) grading based on different methods for proliferation measurement. PHH3 indicates phosphohistone H3.

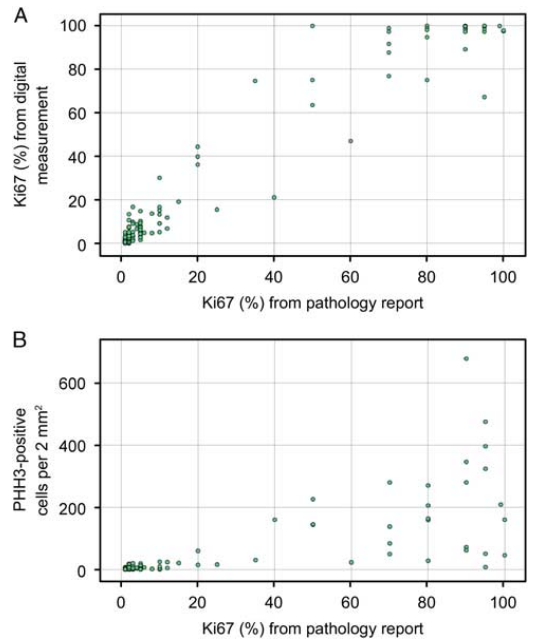


FIGURE 4. A, Scatter plot showing the correlation between the Ki67 index from the pathology report and Ki67 based on digital image analysis. B, Scatter plot showing the correlation between the Ki67 index from the pathology report and digital measurement of the number of phosphohistone H3 (PHH3)-positive cells per 2 mm².

The agreement between grading based on the DIA Ki67 and the pathology Ki67 is shown in Table 3. None of the grade 3 tumors was graded as grade 1 and vice versa. Cases with less correlation between the methods comprised mostly grade 1 and grade 2 tumors, and the percentage was mostly measured higher (ie, > 3%) by DIA than with the pathology Ki67. Among 26 cases with a discrepancy between grades 1 and 2, Ki67 values of 2% to

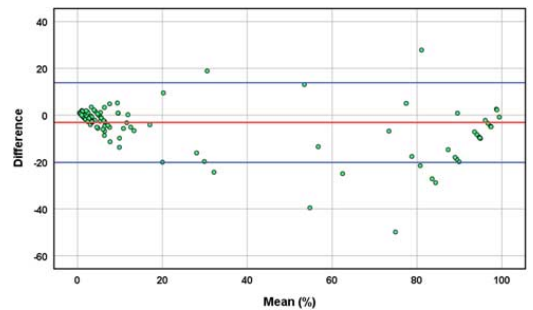


FIGURE 5. A Bland-Altman plot showing the difference Ki67 index against mean value from the pathology report and Ki67 based on digital image analysis.

TABLE 3. Agreement Between Grading of Tumors Based on Digital Image Analysis of Ki67 and Grading From Routine Pathology Reports

	Grade (DIA Ki67) n, (%)			Total, n (%)
	1	2	3	
Grade (routine)				
1	63 (39.6)	22 (13.8)	0	85 (53.5)
2	4 (2.5)	33 (20.8)	1 (0.6)	38 (23.9)
3	0	1 (0.6)	35 (22.0)	36 (22.6)
Total	67 (42.1)	56 (35.2)	36 (22.6)	159

DIA indicates digital image analysis.

4% were found in 24 (92.3%) of the cases by either DIA Ki67 or pathology Ki67.

PHH3 was measured in 145 (145/159 = 91.2%) of the patients. Fourteen patients were excluded because of a lack of available tumor material for analysis. A median of 3 mitoses (range: 0 to 678 cells/mm²) was observed. Figure 4B shows a scatter plot of the distribution of DIA PHH3 and the pathology Ki67. The observed kappa between grading based on the DIA PHH3 and pathology Ki67 was 0.742. (95% CI: 0.65-0.83). The agreement between grading based on DIA PHH3 and the pathology Ki67 is shown in Table 4. For the DIA of PHH3, there were no grade 3 tumors that were graded as grade 1. Moreover, 35 NENs were upgraded from grade 1 to grade 2 based on the DIA PHH3 measurement compared with pathology Ki67. In 20 (20/35 = 57.1%) of these tumors, the PHH3 value was 2 or 3.

DISCUSSION

The current study explored several comparative measures for grading by the use of DIA and alternative markers for proliferation. Grading based on the DIA Ki67 showed good reliability compared with grading based on the pathology Ki67. The use of DIA PHH3 for grading did not show similar results, with a higher number of NENs migrating between grades, especially grade 2, as a consequence. Whether this represents true grade migration or just artefacts from variation in scores remains unproven.

This study confirms an excellent agreement between the DIA Ki67 and the pathology Ki67, a finding that is supported by other studies.^{13,29} DIA can improve the reliability and reproducibility of grading in routine

TABLE 4. Agreement Between Grading of Tumors Based on Digital Image Analysis of Phosphohistone H3 and Grading from Routine Pathology Reports

	Grade (DIA PHH3) n, (%)			Total n, (%)
	1	2	3	
Grade (routine)				
1	43 (29.7)	35 (24.1)	0	78 (53.8)
2	4 (2.8)	28 (19.3)	4 (2.8)	36 (24.8)
3	0	3 (2.1)	28 (19.3)	31 (21.4)
Total	47 (32.4)	66 (45.5)	32 (22.1)	145

DIA indicates digital image analysis; PHH3, phosphohistone H3.

practice.³⁰ Thus, likely the pathology departments with this method or similar DIA available, can use DIA Ki67 as a part of their routine diagnostics. Digital pathology has during recent years, been introduced at more pathology departments, and the numbers are increasing.^{31,32} Manual counting is often difficult because of the high cellularity commonly encountered in these tumors.³⁰ One of the benefits of our DIA method of Ki67 is the automatic separation of stroma and stromal cells from tumor cells. This does not apply to all DIAs, which may partly explain the previously reported poor concordance between the DIA and manual analysis of Ki67 found by others.³³

This study included a consecutive series from a population-representative cohort of GEP-NEN patients in a well-defined region of Norway. Compared with other studies of GEP-NENs, the number of included patients with grades 2 and 3 was high, and the distribution of different grades was more even.^{13,17,30,33-35} A limitation of our study is that almost 40% of the tumor samples were from biopsies. However, this is in line with current routine practice at many centers since surgical specimens are not achievable for all patients, especially patients with advanced disease.

Grading based on the DIA PHH3 agreed less well with the WHO grade based on the pathology Ki67. This is in line with the results of others.^{15,33,36} Accordingly, we believe the DIA and use of PHH3 are not supported for routine use or as an alternative in GEP-NEN grading. Some of the cases with low Ki67 had high PHH3. Others have reported a specific value for PHH3 in PNENs,¹⁴ but we could not confirm or refute this based on the limited number of PNENs.

For both DIA Ki67 and DIA PHH3, the proportion of grade 2 tumors was higher than the routinely reported grading. This illustrates the difficulty in separating grade 1 and grade 2 tumors.^{33,37} A factor that might explain this finding is that the DIA method makes it easier to identify a hot spot than manual evaluation in a busy routine practice. With DIA, measurements can be repeated or several areas can be measured if the hot spot is difficult to identify. The size of the hot spot (500 to 2000 cells) might also influence the grading. A study of G1 and G2 PNENs found that DIA overestimated the Ki67 index compared with manual evaluation. The difference was reduced by increasing the size of the hot spot.³⁸ Kroneman et al³⁷ found that eyeball estimations of Ki67 tended to downgrade more NETs to grade 1 than evaluations by DIA. These studies support our findings. In many cases with a discrepancy, the value of Ki67 or PHH3 was near the cut-off level for the grading criteria. Discussions are ongoing regarding which method should be regarded as the gold standard.^{13,34,35} For breast cancers, there is a debate about whether the manual analysis of Ki67 should be the gold standard since several studies have shown superior prognostic information from DIA.^{39,40}

In conclusion, standardized DIA Ki67 scoring gave similar results as subjective scoring but may be a time-saving supplementary tool in surgical pathology²⁹ that can improve the poor intraobserver and interobserver reliability with manual evaluation methods.⁴¹ DIA PHH3 do not agree so well with routine grading and is not recommended as an alternative to MAI or Ki67 in routine practice.

ACKNOWLEDGMENTS

The authors thank statistician Ingvild Dalen, PhD, Stavanger University Hospital, Norway, for providing help with the statistical methods.

REFERENCES


- Merola E, Rinzivillo M, Cicchese N, et al. Digestive neuroendocrine neoplasms: a 2016 overview. *Dig Liver Dis*. 2016;48:829–835.
- Sandvik OM, Søreide K, Gudlaugsson E, et al. Epidemiology and classification of gastroenteropancreatic neuroendocrine neoplasms using current coding criteria. *Br J Surg*. 2016;103:226–232.
- Modlin IM, Lye KD, Kidd M. A 5-decade analysis of 13,715 carcinoid tumors. *Cancer*. 2003;97:934–959.
- Maggard MA, O'Connell JB, Ko CY. Updated population-based review of carcinoid tumors. *Ann Surg*. 2004;240:117–122.
- Søreide JA, van Heerden JA, Thompson GB, et al. Gastrointestinal carcinoid tumors: long-term prognosis for surgically treated patients. *World J Surg*. 2000;24:1431–1436.
- Lee MS, O'Neil BH. Summary of emerging personalized medicine in neuroendocrine tumors: are we on track? *J Gastrointest Oncol*. 2016; 7:804–818.
- Yao JC, Hassan M, Phan A, et al. One hundred years after "carcinoid": epidemiology of and prognostic factors for neuroendocrine tumors in 35,825 cases in the United States. *J Clin Oncol*. 2008;26:3063–3072.
- Bellizzi AM. Immunohistochemistry in the diagnosis and classification of neuroendocrine neoplasms: what can brown do for you? *Hum Pathol*. 2020;96:8–33.
- Nagtegaal ID, Odze RD, Klimstra D, et al. The 2019 WHO classification of tumours of the digestive system. *Histopathology*. 2020;76:182–188.
- WHO Classification of Tumours. *Digestive System Tumours*, 5 ed. Vol. 1. Lyon, France: IARC Publications; 2019.
- McCall CM, Shi C, Cornish TC, et al. Grading of well-differentiated pancreatic neuroendocrine tumors is improved by the inclusion of both Ki67 proliferative index and mitotic rate. *Am J Surg Pathol*. 2013;37:1671–1677.
- Gudlaugsson E, Skaland I, Janssen EA, et al. Comparison of the effect of different techniques for measurement of Ki67 proliferation on reproducibility and prognosis prediction accuracy in breast cancer. *Histopathology*. 2012;61:1134–1144.
- Tang LH, Gonen M, Hedvat C, et al. Objective quantification of the Ki67 proliferative index in neuroendocrine tumors of the gastroenteropancreatic system: a comparison of digital image analysis with manual methods. *Am J Surg Pathol*. 2012;36:1761–1770.
- Villani V, Mahadevan KK, Ligorio M, et al. Phosphorylated Histone H3 (PHH3) is a superior proliferation marker for prognosis of pancreatic neuroendocrine tumors. *Ann Surg Oncol*. 2016;23 (suppl 5):609–617.
- Ozturk Sari S, Taskin OC, Gundogdu G, et al. The impact of phosphohistone-H3-assisted mitotic count and Ki67 Score in the determination of tumor grade and prediction of distant metastasis in well-differentiated pancreatic neuroendocrine tumors. *Endocr Pathol*. 2016;27:162–170.
- Sun A, Zhou W, Lunceford J, et al. Level of phosphohistone H3 among various types of human cancers. *BMJ Open*. 2012;2:e001071.
- Tracht J, Zhang K, Pekar D. Grading and prognostication of neuroendocrine tumors of the pancreas: a comparison study of Ki67 and PHH3. *J Histochem Cytochem*. 2017;65:399–405.
- Skaland I, Janssen EA, Gudlaugsson E, et al. Validating the prognostic value of proliferation measured by phosphohistone H3 (PHH3) in invasive lymph node-negative breast cancer patients less than 71 years of age. *Breast Cancer Res Treat*. 2009;114:39–45.
- Bossard C, Jarry A, Colombeix C, et al. Phosphohistone H3 labelling for histoprostic grading of breast adenocarcinomas and computer-assisted determination of mitotic index. *J Clin Pathol*. 2006; 59:706–710.
- Ribalta T, McCutcheon IE, Aldape KD, et al. The mitosis-specific antibody anti-phosphohistone-H3 (PHH3) facilitates rapid reliable grading of meningiomas according to WHO 2000 criteria. *Am J Surg Pathol*. 2004;28:1532–1536.
- American Joint Committee on Cancer Staging Manual, 8th ed. Cham, Switzerland: Springer International Publishing AG; 2017.
- Gentil Perret A, Mosnier JF, Buono JP, et al. The relationship between MIB-1 proliferation index and outcome in pancreatic neuroendocrine tumors. *Am J Clin Pathol*. 1998;109:286–293.
- Klöppel G, Couvelard A, Perren A, et al. ENETS Consensus Guidelines for the Standards of Care in Neuroendocrine Tumors: towards a standardized approach to the diagnosis of gastroenteropancreatic neuroendocrine tumors and their prognostic stratification. *Neuroendocrinology*. 2009;90:162–166.
- Skaland I, Janssen EA, Gudlaugsson E, et al. Phosphohistone H3 expression has much stronger prognostic value than classical prognosticators in invasive lymph node-negative breast cancer patients less than 55 years of age. *Mod Pathol*. 2007;20:1307–1315.
- Dumars C, Foubert F, Touchefeu Y, et al. Can PPH3 be helpful to assess the discordant grade in primary and metastatic enteropancreatic neuroendocrine tumors? *Endocrine*. 2016;53:395–401.
- Cohen J. Weighted kappa: nominal scale agreement with provision for scaled disagreement or partial credit. *Psychol Bull*. 1968;70:213–220.
- Koo TK, Li MY. A guideline of selecting and reporting intraclass correlation coefficients for reliability research. *J Chiropr Med*. 2016; 15:155–163.
- Bland JM, Altman DG. Comparing methods of measurement: why plotting difference against standard method is misleading. *Lancet*. 1995;346:1085–1087.
- Satturwar SP, Pantanowitz JL, Manko CD, et al. Ki-67 proliferation index in neuroendocrine tumors: can augmented reality microscopy with image analysis improve scoring? *Cancer Cytopathol*. 2020;128: 535–544.
- Reid MD, Bagci P, Ohike N, et al. Calculation of the Ki67 index in pancreatic neuroendocrine tumors: a comparative analysis of four counting methodologies. *Mod Pathol*. 2015;28:686–694.
- Tschuchnig ME, Oostingh GJ, Gadermayr M. Generative adversarial networks in digital pathology: a survey on trends and future potential. *Patterns (N Y)*. 2020;1:100089.
- Jahn SW, Plass M, Moinfar F. Digital pathology: advantages, limitations and emerging perspectives. *J Clin Med*. 2020;9:3697.
- Hacking SM, Sajjan S, Lee L, et al. Potential pitfalls in diagnostic digital image analysis: experience with Ki-67 and PHH3 in gastrointestinal neuroendocrine tumors. *Pathol Res Pract*. 2020;216:152753.
- Dhall D, Mertens R, Brese C, et al. Ki-67 proliferative index predicts progression-free survival of patients with well-differentiated ileal neuroendocrine tumors. *Hum Pathol*. 2012;43:489–495.
- Goodell PP, Krasinskas AM, Davison JM, et al. Comparison of methods for proliferative index analysis for grading pancreatic well-differentiated neuroendocrine tumors. *Am J Clin Pathol*. 2012;137:576–582.
- Kim MJ, Kwon MJ, Kang HS, et al. Identification of phosphohistone H3 cutoff values corresponding to original WHO grades but distinguishable in well-differentiated gastrointestinal neuroendocrine tumors. *Biomed Res Int*. 2018;2018:1013640.
- Kroneman TN, Voss JS, Lohse CM, et al. Comparison of three Ki-67 index quantification methods and clinical significance in pancreatic neuroendocrine tumors. *Endocr Pathol*. 2015;26:255–262.
- Owens R, Gilmore E, Bingham V, et al. Comparison of different anti-Ki67 antibody clones and hotspot sizes for assessing proliferative index and grading in pancreatic neuroendocrine tumors using manual and image analysis. *Histopathology*. 2020;77:646–658.
- Stålhammar G, Robertsson S, Wedlund L, et al. Digital image analysis of Ki67 in hot spots is superior to both manual Ki67 and mitotic counts in breast cancer. *Histopathology*. 2018;72:974–989.
- Klauschen F, Wienert S, Schmitt WD, et al. Standardized Ki67 diagnostics using automated scoring—clinical validation in the GeparTrio Breast Cancer Study. *Clin Cancer Res*. 2015;21: 3651–3657.
- Trikalinos NA, Chatterjee D, Lee J, et al. Accuracy of grading in pancreatic neuroendocrine neoplasms and effect on survival estimates: an institutional experience. *Ann Surg Oncol*. 2020;27:3542–3550.

**Errata for
Use of quantitative pathology to improve grading and
predict prognosis in tumours of the gastrointestinal
tract**

Dordi Lea



Thesis for the degree philosophiae doctor (PhD)
at the University of Bergen

13/12-21 Dordi Lea  17.12.21
(date and sign. of candidate) (date and sign. of faculty)

Errata

Page 4: Missing text: Added “Especially thanks to Linda Hatleskog for her excellent linguistic skills, which have improved this thesis”.

Page 10: Changing reference from “(2017) Vol. 37, 675–684” to ”2017; 37 (2):675–684”.

Page 23: Deletion of space in table.

Page 45, 47, 70: Changing capital letters to small letters in chromogranin A, synaptophysin and gastrin.

Page 54, 81 and 84: Missing -, added in T-cell/T-cells.

Page 42, 72 and 87: Missing space added after punctuation.

Page 67: Missing text: “To improve the prognostic value of grading using digital image analysis of Ki-67 compared to manual evaluation with a light microscope (**Paper III**);” - corrected to “To improve the prognostic value of grading using digital image analysis of Ki-67 in GEP-NENs compared to manual evaluation with a light microscope (**Paper III**);”

Page 86 and 89: Deletion of space before punctuation.



Graphic design: Communication Division, UIB / Print: Skjipes Kommunikasjon AS



uib.no

ISBN: 9788230852491 (print)
9788230869437 (PDF)